ABSTRACT

Title of dissertation: IDENTIFICATION AND ENGINEERING BACTERIOPHAGE ENDOLYSINS FOR INACTIVATION OF GRAM-POSITIVE SPORE-FORMING BACILLI

Irina V. Etobayeva, Doctor of Philosophy, 2018

Dissertation Directed by: Associate Professor Daniel C. Nelson
Institute for Bioscience and Biotechnology Research and
Department of Veterinary Medicine

This dissertation concentrates on the study of the antibacterial potential of bacteriophage-encoded endolysins derived from phages that infect the Gram-positive *Bacillus cereus sensu lato* group. Bacteriophage-encoded endolysins are peptidoglycan hydrolases that have been identified as important factors in the phage life cycle. Endolysins are encoded by phage late genes during an intracellular infection cycle to lyse the bacterial cell wall from within and allow phage progeny release. Endolysins derived from phages of Gram-positive bacterial hosts are equipped with an enzymatic domain that hydrolyzes conserved covalent bonds in bacterial peptidoglycan, and a cell wall binding domain that ensures proper attachment of endolysins to bacilli. In this study three novel endolysins, PlyP56, PlyN74, and PlyTB40 have been discovered and identified. The biochemical analysis shows that all three endolysins have relatively broad antimicrobial activity against organisms of the *B. cereus* group with the optimal lytic activity at physiological pH (pH 7.0–8.0), over a broad temperature range (4–55°C), and at low concentrations of NaCl (<50 mM).

The domain shuffling engineering studies were undertaken to observe enhancements of bacteriolytic properties of chimeric lysins that retained their specificity to *B. cereus* species. Finally, these studies have identified a new development in lysis of peptidoglycan of Gram-positive *B. cereus* group of organisms by phage-encoded endolysins. When grown to stationary phase, bacilli, especially, in overnight cultures become more resistant to lysis despite the evidence that the cell wall domains bind the bacterial surface. In light of these findings, I hypothesize that *B. cereus* group of species have evolved complex behaviors to interact with phage by modulating surface associated secondary polymers throughout the maturation of the bacilli in order to render them more resistant to the lytic action of phage encoded endolysins, which, contributes to bacterial survival from phage infection.

IDENTIFICATION AND ENGINEERING BACTERIOPHAGE ENDOLYSINS FOR INACTIVATION OF GRAM-POSITIVE SPORE-FORMING BACILLI

by

Irina V. Etobayeva

Dissertation submitted to the Faculty of the Graduate School of the
University of Maryland, College Park, in partial fulfillment
of the requirements for the degree of
Doctor of Philosophy
2018

Advisory Committee:
Associate Professor Daniel C. Nelson, Chair
Associate Professor George Belov
Associate Professor Kasey M. Moyes
Associate Professor Meiqing Shi
Professor Shunyuan Xiao

Acknowledgements

First, I wish to thank my advisor Dr. Daniel Nelson, for all his help and advice during my dissertation research at the Institute for Bioscience and Biotechnology Research and the University of Maryland.

I wish to thank members of my lab, Dr. Sara Linden and Xiaoran Shang for their guidance and for bouncing ideas during our conversations. Additionally, I would like to thank members of the Xiao lab, Dr. Harley King for assistance with some of my experiments and patient guidance. Aside from that I am thankful I had a chance to meet our international research interns, Dr. Yang Zhou and Dr. Hang Yang. I feel that our research together made me better equipped to achieve more in future career.

I would like to thank my kids, Val, Juan, and Andrea, for being with me during this exciting and challenging time. It was not an easy journey for all of us, but we kept strong together. I wish to express my sincere gratitude for having children like you. Thank you for being with me during all of the ups and downs.

The research described in this dissertation was carried out by me while I was assigned by the US Navy to the University of Maryland for duty under instructions. I would like to thank the Naval Medical Professional Development Center, Bethesda, MD, and personally thank CAPT Cary M. Sill, CAPT Phillip Sanchez, and CDR Miguel Santiesteban for mentorship and for entrusting me to complete this Doctorate degree. I thank my supervisor, LCDR (Ret.) Glenn A. Smith for believing in me and for many meaningful conversations. I reached to this point because of all of your help, mentorship, and guidance.

Table of Contents

List of Tables

Chapter 1

Chapter 2

Chapter 3

List of Figures

Chapter 1

Chapter 2

Chapter 3

Chapter 5

List of Abbreviations

6xHIS tag	Hexahistidine tag
AA	Amino acid
Ala	Alanine
Asp	Asparagine
ATCC	American Type Culture Collection
bceT	*B. cereus* enterotoxin T
BEI Resources	Biodefense and Emerging Infections Research Resources
BHI	Brain-heart infusion
BSL	Biosafety level
CBD	Cell wall binding domain
CBRs	Choline binding repeats
CCWP	Carbohydrate cell wall polymer
CDC	Center for Disease Control and Prevention
CFU	Colony forming unit
ChBD	Choline binding domain
Cry	Crystal protein
Cys	Cysteine
DMSO	Dimethyl sulfoxide
DNA	Deoxyribonucleic acid
EA1	Extractable antigen 1
EAD	Enzymatically active domain
EDTA	Ethylenediaminetetraacetic acid
EF	Edema factor
ET	Edema toxin
FDA	U. S. Food and Drug Administration
FoodNet	U.S. Foodborne Diseases Active Surveillance network
Gal	Galactose
GlcNAc	N -Acetylglucosamine
Gln	Glutamine
Glu	Glutamic acid
HBL	Hemolysin BL
His	Histidine
LB	Luria-Bertani
Leu	Leucine
LF	Lethal factor
LT	Lethal toxin
Man	Mannose
mDAP	meso-diaminopimelic acid
MurNAc	N– Acetylmuramic acid
NCBI	National Center for Biotechnology Information
Nhe	Non - hemolytic enterotoxin
OD	Optical density

ORF	Open reading frame
P	Phosphate
PA	Protective antigen
PBS	Phosphate buffered saline
PCR	Polymerase chain reaction
PDB	Protein data bank
Phe	Phenylalanine
PMSF	Phenylmethylsulfonyl fluoride
Pro	Proline
Sap	Surface array protein
SCWP	Secondary cell wall polysaccharide
SDS-PAGE	Sodium dodecyl sulfate polyacrylamide gel electrophoresis
SH3	src homology 3 domain
SOP	Standard operation procedure
Tyr	Tyrosine
USDA	U. S. Department of Agriculture

1 Introduction and Background

1.1 Introduction

Bacillus cereus species are Gram-positive rod-shaped microorganisms that form drought tolerant spores. Members of these species are highly abundant soil bacilli that vary in their capability to cause diseases ranging from mild food poisoning to severe illness. Contamination of raw food with bacilli initially starts in soil with contaminated water and later during food preparation in processing facilities. Concern related to emergence of broad spectrum antibiotic resistant bacteria (Ventola, 2015; Zaman et al., 2017) and application of broad-spectrum antibiotics for food preservation expedited the need for an alternative to antibiotics therapeutics and food preservatives capable of selective bactericidal action (Briers and Lavigne, 2015). A number of new endolysins, also known as enzybiotics (Heselpoth et al., 2018), with lytic activity against a broad range of bacteria have been discovered to date, and their enzymatic mechanisms characterized. However, there are only limited reports related to endolysins that target and effectively lyse Gram-positive spore-forming species (Fischetti, 2010).

Endolysins are enzymes encoded by phage during an intracellular replication cycle. In general, they comprise of two structural units, an enzymatically active domain (EAD) attached via a short linker to a cell wall binding domain (CBD). Once synthesized at the end of phage life cycle, endolysins target and cleave evolutionarily preserved covalent bonds within the peptidoglycan of bacterial cell wall. Ligands on the surface of bacteria serve as anchors facilitating attachment of CBDs and association with bacteria. Endolysins lyse the cell wall of host bacteria “from within” and allow phage progeny release (Fischetti, 2008; Nelson et al., 2012b; Schmelcher et al., 2012).

Furthermore, it is reported that endolysins applied extrinsically retain their enzymatic activity by lysing bacteria "from without" (Abedon, 2011).

Characterization and engineering of endolysins specific to spore-forming bacilli has broad application in medicine for controlling bacterial contamination, decontamination efforts, designing targeted antibacterial therapeutics, in diagnostics for development of rapid detection assays such as diagnostics based on the modular CBD subunits (Kikkawa et al., 2007; Schmelcher and Loessner, 2014), in agriculture for food preservation and animal treatment, and for environmental decontamination efforts.

In this dissertation I aim to identify novel *Bacillus*-specific phage endolysins, biochemically characterize their properties, and further engineer them to enhance enzymatic properties and expand host spectrum. I used domain swapping engineering strategies to improve their enzymatic properties and affinities for the peptidoglycan substrate.

1.2 Bacteriophage-Derived Peptidoglycan Hydrolases: Endolysins

1.2.1 History of Bacteriophage Discovery

Viruses of bacteria, otherwise called bacteriophages, or phages, are the largest known group of viruses (Clokie et al., 2011; Comeau et al., 2008). Frederick Twort, an English physician, first discovered and described them in 1915 (Twort, 1915), while he was experimenting with the contaminating *Staphylococcus* bacteria from the vaccinia virus vaccine. Twort was having a problem propagating vaccinia virus from the vaccine due to contaminating bacteria. During an unsuccessful attempt to propagate the virus, he observed a peculiar phenomenon – clear glassy zones on otherwise uniform bacterial lawn, which upon microscopy revealed the debris of dead bacteria. One of three hypotheses that he proposed to explain this phenomenon was an infection

of bacteria with the “ultra-microscopic virus”. This agent could pass through the bacterial filters, and, also, could be transferred from one colony to the other. In 1915 Twort published an article with this data but he never attempted to determine the nature on how this agent worked.

Two years later, in 1917, the French-Canadian microbiologist at the Pasteur Institute, Félix d’Hérelle, independently from Twort has discovered the same type of infecting agent. He immediately proposed the parasitic viral nature of the agent and named it bacteriophage, which literally means bacteria-eater from the Greek word “phagein” that is “to devour” (d’Herelle, 1917; Publications service, 2007). After this discovery, d’Hérelle developed a theory about parasitic existence of the bacteriophages in their bacterial host. Since this time, the potential of using phages to treat and control bacterial infections has attracted attention of microbiologists to bacteriophages all over the world. Therapeutic application of bacteriophages was proposed and was successfully tested by d’Hérelle himself and also independently by other scientists (Bruynoghe & Maisin, 1921; d’Herelle & Smith, 1926).

Noteworthy, spontaneous lysis of bacteria has been described decades before the discovery of bacteriophages either by Twort or d’Hérelle. In 1892, Kruse and Pansini, who studied host protective immunity in pneumococcal infections, observed autolysis of pneumococci during the infection (Wadsworth, 1912). A Russian microbiologist, Gamaleya, in 1898, described bacteriolytic substances that lysed bacilli of *B. anthracis*. He could experimentally transfer lysogenic properties from *B. anthracis* cell lysate to new bacterial culture naming this phenomena the bacterial lysis (Bardell, 1982). However, despite all these observations, scholars were unable to identify the agent that caused bacterial lysis, although, they noticed its significance for the protection against diseases. d’Hérelle, on the other hand, persevered in studying the properties of bacteriophages. He determined that phages could exponentially replicate and destroy pathogenic

bacteria, indicating that they also could play an important role in a fight against of infectious diseases. He developed and described a method for determining a number of bacteriophage particles by introducing progressively decreasing concentrations of bacteriophages into a liquid culture of bacteria (d'Herelle & Smith, 1926). Subsequently, bacterial cultures were aliquoted and evenly smeared on top of solid agar and cultivated for bacterial growth. Single phage particles then could be enumerated by the number of clearing spots, called "plagues", on the bacterial lawn. This plague assay, with some modifications, is used for enumeration of phage particles at the present time.

On a large scale, bacteriophages first were used for prevention and treatment of cholera epidemics in colonial India in the 1920s and 1930s by the British medical officer Lieutenant Colonel Morison (Merril et al., 2003). The effort was originally initiated by d'Hérelle when he was invited by the British government to work in India on phage therapy of the plague. His visit led to an establishment of "The Bacteriophage Inquiry" project in India. Therapy with phages has proved to be quite effective in treatment of patients, while prevention of cholera epidemics with a release of phages into the drinking water was less understood (Summers, 2001).

Application of phages for therapeutic use had rapid translation to commercial products in the United States in the 1920s and 1930s. The large pharmaceutical companies, Eli Lilly & Co, Swan-Myers division of Abbot Laboratories, and Parke-Davis sold various phage 'jel' products and bacteriophage filtrate preparations to threat *Streptococcus*, *Staphylococcus* and colon bacilli infections (Straub and Applebaum, 1933). However, since the discovery of low molecular weight antibiotics with effective antibacterial properties, which were also easy to manufacture, the production of bacteriophage products began to be replaced by commercialized antibiotics. Later, new standards set for the drug discovery and manufacture by the Council on Pharmacy and

Chemistry of the American Medical Association, and the start of World War II, diminished the initial enthusiasm in phage therapy in the West and soon after all antimicrobial-related research focused on antibiotic-related therapy.

Before World War II had taken over Europe, in 1931, d'Hérelle and his Russian student, George Eliava, produced the first commercial anticholera phage formulation at the Pasteur Institute established in the Soviet Republic of Georgia. d'Hérelle played important role in the establishment of this institute as well, which is currently named after George Eliava. Shortly after the triumph of first commercialized phage product, Eliava faced an unfortunate fate; he was executed by the Soviet government. d'Hérelle returned to France and was kept under house arrest for the duration of World War II. There is evidence that while in Tbilisi, Georgia, d'Hérelle authored a book called "Bacteriophage and the Phenomenon of Recovery", which was published in 1935 in the Russian language. This book was removed from the circulation soon after the execution of George Eliava and kept secret for official use only by the Soviet government (Chanishvili, 2012). The Soviets subsequently renamed the Pasteur institute into the State Serum and Vaccine Institute, also known as the Eliava institute. It became a major facility for production of phage formulations in the Soviet Union for the duration of World War II and the Cold War. The Eliava institute continues the legacy of d'Hérelle to the present day and is currently the largest bacteriophage research center in the world (Stone, 2002; Sulakvelidze et al., 2001).

While phage therapy was slowly abandoned in the West, in the East European block, in countries like Russia, Republic of Georgia, and Poland, bacteriophage therapy has continued to develop even after the discovery of antibiotics. The phage program there has successfully developed, partially, due to economic reasons since antibiotics were not readily available in these countries. Also, huge numbers of wounded warriors from the World War II and the Russo-Finnish

War of 1939, whom required immediate interventions to prevent and treat bacterial infections, had inevitably served their role in human experimentation contributing to the success of the phage program (Summers, 2001). Russian and Polish scientists have achieved and reported significant successes with phage therapy in treating contaminated with bacteria wounds, gastrointestinal and skin infections, and even promising phage applications in patients with the bacterial sepsis and pneumonia (Alisky et al., 1998). Despite significant progress of the phage therapy in these countries, most of the experimental data and data from the clinical trials remain unknown to this day and is buried in the archives of the Russian Academy of Sciences. Most of published reports sealed in Russia or Poland during the Cold War. After the fall of the Soviet Union there have been only minor attempts to consolidate these findings in a limited number of international publications.

At the present time, countries of the East European block and former Soviet Republics continue to utilize phage therapy in their common medical practice. There are commercialized phage derived gels and polyvalent phage filtrate preparations against various Gram-positive and Gram-negative bacteria produced in Poland, the Republic of Georgia and the Russian Federation. These phage-derived therapeutics are tested for safety and sold as over the counter medicines in the local apothecaries (Bagaeva et al., 2015). Unfortunately, the wealth of research findings from these countries often lacks blinded control comparators, and therefore does not satisfy the strict requirements of the United States Department of Agriculture (USDA) or the Food and Drug Administration (FDA) for new drugs and biologicals, so the phage-derived products are limited to markets of these countries.

For the past two decades, wide spread antibiotic resistance of bacteria has revived interest in phage therapy worldwide (Domingo-Calap and Delgado-Martínez, 2018). Also, unknown to the general population and even many scientists, phage therapy was approved by FDA in the US in a

single case to intervene a lethal infection in a coma patient with a multidrug resistant strain of *Acinetobacter baumannii* (Schooley et al., 2017). The personalized phage cocktail formulation used for this experimental application has rescued mice infected with this bacteria (Regeimbal et al., 2016). Unfortunately, despite of the positive outcome and complete recovery of the patient in this case, phage therapy still remains in its infancy in the United States. Nevertheless, since the laws have been very strict against application of whole replicating organisms for human therapy, the interest has been shifted to a more manageable and marketable approach: the phage-encoded endolysins that are capable of lysing bacteria on their own.

1.2.2 Phage Endolysins and Their Role in Bacterial Lysis

Phage-encoded endolysins, or peptidoglycan (PG) hydrolases, have been researched for several decades now (Fischetti, 2008; Sheehan et al., 1997). Currently, several products that contain endolysins have completed their preclinical testing and advanced to Phase III development (Gerstmans et al., 2018). Bacteriophage endolysins have been researched on and off as a promising antibacterials against persisting pathogens for the past two decades (Borysowski et al., 2006). This interest has been recently induced by an emergence of microorganisms with a broad resistance to antibiotics (Zaman et al., 2017).

Endolysins are enzymes that are encoded by phage late genes and translated during an intracellular replication cycle. Once, synthesized at the end of phage parasitic life cycle, endolysins accumulate in the cytoplasm of the host bacteria and lyse bacterial PG. Released phage virions continue the infection cycle by infecting the next susceptible bacteria (Fischetti, 2010). While endolysins lyse bacteria from within, recombinant lysins can compromise bacterial cell wall from the outside in the absence of a bacteriophage delivery system (Loeffler et al., 2001; Royet and

Dziarski, 2007; Schuch et al., 2002; Shen et al., 2016). The lysis of bacteria from the outside is usually common to Gram-positive bacteria, since they lack outer membranes and have an exposed cross-linked peptidoglycan network susceptible to lysis with PG hydrolases. In Gram-negative cells, the outer membrane constitutes an efficient barrier that prevents lysis from without with native endolysins (Figure 1-1A) (Loessner, 2005).

Typically, endolysins from phages that infect Gram-positive bacteria utilize very similar modular design that comprises an N-terminal enzymatically active domain (EAD) fused via short linker with the divergent C-terminal cell wall binding domain (CBD). While the EAD confers catalytic activity to endolysins by cleaving covalent bonds within the PG polymer, the CBD renders specificity to bacterial species by binding conserved ligand(s) on the cell wall of susceptible bacteria (Nelson et al., 2012). Endolysins from phages infecting Gram-positive bacteria usually range in size between 25 to 40 kDa (Schmelcher et al., 2012).

According to the enzymatic activity of their modular EADs, endolysins have been classified into the six different groups (Figure 1-1B): (1) N-acetylmuramoyl-L-alanine amidase; (2) L-alanoyl-D-glutamate endopeptidase; (3) D-glutamyl-m-DAP endopeptidase (this activity has not yet been identified in a phage endolysin); (4) interpeptide bridge-specific endopeptidases such as a L-alanoyl-D-glutamate endopeptidase; (5) N-acetyl-β-D-glucosaminidase; and (6) N-acetyl-β-D-muramidase and lytic transglycosylase (Loessner, 2005; Hermoso et al., 2007).

In contrast, CBDs possess no enzymatic activity, and, rather, function as anchors that bind to conserved ligands, which are usually carbohydrate or teichoic acid molecules on the bacterial cell wall (Fischetti, 2008). The specificity of endolysins is often dictated by the binding range of their CBDs. A species-specific affinity of CBDs allows for selection of endolysins with targeted

specificity against bacterial species, strains, and even serovars (Schmelcher et al., 2010; Schmelcher and Loessner, 2014).

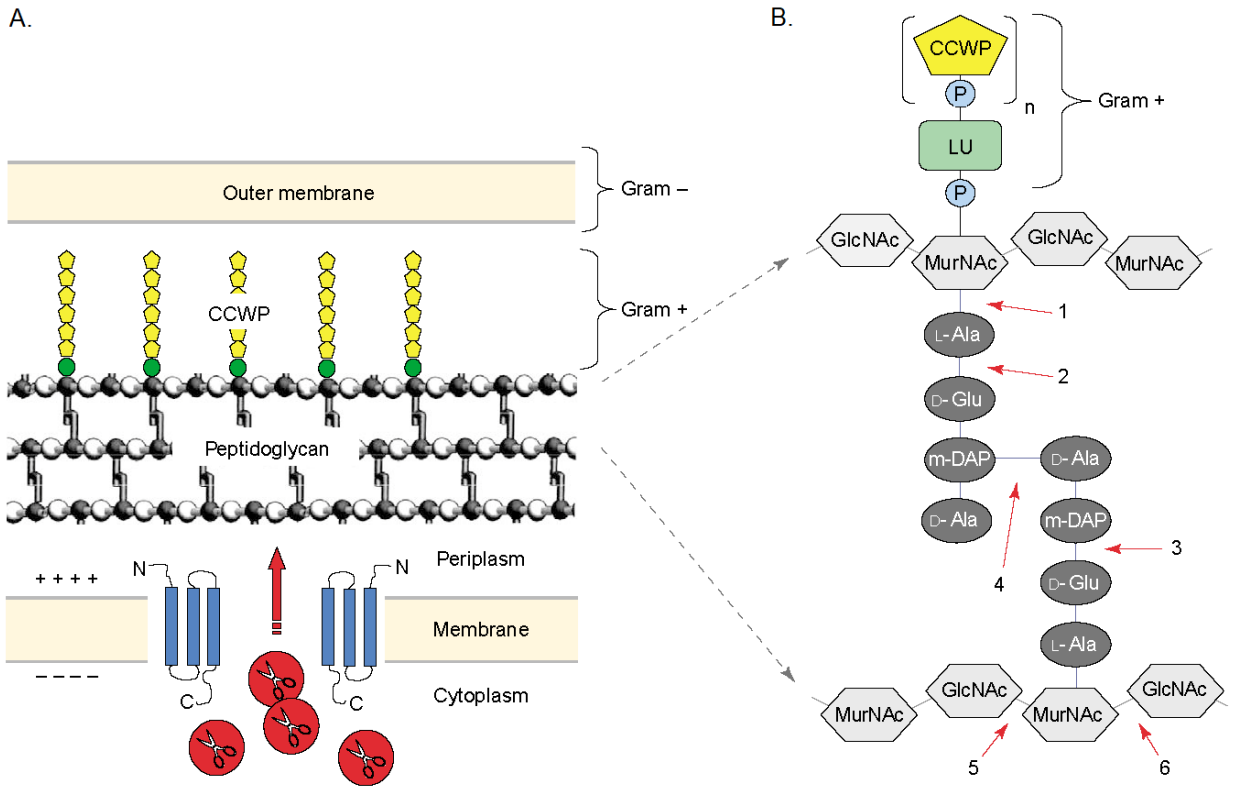

Figure 1-1. Bacterial cell wall structure and endolysin targets. (**A**) Schematic representation of the bacterial cell wall. (Blue) – Choline proteins; (Red) – Endolysins. (**B**) The structure of a type A1γ peptidoglycan is common in Gram-positive *Bacillus* and *Listeria* species and Gram-negative bacteria such as *E. coli*. The bonds cleaved by endolysins are indicated by red arrows and numbers: (1) N-acetylmuramoyl-L-alanine amidase; (2) L-alanoyl-D-glutamate endopeptidase; (3) D-glutamyl-m-DAP endopeptidase (this activity has not yet been identified in a phage endolysin); (4) interpeptide bridge-specific endopeptidases; (5) N-acetyl-β-D-glucosaminidase; and (6) N-acetyl-β-D-muramidase and lytic transglycosylase. Abbreviations: (CCWP) – carbohydrate cell wall polymer; (Glc*N*Ac) – N-acetyl glucosamine; (LU) – linkage unit; (m-DAP) – meso-diaminopimelic acid; (Mur*N*Ac) – N-acetyl-muramic acid; (P) – phosphate group. (Adopted from "Bacteriophage endolysins—current state of research and applications," by M. J. Loessner, 2005, *Current opinion in microbiology*, *8*(4), p. 481).

The structure of endolysins from phages of Gram-positive bacteria can also be comprised of multiple domains, with one or more CBDs and/or EADs combined together (Figure 1-2). This divergent structural appearance of endolysins usually tends to correlate with the bacterial host that phages have been isolated from. The majority of single EAD and CBD combinations have been identified in endolysins from the *Listeria* phages, such as PlyPSA and Ply500, and from the *Bacillus* phages (Etobayeva et al., 2018). In some cases, endolysins can have several CBDs linked together. This modular structure has been discovered in streptococcal phage endolysins, Cpl-1 and Cpl-7. A presence of two EADs has been reported in staphylococcal and streptococcal phage endolysins, LysK and B30, respectfully. Notably, the streptococcal λSA2 endolysin has two EADs uniquely positioned one at each terminus of the endolysin rather than both at the N-terminus as is observed in LysK and B30 (Schmelcher et al., 2012).

Additionally, the full-length monomeric endolysins produced from a single gene have been reported to dimerize with a truncated CBD that had been produced through an alternative translation start site within the endolysin gene. CD27L, a *Clostridium difficile*-specific endolysin, and CTP1L from a *Clostridium tyrobutyricum* phage, are both produced as a single EAD-CBD combination associated with an additional CBD that is believed to help amplify the lytic activity of these enzymes (Dunne et al., 2016). A streptococcal endolysin, PlyC, is structurally unique among endolysins, since it assembles into a multimeric complex of eight CBDs and two EADs, with the CBDs and EADs encoded by two separate genes (Nelson et al., 2006). None of the aforementioned structural modulations have been identified in *Bacillus* phage endolysins.

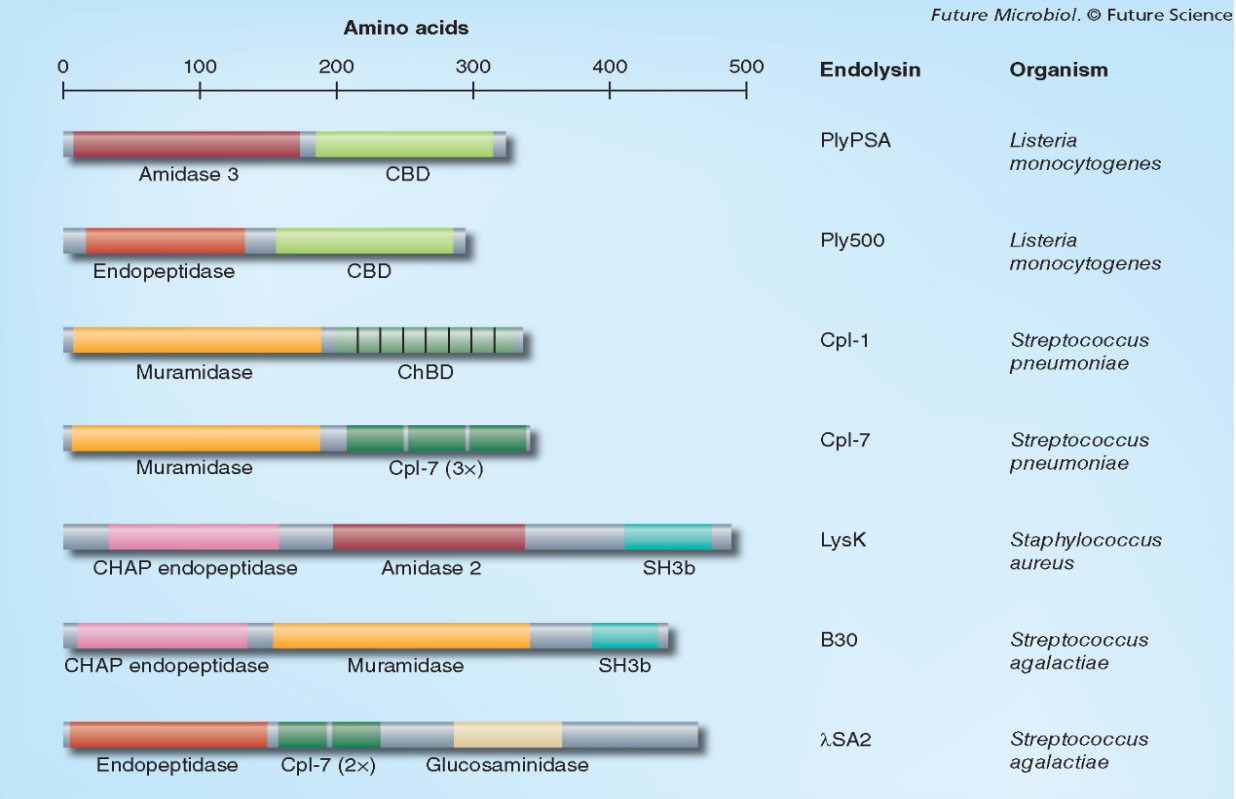

Figure 1-2. Modular architecture of selected phage endolysins. Abbreviations: (CBD) Cell wall binding domain; (ChBD) Choline binding domain; (Cpl-7) Cpl-7-like cell wall binding domain; SH3b: Bacterial Src homology 3 domain. (Adopted from "Bacteriophage endolysins as novel antimicrobials," by M. Schmelcher et al., 2012, *Future microbiology*, *7*(10), p. 1149).

1.2.3 Diversity of EAD Architectures in Endolysins from Phages Infecting *Bacillus* Species

The endolysins that have been expressed and studied are from the *Bacillus* phages specific to the *B. cereus sensu lato* group of organisms with the *B. cereus, B. anthracis* and *B. thuringiensis* being the representative species. These endolysins have a classic organization with a modular design of the single EAD-CBD combination. Furthermore, the EAD architectures from identified endolysins can be grouped into four distinct families: GH25, MurNAc_LAA, PGRP, and VanY super families (Table 1-1).

A GH25-super family EAD architecture has been discovered in *B. cereus* phage lysins PlyB (Porter et al., 2007) and Plyβ (Paskaleva et al., 2015), as well as in the *B. anthracis* phage endolysin, PlyPH (Yoong et al., 2006), and in the *B. thuringiensis* phage lysin, PlyBt33 (Yuan et al., 2012). The crystal structure of PlyB superimposed onto another GH-25 enzyme, the pneumococcal Cpl-1 endolysin (Hermoso et al., 2003), suggests it possesses muramidase lytic activity with active residues Asp_6, Asp_{90}, $Glu_{92,}$ and Asp_{171} that are strictly conserved among enzymes with GH-25 architecture. A muramidase lytic activity was experimentally determined later for PlyB and Plyβ (Paskaleva et al., 2015).

The Amidase_2 EAD architecture of the PGRP superfamily has been identified in one *B. cereus* phage endolysin, LysBPS13 (Park et al., 2012), and *B. anthracis* phage lysins, PlyG and PlyL (Kikkawa et al., 2008; Low et al., 2005; Schuch et al., 2002). In contrast, the MurNAc_LAA superfamily Amidase_3 architecture was more prevalent in EADs of the *B. cereus* phage endolysins, such as in LysPBC1 and LysPBC4 (Kong and Ryu, 2015; Na et al., 2016) although it was present in one *B. anthracis* phage lysin, AP50-31 (Park et al., 2018). Despite these two amidases had different protein folds they have shared an N-acetylmuramoyl-L-alanine amidase

lytic activity that is commonly predicted in endolysins from *Bacillus* phages (Loessner et al., 1997; Peng and Yuan, 2018).

Up to the present time only one EAD architecture of the VanY superfamily has been discovered in *B. cereus* specific phage (Son et al., 2012). LysB4, an endolysin from this phage possesses an N-alanoyl-D-glutamate peptidase activity, which is unique among *Bacillus* endolysins. In conclusion, amidase architectures have been prevalent among EAD structures of *Bacillus* phage endolysins with the N-acetylmuramoyl-L-alanine amidase lytic activity.

Table 1-1. EAD architectures identified in B*. cereus* group specific lysins.

Lysin	EAD architecture	Lytic mechanisms	Origin	Reference
AP50-31	Ami_3/MurNAc-LAA	Putative N-acetylmuramoyl-L-alanine amidase	*B. anthracis* phage AP50, 2 ORFs	(Park et al., 2018; Sozhamannan et al., 2008)
PlyG	Ami_2/PGRP	N-acetylmuramoyl-L-alanine amidase	*B. anthracis* phage γ	(Kikkawa et al., 2008; Schuch et al., 2002)
PlyL	PGRP	N-acetylmuramoyl-L-alanine amidase	*B. anthracis* Ba02-prophage γ	(Low et al., 2005)
PlyPH	GH25-PlyB-like muramidase	Muramidase	*B. anthracis* Ames prophage BA2805	(Paskaleva et al., 2015; Yoong et al., 2006)
PlyBt33	GH25 hydrolase	N-acetylmuramoyl-L-alanine amidase	*B. thuringiensis* phage BtCS33	(Yuan et al., 2012)
LysB4	Peptidaze_M15_4/ VanY	L-alanoyl-D-glutamate endopeptidase	*B. cereus* phage B4	(Son et al., 2012)
LysPBC1	Ami_3/MurNAc-LAA	Putative N-acetylmuramoyl-L-alanine amidase	*B. cereus* phage PBC1	(Kong and Ryu, 2015)
LysPBC4	Ami_3/MurNAc-LAA	Putative N-acetylmuramoyl-L-alanine amidase	*B. cereus* phage PBC4	(Na et al, 2016)
LysPBS13	Ami_2/PGRP	N-acetylmuramoyl-L-alanine amidase	*B. cereus* phage BPS13	(Park et al., 2012)
Ply12	Amidase	N-acetylmuramoyl-L-alanine amidase	*B. cereus* phage 12826	(Loessner et al., 1997)
Ply21	Amidase	N-acetylmuramoyl-L-alanine amidase	*B. cereus* phage TP21	(Loessner et al., 1997)
PlyB	GH25-like lysozyme	Putative muramidase (lysozyme)	*B. cereus* phage Bcp1	(Porter et al., 2007)
Plyβ	GH25-PlyB-like muramidase	Muramidase	*Bacillus* phage bg1	(Paskaleva et al., 2015)
PlyBa	not determined but not amidase	not identified	*B. cereus* phage Bastille	(Loessner et al., 1997)
PlyHSE3	not identified	Putative N-acetylmuramoyl-L-alanine amidase	*B. cereus* phage vB_BceM-HSE3	(Peng and Yuan, 2018)
PlyN74	Ami_2/PGRP	Putative N-acetylmuramoyl-L-alanine amidase	*B. cereus* phage Nigalana	in this work
PlyP56	Peptidaze_M15_4/ VanY	Putative L-alanoyl-D-glutamate endopeptidase	*B. cereus* phage Phrodo	in this work
PlyTB40	Ami_3/MurNAc-LAA	Putative N-acetylmuramoyl-L-alanine amidase	*B. cereus* phage Tsar Bomba	in this work

1.3 *Bacillus cereus* a Model Organism of Ubiquitous Nature

1.3.1 B. cereus a Major Food Contaminant

B. cereus is a Gram-positive facultative anaerobe that is indigenous to soil and forms drought-tolerant endospores resistant to environmental stress. *B. cereus* resides in a wide variety of environments such as soils, vegetation, natural water bodies, produce, animal feed and processed food from food processing facilities (Drobniewski, 1993; Kramer and Gilbert, 1989). The morphology of bacilli and hydrophobic nature of spores allows their adhesion to various surfaces, which can lead to formation of biofilms on vegetables (Elhariry, 2011) and industry equipment (Andersson et al., 1995). Multiple reports suggest that *B. cereus* bacilli and the spores have been isolated from different raw and processed types of foods, such as cereals and their derivatives, raw milk and pasteurized dairy products, vegetables, animal feed, different meats and processed meat products. Additionally, viable *B. cereus* spores have been isolated from dehydrated foods, dried powdered foods, and spices (Kramer and Gilbert, 1989).

B. cereus is a common foodborne pathogen. The bacilli isolated from food commonly have been associated with virulence factors (Bottone, 2010; Guinebretière et al.,2002; Stenfors Arnesen et al., 2008). Psychotropic strains of *B. cereus* isolated from ice cream have adapted to grow quickly in low temperatures and have retained their enterotoxigenic genes (Zhou et al., 2010). *B. cereus* in its spore form can survive cooking temperatures, and without sufficient cooling can germinate and secrete emetic toxin causing food poisoning. Imported cooked rice is the most common food associated with food poisoning (Drobniewski, 1993). In addition, recent studies have identified multiple pathogenic *B cereus* strains in soy beans (Yim et al., 2015). The spores of psychrotolerant *B. cereus* strains can survive and germinate in pasteurized milk into vegetative bacilli, and in the absence of competing microflora, produce emetic toxin (Andersson et al., 1995).

B. cereus produces two types of toxins, the emetic toxin, cereulide, and two 3-protein heat labile enterotoxins, the Non-hemolytic enterotoxin (Nhe) and Hemolysin BL (HBL) (Granum and Lund, 2006). Based on toxin synthesis, *B. cereus* causes two types of foodborne illnesses – emetic (vomiting) and diarrheal syndromes. An intoxication that is caused by ingestion of a cereulide is an emetic syndrome. The cereulide is a cyclic peptide toxin that is secreted in food during bacterial growth. It is highly stable and tolerant to heat, withstanding temperatures up to 121°C for 90 minutes. The cereulide is also resistant to acid peptide digestion (Drobniewski, 1993). An emetic syndrome usually has a short incubation time and fast recovery. The symptoms associated with this syndrome are nausea, vomiting and abdominal cramping (Kramer and Gilbert, 1989). The diarrheal syndrome is caused by two 3-protein heat labile enterotoxins, Nhe and HBL, which are formed in the intestine after ingestion of the organism. Symptoms are usually mild with abdominal cramps, watery diarrhea and nausea (Stenfors et al., 2008). In rare cases, both types of toxins can be produced (Montville and Matthews, 2005). Usually, these two forms of intoxications are self-limiting and last for a short period of time, so, they are rarely reported (Drobniewski, 1993). While the diarrheal type of *B. cereus* poisoning resembles foodborne illness caused by *Clostridium perfringens*, the emetic type of poisoning is similar to *Staphylococcus aureus* food poisoning, and is often linked to rice (Kramer and Gilbert, 1989).

A number of other enterotoxins are isolated from *B. cereus* strains that caused outbreaks of food poisoning, including the cytotoxin CytK (Lund et al., 2000), the enterotoxin entFM, and *B. cereus* enterotoxin T (bceT), all of which contribute to the virulence of *B. cereus* but may not play a major role in food poisoning (Choma and Granum, 2002; Luxananil et al., 2003). In addition to enterotoxin synthesis, *B. cereus* may also produce exotoxins and membrane degrading enzymes (Drobniewski, 1993).

B. cereus pathogens have been associated with non-food related illnesses, although, this occurs rarely. *B. cereus* bacilli have been found in postsurgical and traumatic wounds, and on surfaces of orthopedic implanted devices (Gallo et al., 2011). *B. cereus* can also cause opportunistic infections, especially in immunocompromised individuals, such as septicemia, catheter associated infections (Koch and Arvand, 2005), meningitis and a pneumonia strikingly resembling an inhalational anthrax (Hoffmaster et al., 2004, 2006). *B. cereus* has also been known to occasionally cause localized eye infections in humans, which can lead to permanent blindness (Drobniewski, 1993).

1.3.2 B. cereus sensu lato Group of Organisms: *B. cereus, B. anthracis,* and *B. thuringiensis*

The *B. cereus* group of species is made of ubiquitous spore-forming organisms highly abundant in soil, vegetation and natural water bodies. *Bacillus* organisms produce large vegetative bacilli that are about 3 to 5 μm in length and 1 to 1.12 μm in diameter with ellipsoidal spores that do not distend the sporangia (Kramer & Gilbert, 1989). They range in their virulence types and phenotypes from species to species, being mostly opportunistic pathogens (Stenfors Arnesen et al., 2008). From the soil, bacilli and spores easily disseminate to food and cause a range of foodborne symptoms in animals and humans. *B. cereus, B. anthracis, B. thuringiensis* are closely related species that are the representative members of this group (Aronson, 1993; Han et al., 2006).

B. cereus species have been considered an ancestral species within the *sensu lato* group (Helgason et al., 2000). All distinguishing features of the other two species, *B. anthracis* and *B. thuringiensis*, are encoded by genes located on highly mobile plasmids (Rasko et al., 2004; Thomas et al., 2000). The *B. cereus* group of organisms evokes a high degree of concern for its ability to exchange transmissible plasmids among each other. In this retrospect, *B. anthracis* have often been

described as clones of *B. cereus*, making these two species difficult to differentiate from each other (Hill et al., 2004; Keim et al., 2000). For instance, emetic *B. cereus* strains can be involved in a conjugative plasmid transfer in food between bacilli of *B. cereus* and *B. thuringiensis* (Van der Auwera et al., 2007), which imposes a threat of pathogenicity genes being transferred across these species.

B. anthracis is the etiological agent of anthrax. It is normally a disease of herbivores, but humans are also susceptible to it. Anthrax disease presents in three forms: cutaneous anthrax, gastrointestinal anthrax, and inhalational anthrax depending on the route of infection. Cutaneous anthrax is most common form of disease, historically known as "wool sorters disease", since exposure often was limited to workers at the wool sorting facilities. Gastrointestinal anthrax and inhalational anthrax are the most severe forms of anthrax caused by ingestion or inhalation of the spores by a mammalian host. The ability of *B. anthracis* spores to become airborne led to development of a bio-weapon containing anthrax spores during the Cold War. An accidental release of spores in 1979 in Sverdlovsk led to numerous deaths (Abramova et al., 1993).

The main virulence factors of *B. anthracis* are a series of toxins and a poly-D-glutamic acid capsule, which are encoded by two mobile plasmids, pXO1 and pXO2, respectively. The coding region on the pXO2 virulence plasmid for the capsule is made of the three genes *capB*, *capC,* and *capA* (Makino, et al., 1989). In the absence of capsule, the *B. anthracis* outer cell wall consists of the S-layer that overlay the PG. The S-layer is made of two proteins, the surface array protein (Sap) and the extractable antigen 1 (EA1) (Mesnage et al., 1997). The toxins are encoded by the pXO1 virulence plasmid and are composed of three main proteins, protective antigen (PA), lethal factor (LF), and edema factor (EF). A combination of PA and LF produces a lethal toxin (LT), which, when assembled together can lead to death of an infected animal. A combination of PA and

EF produces an edema toxin (ET), which produces edema in the skin (Mock and Fouet, 2001). Interestingly, these proteins are not toxic separately.

B. thuringiensis is closely related to the *B. cereus* species (Carlson et al., 1994). During sporulation, *B. thuringiensis* produces parasporal crystals made of the Crystal (Cry) proteins, also called δ-endotoxins, which are toxic to insects (Roh et al., 2007). Due to this property, *B. thuringiensis* Cry proteins are often used as biological insecticides (Ghribi et al., 2004). The Cry proteins are encoded by the *cry* genes located on a mobile plasmids similar to *B. cereus* and *B. anthracis* (Gonzalez and Carlton, 1980). Except for the presence of this plasmid, *B. thuringiensis* cannot be differentiated from *B. cereus*.

1.3.3 Emerging Antibiotic Resistance in *B. cereus* Strains

Emergence of antibiotic resistant species from the *B. cereus* group of organisms is a highly concerning (Ikeda et al., 2015). Cases of food contamination with antibiotic resistant *B. cereus* isolates have been reported worldwide (Arslan et al., 2014; Kim et al., 2015; Merzougui et al., 2014; Park et al., 2009; Yim et al., 2015). *B. cereus* is naturally resistant to β – lactam antibiotics as it produces β – lactamases unlike *B. anthracis* (Drobniewski, 1993). *B. cereus* is generally susceptible to treatment with clindamycin, vancomycin, gentamicin, chloramphenicol, and erythromycin. However, *B. cereus* species have been reported to gain resistance to some of these antibiotics. A case of reported erythromycin-resistance has been discovered in *B. cereus* isolates from ricotta processing facilities (da Silva Fernandes et al., 2014). Additionally, it was experimentally confirmed that during bacterial conjugation between *B. thuringiensis* and *B. cereus*, two related species of the *B. cereus* group of organisms, exchange of their plasmids in rice pudding and milk was about ten-fold higher than transfer of the plasmids in Luria - Bertani growth

medium (Van der Auwera et al., 2007). These facts confirm that horizontal gene transfer is possible among the *B. cereus* group of species. These findings are alarming since *B. cereus* can also harbor pathogenicity genes via plasmids, including *B. anthracis*.

B. cereus food poisoning accounts for 63,400 incidences of food poisoning in the United States, annually. This is only about 2% out of all reported food poisoning cases based on a Centers for Disease Control and Prevention (CDC) report (Scallan et al., 2011). Nevertheless, the incidences of confirmed outbreaks of foodborne illnesses caused by *B. cereus* are widely underreported in the U.S. since they are not tracked by the U.S. Foodborne Diseases Active Surveillance network (FoodNet) (CDC, 2015). Interestingly, European surveillance reports *B. cereus* food poisoning as being a major causative agent of foodborne illnesses in the Netherlands with a significant percentage of the outbreaks due to *B. cereus* contaminated rice dishes from Chinese restaurants (Tirado and Schmidt, 2001).

Contaminated foods imported from developing countries are often implicated in *B. cereus* associated food poisoning. This is concerning due to the use of antibiotics in these countries without proper prescriptions, which contributes to development of resistant bacterial species. *B. cereus* has been found in food in both its vegetative cell and endospore forms (Kramer and Gilbert, 1989). For example, a food safety study in South Korea identified 87 *B. cereus* strains in traditional Korean soy bean products that are often being marketed internationally. The study also identified 47 out of 88 food samples from Korean soy bean products positive for *B. cereus* contamination with bacterial burdens up to 10^4 colony forming units (CFU) per gram of food. Same products have been contaminated with multiple *B. cereus* species that were highly resistant to β – lactam antibiotics such as ampicillin, penicillin, cefepime, imipenem, and oxacillin. Fifteen of these strains harbored at least one enterotoxin gene, and one strain contained an emetic toxin gene (Yim

et al., 2015). Another group in Brazil discovered that in addition to β - lactamase resistance, 9.5 % of *B. cereus* isolates from a ricotta cheese production facility were resistant to erythromycin (da Silva Fernandes et al., 2014). Chinese food is also often associated with *B. cereus* mediated foodborne outbreaks (Tirado & Schmidt, 2001).

1.3.4 Architecture of Gram-Positive Bacilli: Peptidoglycan and Cell Wall-Associated Structures

The bacterial cell wall is a complex and ordered system of layers that prevents entry of foreign macromolecules into the bacterial cell. In prokaryotic organisms, Gram-positive bacteria contain two layers; a cell membrane and a peptidoglycan layer. In contrast, Gram-negative bacteria have a three layers; the internal cell membrane, a peptidoglycan layer, and outer cell membrane. In addition to serving as a barrier, the peptidoglycan layer maintains shape of the bacteria and anchors cell wall associated polymers. such as proteins (Dramsi et al., 2008) and teichoic acids (Neuhaus and Baddiley, 2003).

The peptidoglycan layer of Gram-positive bacteria provides stiffness to the bacterial cell wall. It supports the shape of bacterial cell and ensures its integrity. In general, the peptidoglycan of bacteria consists of linear glycan strands cross-linked with short peptides (Vollmer et al., 2008). These strands are made of alternating *N*–acetylglucosamine (Gln*N*Ac) and *N*–acetylmuramic acid (Mur*N*Ac) residues linked via β-(1 → 4) bonds (Figure 1-3). The D-lactoyl group of each Mur*N*Ac is substituted with a peptide stem that consists of L-Ala-γ-D-Glu-mDAP-D-Ala-D-Ala, where

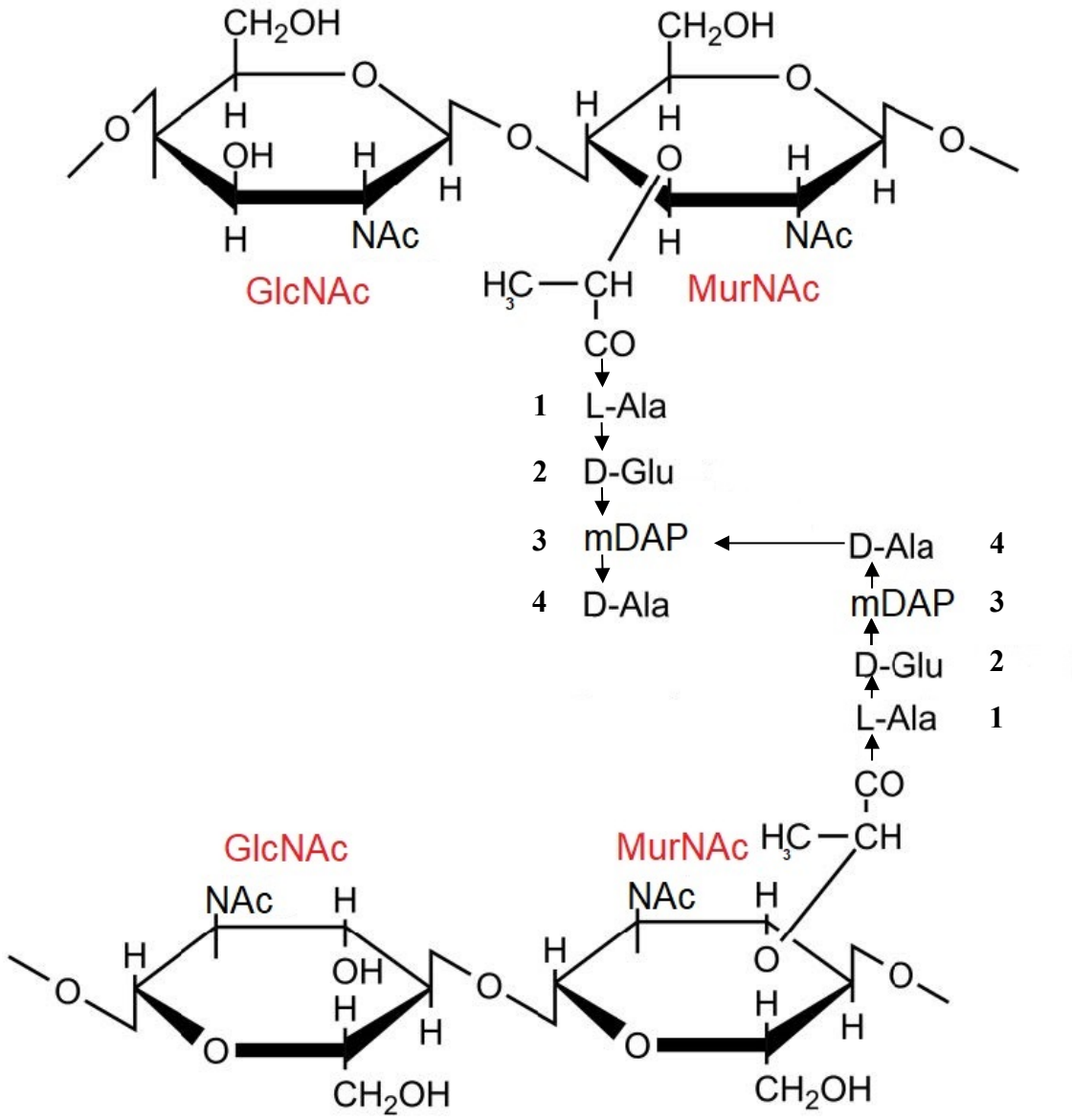

Figure 1-3. Fragment of cross-linked A1γ peptidoglycan. For simplicity of representation abbreviations indicate: (Gln*N*Ac) – *N* -Acetylglucosamine; (Mur*N*Ac) – *N* – Acetylmuramic acid; (mDAP) – meso-diaminopimelic acid; (*N*Ac) – N – acetyl group. The amino acid positions in the peptide stem: (1) L-Ala; (2) D-Glu; (3) mDAP; (4) D-Ala. The glycan strand consists of the alternating Gln*N*Ac and Mur*N*Ac residues linked by β-(1 → 4) bonds. This type of peptidoglycan structure, where mDAP and D-Ala are directly cross-linked at the position 3 – 4, is typical in *Bacillus*, *Listeria* species and Gram-negative bacteria.

mDAP is meso-diaminopimelic acid. This peptide stem represents structure of the nascent peptidoglycan. D-Ala, the last residue of the peptide stem is lost in the mature peptidoglycan. The stem peptides crosslink glycan strands, and in turn are linked to each other directly via mDAP – D-Ala residues at the position 3-4. This is an A1γ peptidoglycan typical in Gram-positive bacteria like *Bacillus* and *Listeria* species and in many Gram-negative bacteria (Vollmer et al., 2008).

Soon after the glycan strands synthesized, they are structurally modified in many bacteria. For instance, the N-deacetylation and O-acetylation contribute to bacterial resistance to lysis by lysozyme (Vollmer, 2008). Lysozyme, also known as muramidase, hydrolyses the glycan strands of peptidoglycan between the C1 of Mur*N*Ac and the C4 of Glc*N*Ac residues. N-deacetylation of Glc*N*Ac to Glc*N* (non-acetylated glucosamine) in *B. cereus* renders the organism resistant to lysis with lysozyme (Araki et al., 1971). Similarly, N-deacetylation of Mur*N*Ac to Mur*N* in the peptidoglycan of *B. anthracis* also accounts for the observed resistance to lysozyme. Lysozyme activity was restored after isolated *B. anthracis* cell walls were chemically N-acetylated by acetic anhydride (Zipperle Jr. et al., 1984). Other *Bacillus* species, including *B. anthracis*, *B. thuringiensis* and *B. subtilis* strain 168, also have deacetylated Glc*N* and Mur*N* residues in their peptidoglycan (Vollmer, 2008).

The secondary cell wall polysaccharides (SCWP) contain different compositions based on the *Bacillus* species. The SCWP of *B. anthracis* is comprised of an amino sugar backbone of →4)-β-D-Man*pN*Ac-(1→4)-β-D-Glc*pN*Ac-(1→6)-α-D-Glc*pN*Ac-(1→, where the α-Glc*N*Ac residue has been substituted with α-Gal and β-Gal at O3 and O4 positions, respectively, and the β-Glc*N*Ac substituted with α-Gal at the O3 position (Choudhury et al., 2006). A similar structure has been conserved in the pathogenic *B. cereus* strain G9241 with an additional α-Gal substitution on 50% of the β-Man*pN*Ac residues at the O3 position (Forsberg et al., 2011). Remarkably, the SCWP

from the *B. cereus* ATCC 10987 strain that are not associated with the diseases, consists of a →4)-β-D-Man*pN*Ac-(1→4)-β-D-Glc*pN*Ac-(1→6)-α-Gal*pN*Ac-(1→backbone, where the α-Gal*N*Ac is substituted at O3 with a β-Gal residue and the β-Man*N*Ac acetylated at O3 (Leoff et al., 2008). Overall, a common SCWP structure that consists of a -Man*N*Ac-Glc*N*Ac-Hex*N*Ac- backbone has been modified with the terminal galactosyl (Gal) or glucosyl (Glc) residues or non-carbohydrate substituents such as acetyl, amino or pyruvyl groups in different *Bacillus* species (Ganguly et al., 2013).

1.4 Development of Endolysins as Novel Antibacterials

1.4.1 Engineering Strategies

Chimeragenesis consisting of an interchange of the functional domains is one of the most common endolysin engineering strategies that have been utilized to create recombinant lysins targeting Gram-positive bacteria. The modular structures of Gram-positive endolysins, which are composed of EAD and CBD domains, gives rise to domain shuffling approaches to alter properties of the fusion enzyme by modifying their catalytic and binding properties. A recombination of domains from different origins can lead to chimeric endolysins with altered properties that recognize and act upon different species, which, is generally dictated by the binding specificity of their CBDs. This approach finds support in the discovery of many chimeric endolysins with a broad range of activity against different bacterial pathogens (Croux et al., 1993; Pires et al., 2016; São-José, 2018). Bioinformatic analysis suggests naturally occurring endolysins have evolved by similar recombination events and exchange of these genes between bacteriophages as well with their bacterial host (Díaz et al., 1990; Hendrix, 2002; Sheehan et al., 1996).

An evolution mutagenesis method is based on the simulation of the evolutionary processes *in-vitro* at the molecular level to obtain endolysins with desired lytic properties. A typical experiment of creating a mutant form of a lysin by this method of molecular evolution involves three steps: 1) obtaining a library of mutant DNA using random mutations or permutations that can be introduced by an *E. coli* mutator strain; 2) testing and selecting resulting mutants with desired lytic properties; 3) cloning selected variants and extracting DNA plasmid for sequencing to determine the nature and number of substitutions compared to the native lysin (Heselpoth et al., 2018).

The structure-based mutagenesis method is a rational design approach based on the analysis of the amino acid sequences and three-dimensional (3D) crystal structures of known endolysins. Appropriate amino acid substitutions are introduced into the primary sequence of the candidate lysin using a site-directed mutagenesis. These residues are identified from the microenvironment and interactions of amino acids in the know endolysin molecule, presumably, responsible for enzymatic or binding activity. If the new mutant does not have the desired lytic or binding activity, the cycle of operations is repeated again (Heselpoth et al., 2018). This approach is most commonly used for directed mutagenesis of the metal ion coordinating residues in the enzymatic pocket to enhance lytic activity of the lysin (Heselpoth et al., 2015), or enhance stability of the enzyme, or for point-mutation of residues that facilitate dimerization of the lysin.

Engineering approaches for endolysins directed toward Gram-negative bacteria differ in one important aspect. The outer membrane of these bacteria are refractory to an exogenous application of endolysins. Therefore, membrane permeabilizing peptides are usually attached to these phage endolysins. Hydrophobic, polycationic, and amphipathic peptides are effective in outer membrane penetration of different outer membrane types of the Gram-negative bacteria. A

fusion of the endolysins with these short peptides can alter the hydrophobic, amphipathic or cationic characteristics of the endolysin giving them specific membrane-destabilizing properties. The hydrophobic peptides reduce hydrophobic stacking of the outer membrane leaflet and cause outer membrane destabilization by intercalating into the lipid A acyl chain-phospholipid moieties of the outer membrane (Nikaido, 2003). For example,e the Phe-Phe-Val-Ala-Pro penta-peptide motif has hydrophobic properties and is reported to adopt a protruding β-strand conformation upon interaction with the bacterial outer membrane (Ibrahim et al., 1994). Similar to polymyxin B or poly-L-lysine, polycationic peptides induce outer membrane permeabilization by displacement of the stabilizing Ca^{2+} and Mg^{2+} ions, which causes formation of the cracks in the outer membrane (Hancock et al., 1991; Vaara and Vaara, 1981). Amphipathic peptides can likewise permeabilize both the Gram-negative outer membrane and the cytoplasmic membrane (Oren and Shai, 1998). The α4 (During et al., 1999), ArtiMW2 (Yan and Adams, 1998), Parasin1 (Park et al., 1998), and Lycotoxin1 (Adão et al., 2008) peptides are all small, linear amphipathic peptides. They share a similar α-helical structure with one side of the helix covered by positively charged residues and the opposite side by hydrophobic residues. It has been experimentally determined that the basic Lys residue at the N-terminus of Parasin1 is essential for its membrane binding activity as deletion of this residue resulted in poor membrane-binding and permeabilizing activity (Koo et al., 2008).

1.4.2 Perspectives on Endolysin-Related Applications in Medicine, Food Safety and Agriculture

The rapidly growing incidence of bacterial resistance to antibiotics has enhanced the search for alternative antibacterial agents to control these species. It is hypothesized that the co-evolution of bacteriophages and their host bacteria has led to evolution of peptidoglycan hydrolases that bind

to bacterial cell wall and hydrolyze conservative covalent bonds in the peptidoglycan (Poullain, 2007). Therefore, the probability of development of resistance in bacteria to these enzymes is very low; otherwise bacteriophages would have gradually disappeared in the course of natural selection. Similar assumptions have been confirmed by the experiments on *S. aureus* cells treated with the fusion enzyme, LysK-Lysostaphin (Donovan et al., 2009), and on bacilli of *B. anthracis* exposed to low concentrations of the PlyG endolysin (Fischetti, 2005). Even an acceleration of bacterial mutagenesis under the action of an ethyl ester of methanesulfonic acid did not lead to an appearance of strains resistant to lysis with endolysins. At the same time, an analogous procedure led to an increase in resistance of investigated bacteria to novobiocin and streptomycin by 3 - 4 log orders (Fischetti, 2010). Despite these facts, cases of bacterial resistance to non-bacteriophage encoded peptidoglycan hydrolases are known. Resistance to lysis by human lysozyme, a muramidase, can be achieved, for example, by O-acetylation or N-deacetylation of the bacterial peptidoglycan (Vollmer, 2008). A modification of hydrolysable sites in the peptidoglycan or binding sites can also lead to bacterial resistance to peptidoglycan hydrolases (Schmelcher et al., 2012), but at the moment, no cases of such occurrence have been discovered for phage endolysins.

One great advantage of peptidoglycan hydrolases is their targeted specificity to one or few bacterial species, making them very promising for medical applications. The phage endolysins work exclusively on target group of bacteria without affecting the commensal microflora (Pires et al., 2016). Such specificity is uncommon for traditional antibiotics and chemical antiseptics. However, systemic application of endolysins carries the risk of releasing peptidoglycan fragments of disrupted bacterial cell walls into the blood stream. Fragmented peptidoglycan primes the host immune pro-inflammatory response and cytokine release by immunocompetent cells as shown by the example of an intravenous administration of pneumococcal phage lysin, Cpl-1 (Fischetti,

2010). Cpl-1 caused an increase in the concentration of pro-inflammatory cytokines in mice (Entenza et al., 2005). However, the levels of the cytokine release can be modulated to acceptable levels with the titration of endolysins to find an effective therapeutic dose. It was experimentally proven that a streptococcal lysin, PlyC, at varying doses up to 50 μg/mL was not toxic to the bovine blood polymorphonuclear leukocytes (Scholte et al., 2018). Additionally, domain engineering can modulate enzymatic activity and/or specificity of lysins, which was found quite effective in achieving desired enzymatic properties for selected endolysins (Croux et al., 1993; Gerstmans et al., 2018). Recent advancements in endolysins research and announcements that several products based on phage-derived endolysins are being advanced to the Phase III clinical trials shows that phage endolysins can be developed into the antibacterial products and further commercialized (Gerstmans et al., 2018).

Application of endolysins in the food industry and agriculture has received a lot of attention and has been documented in multiple publications (Callewaert et al., 2011). The specificity of endolysins to peptidoglycan substrates and bacteriophages to their bacterial host provide various potential opportunities for their application, from detection of microorganisms in food to controlling bacterial populations in raw food and preserves. As a rule, the specificity of bacteriophages to bacteria is much more limited than that of their endolysins, which typically have a broader host range (Nelson et al., 2012). One notable exception is some *Listeria* endolysins, which have been described to have serovar specificity (Schmelcher and Loessner, 2014). Lytic enzyme of the *Clostridium* phage CTP1 has inhibited growth of *Clostridium tyrobutyricum* in developing cheese without affecting the microorganisms that ensure product maturation (Mayer et al., 2010). Similar antibacterial effects have been reported for application of endolysins in dairy products (Callewaert et al., 2011). Nevertheless, more broadly specific phage endolysins can be

used to control populations of microorganisms in food. Such endolysins in purified form can be utilized to extend food shelf life, while the others with narrow specificity would be indispensable to control growth of specific bacterial species, such as psychrotolerant *L. monocytogenes* or *C. tyrobutyricum.*

In addition to applications in food, endolysins can be used in agriculture to control infections with pathogenic bacteria in livestock. In fact, the *S. aureus*-derived peptidoglycan hydrolase, lysostaphin, has proven to be quite effective against staphylococcal infections that cause mastitis in cows. This is the first recombinant enzyme used for treatment and prevention of mastitis, an inflammation of the mammary glands in cows, which has accounted for huge loses in the dairy industry (Oldham and Daley, 1991). The recombinant PlyC lysin is a phage-encoded lysin that currently has been researched for its potential to treat mastitis caused by streptococcal species (Scholte et al., 2018), and as disinfectant for equipment and various working surfaces in stables to prevent contamination by *S. equi*, a pathogen that can cause suffocation of horses (Hoopes et al., 2009).

In conclusion, over the past 10 years, a number of publications describing isolation and characterization of new endolysins has increased exponentially. Positive changes pertaining use of the phage-encoded endolysins in medicine, agriculture and, in particular, the food industry should be expected soon based on a decision of the U. S. Food and Drug Administration to allow application of the *Listeria* bacteriophages in certain foods (Schmelcher et al., 2012).

2 Discovery and Biochemical Characterization of PlyP56, PlyN74, and PlyTB40 – *Bacillus* Specific Endolysins

This chapter, in part, is published as:

Etobayeva, I., Linden, S.B, Alem, F., Harb, L., Mosier, P.D., Johnson, A.A., Temple, L., Hakami, R.M and Neslon, D.C. (2018). Disovery and biochecmical characterization of plyP56, PlyN74, and PlyTB40 – *Bacillus* specific endolysins. *Viruses, 10*(5), p.276.

Abstract

Three *Bacillus* bacteriophage-derived endolysins, designated PlyP56, PlyN74, and PlyTB40, were identified, cloned, purified, and characterized for their antimicrobial properties. Sequence alignment revealed these endolysins have an N-terminal enzymatically active domain (EAD) linked to a C-terminal cell wall binding domain (CBD). PlyP56 has a Peptidase_M15_4/VanY superfamily EAD with a conserved metal binding motif and displays biological dependence on divalent ions for activity. In contrast, PlyN74 and PlyTB40 have T7 lysozyme-type Amidase_2 and carboxypeptidase T-type Amidase_3 EADs, respectively, which are members of the MurNAc-LAA superfamily, but are not homologs and thus do not have a shared protein fold. All three endolysins contain similar SH3-family CBDs. Although minor host range differences were noted, all three endolysins show relatively broad antimicrobial activity against members of the *Bacillus cereus sensu lato* group with the highest lytic activity against *B. cereus* ATCC 4342. Characterization studies determined the optimal lytic activity for these enzymes was at physiological pH (pH 7.0–8.0), over a broad temperature range (4–55^{o}C), and at low concentrations of NaCl (<50 mM). Direct comparison of lytic activity shows the PlyP56 enzyme to be twice as effective at lysing the cell wall peptidoglycan as PlyN74 or PlyTB40, suggesting PlyP56 is a good candidate for further antimicrobial development as well as bioengineering studies.

2.1 Introduction

The *Bacillus* genus consists of a diverse collection of aerobic organisms that are common residents of the soil and occasionally become opportunistic pathogens of humans. *Bacillus* species are Gram-positive, rod-shaped bacilli that also form endospores, which allow their survival under adverse environmental conditions. Once these conditions are resolved, endospores germinate into vegetative bacilli to continue their life cycle. From the soil, vegetative bacilli or endospores can be transmitted to humans or animals via contaminated water and produce. Resistant to irradiation, endospores allow the bacteria to remain dormant for long periods of time on surfaces in food-processing facilities, making it virtually impossible to eliminate pathogenic bacilli from the environment (Leggett et al., 2012).

Although the majority of bacilli are relatively harmless to humans and animals (Ceuppens et al., 2013), genetically related species of the *B. cereus sensu lato* group are capable of causing clinical disease and toxin-mediated food poisoning. Among these species, the most phenotypically related are *B. cereus*, *B. anthracis*, and *B. thuringiensis* (Okinaka and Keim, 2016). B. cereus is capable of producing both emetic and diarrheal toxins. These species are opportunistic pathogens and widespread food contaminants highly resilient to pasteurization efforts (Leggett et al., 2015). In addition to causing gastrointestinal conditions, *B. cereus* species are also capable of causing ocular infections (Gherardi, 2016) and catheter-associated blood stream infections (Kutsuna et al., 2017). *B. anthracis* is an obligate pathogen and the etiologic agent of anthrax. While this organism generally is restricted to grazing animals, systemic anthrax has a high fatality rate in humans due to secretion of a three-protein toxin. While *B. cereus* and *B. anthracis* are known for causing disease and food poisoning in humans and animals, *B. thuringiensis* is an insect pathogen and its parasporal crystal proteins are used as an insecticide (Aronson, 1993). Otherwise, the three

members of the *B. cereus sensu lato* group have very little differences in their genomes and often share the same plasmid-associated pathogenicity genes, which make it difficult to differentiate the species from one another (Hoffmaster et al., 2006).

A growing number of reports about multidrug resistant *B. cereus* isolates in food have been reported worldwide (Khasnabis et al., 2017; Kim et al., 2015; Merzougui et al., 2014), which has prompted a search for an alternative to conventional antibiotics. Bacteriophage-encoded endolysins have been researched as one such alternative (Fischetti, 2005; Loessner, 2005). Endolysins are enzymes encoded by the late genes during a bacteriophage replication cycle. Once synthesized, endolysins target evolutionarily conserved covalent bonds within the bacterial peptidoglycan, lysing host bacteria from the inside to allow bacteriophage progeny release into the extracellular environment (Fischetti, 2010). Significantly, endolysins applied extrinsically also can compromise the peptidoglycan integrity in the absence of a bacteriophage delivery system (Loeffler et al., 2001; Royet and Dziarski, 2007; Schuch et al., 2002; Shen et al., 2016).

Typically, endolysins derived from bacteriophage that infect Gram-positive hosts consist of two domains: a conserved N-terminal EAD fused via a short linker sequence to a C-terminal CBD (Nelson et al., 2012b). Based on the cleavage sites of one of the major covalent bonds within the bacterial peptidoglycan polymer, EADs are divided into five conserved classes: muramidases, glucosaminidases, endopeptidases, L-alanine amidases, and lytic transglycosylases. In contrast, CBDs are diverse in sequence and confer targeted specificity to a bacterial species or strain by binding a conserved carbohydrate moiety on the bacterial cell surface (Schuch et al., 2013).

In this study, I identified and characterized three novel *B. cereus* endolysins, PlyP56, PlyN74, and PlyTB40, each with different EADs but homologous CBDs. I found that these endolysins were highly active against *B. cereus* species, with lesser activity against other Bacillus

species. Based on characterization of its biochemical properties and specificity, PlyP56 is a more effective endolysins compared to PlyN74 and PlyTB40, but all three are amenable to further bioengineering studies.

2.2 Materials and Methods

2.2.1 Bacteriophage Sequence Analysis

Forty-six sequenced *Bacillus*-specific bacteriophage genomes contained in the *Bacillus* Phage Database (bacillus.phagesdb.org) and GenBank were screened for putative endolysins. Each bacteriophage open reading frame (ORF) was searched with the BLASTN, BLASTP, Pfam, and CDD databases. Six published endolysin sequences (LysB4, Ply500, PlyL, PlyPSA, LysBPS13, and phi29) were added for comparison (Korndörfer et al., 2006, 2008; Low et al., 2005; Park et al., 2012; Saedi et al., 1987; Son et al., 2012). Phylogenetic trees were drawn using MEGA7 (Kumar et al., 2016) to determine phylogenetic position of ORFs among *Bacillus* species-specific bacteriophages using the Maximum Likelihood method based on the JTT matrix-based model (Jones et al., 1992). The percentage of trees in which the associated taxa clustered together is shown next to the branches. Initial tree(s) for the heuristic search were obtained automatically by applying Neighbor-Join and BioNJ algorithms to a matrix of pairwise distances estimated using a JTT model, and then selecting the topology with superior log likelihood value.

Genes encoding the *B. cereus* group-specific endolysins Phrodo ORF_56 (AMW62097.1), which was named PlyP56, Nigalana ORF_74 (AMW61226.1) named PlyN74, and TsarBomba ORF_40 (ALA13156.1) named PlyTB40, were selected for expression in *Escherichia coli*.

2.2.2 Bacterial Strains and Growth Conditions

Bacillus strains used in this study are described in Table 2-1. Unless otherwise described, bacterial strains were purchased from the American Type Culture Collection (ATCC). *B. anthracis* strains (both BSL2 and BSL3) were procured from the Biodefense and Emerging Infections Research Resources (BEI Resources). All BSL-3 work was performed according to the established and CDC-approved Standard Operating Procedures/Protocols (SOPs) at the BSL3 containment facility of George Mason University. All standard safety precautions were strictly followed for conduct of the studies, including use of protective personnel equipment and other personal sterile practices specifically designed for safe conduct of BSL3 work. The containment facilities at George Mason University are registered with the CDC to allow possession, use, and transfer of select agents (including *B. anthracis*) and toxins according to specified guidelines. All *Bacillus* strains were propagated in Brain Heart Infusion (BHI) plates or BHI broth at 37ºC and shaken at 200 rpm. DH5α competent and BL21 (DE3) competent *Escherichia coli* strains were used for cloning and protein expression. *E. coli* strains were propagated overnight at 37ºC and shaken at 220 rpm unless otherwise stated. *E. coli* strains were cultured in Luria–Bertani (LB) broth (BD Biosciences, Franklin Lakes, NJ, USA), and/or on LB plates supplemented with 100 µg/mL ampicillin. All chemicals and culture media were acquired from Sigma (St. Louis, MO, USA) unless otherwise stated.

Table 2-1. Relative lytic activity of *Bacillus* bacteriophage endolysins.

Bacterial species	Strains[1]	Bacteriophage Endolysins[2] PlyP56	PlyN74	PlyTB40
B. cereus	**ATCC 4342**	84.9 ± 6.0	69.2 ± 9.8	71.9 ± 12.9
B. cereus	**ATCC 14579**	73.4 ± 1.3	59.7 ± 7.2	40.9 ± 20.5
B. cereus	**ATCC 11778**	79.6 ± 4.4	60.6 ± 4.4	58.2 ± 13.2
B. cereus	**ATCC 13061**	45.8 ± 2.4	37.9 ± 3.8	24.0 ± 8.1
B. thuringiensis	**ATCC 10792**	38.7 ± 5.2	35.8 ± 9.1	25.6 ± 6.6
B. amyloliquefaciens	ATCC 23842	36.5 ± 20.5	23.9 ± 13.8	6.2 ± 2.4
B. circulans	ATCC 4513	53.2 ± 3.2	17.2 ± 5.1	5.5 ± 5.1
B. coagulans	ATCC 7050	8.0 ± 1.7	5.7 ± 7.9	4.6 ± 4.5
B. licheniformis	ATCC 14580	4.6 ± 6.4	30.2 ± 3.6	9.6 ± 3.7
B. megaterium	ATCC 14581	83.9 ± 12.3	30.2 ± 15.5	9.6 ± 1.6
B. pumilus	BJ0050	58.8 ± 15.2	46.1 ± 11.1	32.6 ± 14.4
B. pumilus	ATCC 700814	16.7 ± 18.4	10.9 ± 12.5	2.6 ± 4.3
B. subtilis	ATCC 6051	3.5 ± 1.9	1.4 ± 0.5	0.1 ± 0.2
B. subtilis	ATCC 33608	2.9 ± 2.3	1.6 ± 2.7	0.6 ± 0.8
Lysinb. sphaericus	ATCC 4525	36.9 ± 19.8	18.9 ± 9.4	10.8 ± 3.4
Paenib. polymyxa	ATCC 7070	6.0 ± 4.7	3.7 ± 4.3	3.1 ± 1.5

[1] See Methods for source of species and strains. Strains in bold belong to the *B. cereus sensu lato* group. [2] Activity of endolysins was evaluated via turbidity reduction assay. Values reported are the percent decrease in absorbance (OD600) of cells treated with endolysins normalized to values of untreated cells after 20 min incubation with 100 μg/mL of each endolysin. The starting absorbance of mid-log cells was adjusted to an OD600 of 1.0. Values represent mean values from three independent experiments, run in triplicate.

2.2.3 Cloning of Vector Constructs

Endolysin-encoding genes, *plyP56*, *plyN74*, and *plyTB40*, were codon-optimized for expression in *E. coli* and chemically synthesized by Thermo Fisher (Waltham, MA, USA) in a pMA_T vector. The constructs with EcoRI and XbaI restriction sites and a C-terminal hexahistidine tag (6xHis tag) were subcloned into an arabinose-inducible pBAD24 expression vector, sequenced (Macrogen, Seoul, South Korea) to confirm identity, and eventually transformed into BL21 (DE3) competent *E. coli*. Ampicillin resistant colonies were expanded and once again retested by sequencing. The ApE-A plasmid editor (version number 2.0.47, University of Utah, Salt Lake City, UT, USA) was utilized for DNA sequence manipulations and analysis. Alternatively, the CBDs for each endolysin, corresponding to residues 174–259 for PlyP56, 190–275 for PlyN74, and residues 191–272 for PlyTB40, were cloned identically to the procedures described above for the full-length enzymes, with the exception that the 6xHis tag was placed on the N-terminus for the CBD constructs. Primers for these constructs are contained in Table 2-2.

2.2.4 Recombinant Protein Expression

Overnight cultures of E. coli strain BL21 (DE3) transformed with pBAD24 vectors containing *plyP56*, *plyN74*, or *plyTB40* genes, or their corresponding CBDs, were diluted 1:100 (v/v) with sterile LB broth supplemented with ampicillin (100 μg/mL) and shaken at 220 rpm and 37ºC for approximately 3 h. Once the optical density (OD600) reached 0.8, protein expression was induced with L-arabinose (0.25%). E coli cultures were returned to the shaker which was set at 180 rpm and 18ºC for overnight protein expression (~16 h). The following morning, bacterial cells were pelleted by centrifugation at 5000 rpm for 10 min at 4ºC. The supernatant was discarded and cell pellets were subjected to protein purification.

Table 2-2. Primers for CBD amplification.

Template	Primer	Sequence (5' → 3')*
pBAD24::*plyP56*	IR29-F'	CGTGAATTCATGCATCATCATCATCATCATGATTATGATAGCAGCTGG
	IR30-R'	CGTTCTAGATTATTTAAACGTGCCCCAATA
pBAD24::*plyN74*	IR33-F'	CGTGAATTCATGCATCATCATCATCATCATGATTATGATAGCAGCTGGTTTACC
	IR34-R'	CGTTCTAGATTATTTAAAGGTGCCCCAATAATTCAC
pBAD24::*plyTB40*	IR37-F'	CGTGAATTCATGCATCATCATCATCATCATTATGATAGCAGCTGGTTTACACCG
	IR38-R'	CGTTCTAGATTACTGAAAGGTGCCCCAATAGCTAAT

* Restriction sites underlined

2.2.5 Recombinant Protein Purification

The cell pellets were frozen at –80ºC for 15–20 min before sonication. Frozen pellets were thawed in lysis buffer (phosphate buffered saline supplemented with 10 mM imidazole, 1 mM phenylmethylsulfonyl fluoride (PMSF), pH 7.4) with 185 rpm shaking on an orbital shaker until the pellet dissolved completely. The resulting solution was sonicated (duty cycle 30, output control 6) for 14 min to lyse cells. After sonication, cell debris was removed by centrifugation at 12,000 rpm for 45 min at 4ºC. The supernatant containing soluble protein was filtered with a 0.45 mm filter (Whatman, Maidstone, UK) and recombinant proteins were applied to Mini Profinity™ IMAC Cartridges (Bio-Rad, Hercules, CA, USA) and eluted in 10 mL fractions of 20, 50, 100, 250, and 500 mM imidazole. Proteins were analyzed by SDS-polyacrylamide gel electrophoresis (SDS-PAGE) for purity. Fractions containing homologous recombinant proteins were pooled and dialyzed overnight against PBS (pH 7.4) supplemented with 300 mM NaCl. Protein concentrations were determined by the Bradford assay following manufacturer's instructions (Bio-Rad). Purified proteins were stored at –80ºC in PBS (pH 7.4) supplemented with 15% glycerol.

2.2.6 Turbidity Reduction Assay

Bacteriolytic activity of endolysins was measured via the turbidity reduction assay as described (Nelson et al., 2012). The assay was performed in a standard 96-well titration plate (ThermoFisher Scientific) with an overnight bacterial culture of indicator strain, *B. cereus* ATCC 4342, for all dose range and biochemical characterization studies. For all host range studies, a 4-h culture of mid-log bacteria was used. A change in OD600 was measured every 15 s over the duration of the assay (20 min) on a SpectraMax 190 spectrophotometer (Molecular Devices, San Jose, CA, USA). Briefly, bacterial cells were pelleted at 5000 rpm for 10 min at 4ºC and

resuspended in sterile PBS. A 100 µL volume of cell suspension was added to each well containing 100 µL of each endolysin at a predetermined concentration range such that the starting OD600 was equal to 1.0. Wells with a mixture of only bacteria in PBS served as a negative control and established a settling baseline that was subtracted from the experimental data. Bacteriolysis was quantified as the percentage of activity relative to the lytic activity of 100 µg/mL PlyP56 on *B. cereus* ATCC 4342, which represented 100% activity for all dose range

analysis, and at 50 µg/mL of PlyP56 (100% activity), for all biochemical characterization studies. All experiments were performed in triplicate on three consecutive days.

2.2.7 Plate Lysis (Spot) Assay

In addition to the turbidity reduction assays, *B. cereus* ATCC 4342 and *B. anthracis* strains were assayed via plate lysis assay. Briefly, bacterial cells were harvested and pelleted at their mid-log phase (4-h cultures). Pellets were then washed twice in PBS, resuspended in 12 mL of 0.7% semisolid agar cooled to 50ºC, poured onto square 10-cm petri dishes, and gently tilted to cover the bottom of the dish. Endolysins were serial diluted 10-fold in PBS to make the concentrations 1 mg/mL, 0.1 mg/mL, and 0.01 mg/mL. Spots (10 µL) were made across a row for 10 µg, 1 µg, 0.1 µg endolysin, and PBS with no endolysin served as a buffer control. Plates were dried in a biosafety hood for 15–20 min and incubated face up at 37ºC for 2 h. Clearing zones were assessed at 1 h and 2 h post-spotting.

2.2.8 Characterization of PlyP56, PlyN74, and PlyTB40

The turbidity reduction assays on overnight cultures described above were used to determine optimal lytic conditions. For dose–response studies, endolysins were serially diluted

beginning with a starting concentration of 100 µg/mL. To evaluate enzymatic activity over a pH range of 3.0 to 11.0, bacterial cells were diluted in equal volumes of universal pH buffer (40 mM boric acid and 40 mM phosphoric acid (BP) buffer adjusted to the desired pH with NaOH), and were challenged against each endolysin at a final concentration of 50 µg/mL. The influence of NaCl on lytic activity of endolysins at 50 µg/mL was tested in BP buffer at pH 7.4 supplemented with increasing concentrations of NaCl (0–500 mM). Kinetic stability of endolysins was evaluated as described (Son et al., 2012) with minor modifications. Briefly, endolysins were incubated at indicated temperatures (4ºC, 25ºC, 37ºC, 45ºC, 55ºC, or 60ºC) for 30 min, recovered on ice for 5 min, and subjected to the turbidity reduction assay at previously determined optimal conditions (pH, NaCl) for each endolysin. To evaluate the role of divalent cations in catalytic function, endolysins were dialyzed overnight at 4ºC in Tris-EDTA buffer (20 mM Tris, 20 mM NaCl, 5 mM EDTA, pH 7.4) to remove any residual metal ions. Subsequently, one half of the EDTA-treated endolysins was stored overnight at 4ºC and the second half was dialyzed overnight in Tris-buffered saline (TBS) (pH 7.4) supplemented with 6 mM $CaCl_2$ or 6 mM $MgCl_2$. Lysis of *B. cereus* ATCC 4342 was assayed via turbidity assay and untreated endolysins served as a control.

2.2.9 Spectrum of Lytic Activity

The host range of the endolysins was accessed via turbidity reduction assay. Overnight cultures of all bacilli were diluted 1:100 and incubated an additional 4 h in fresh media. Cultures were then exposed to each endolysin at a concentration of 100 µg/mL in the 96-well plate and lytic activities were represented as the percentage of lysis relative to 100% activity of each endolysin against the *B. cereus* ATCC 4342 indicator strain after 20 min incubation. Alternatively, the plate lysis assay described above was used to determine the host range against several *B. anthracis*

strains, where +, ++, and +++ indicates an observed clearing zone for 10 µg, 1 µg, and 0.1 µg, respectively, of each endolysin.

2.2.10 Fluorescent Labeling of CBDs

Purified CBDs were chemically crosslinked to an amine-reactive AlexaFluor® 555 fluorescent dye (Thermo Fisher Scientific) according to the manufacturer's instructions with minor modifications. Briefly, 0.5 mL of CBD (2.0 mg/mL) was mixed with 50 µL of 1 M sodium bicarbonate and 100 µL of the AlexaFluor® 555 dye (2.0 mg/mL in DMSO). The reaction mixture was incubated at room temperature for 1 h with constant stirring. Unreacted dye was removed by application to a PD-10 desalting column (GE Healthcare, Cincinnati, OH, USA). The fractions with labeled CBDs were collected and stored at 4ºC for future use to visualize binding.

2.2.11 CBD-Binding Assay

Overnight cultures of bacilli were pelleted at 5000 rpm for 10 min at 4ºC, resuspended in sterile PBS, and washed a second time. Cell suspension aliquots (100 µL) were mixed with 10 µL of each labeled CBDs in separate reactions, and incubated on ice for 10 min. The reaction in absence of fluorescent dye served as a control. After incubation, labeled bacterial cells were pelleted and washed with ice-cold PBS and diluted to 100 µL again. An aliquot (~1 µL) of this mixture was applied to a glass slide, sealed with a glass coverslip, visualized with an Eclipse 80i epifluorescent microscope (Nikon, Tokyo, Japan), and NIS-Elements software (version number 3.22.15, Nikon) was used for image analysis.

2.2.12 Structural Modeling of Bacillus Bacteriophage Endolysin EADs

The amino acid sequences of PlyP56, PlyN74, and PlyTB40 were submitted to the HHPred server (Soding et al., 2005) to identify appropriate homology modeling templates of known structures. The phylogenetically closest structurally characterized homolog in the RCSB Protein Data Bank (PDB) (Berman et al., 2000) was identified and selected from the resulting HHPred hit list for each endolysin EAD based on maximal percent identity. For PlyP56, the L-alanoyl-D-glutamate peptidase from *Listeria monocytogenes* bacteriophage A500, known as Ply500 (Korndörfer et al., 2008), was selected (PDB ID: 2VO9; 1.8 Å resolution) with 70% identity (E-value = 2×10^{-75}). For PlyN74, the N-acetylmuramoyl-L-alanine amidase from *B. anthracis* ϡ prophage Ba02, known as PlyL (Low et al., 2005b), was selected (PDB ID: 1YB0; 1.86 Å resolution) with 53% identity (E-value = 7×10^{-49}). For PlyTB40, another N-acetylmuramoyl-L-alanine amidase with a different fold was selected (PDB ID: 1XOV; 1.8 Å resolution) from *L. monocytogenes* bacteriophage PSA, known as PlyPSA (Korndörfer et al., 2006), with 37% identity (E-value = 3×10^{-25}). The template and target amino acid sequences for each EAD were subsequently aligned with Clustal X 2.1 (Larkin et al., 2007) using the default parameters. From each alignment (see Figures 2-1, 2-2, and 2-3), a percent identity (%I = number of identical alignment positions/total number of alignment positions) and percent similarity (%S = [number of identical alignment positions + number of 'strong similarity' alignment positions]/total number of alignment positions) was calculated (PlyN74–1YB0: %I = 51.3, %S = 64.1; PlyP56–2VO9: %I = 70.1, %S = 81.6; PlyTB40–1XOV: %I = 36.3, %S = 53.2). Gaps (i.e., insertions and deletions) were included in the total number of alignment positions. Using the sequence alignments from Clustal X and the template structures from the PDB, the automodel function of MODELLER 9.16 (Fiser et al., 2000; Sali and Blundell, 1993) was used to generate a population of 100 homology

models for each EAD. The model with the lowest Discrete Optimized Protein Energy (DOPE) (Shen and Sali, 2006) score from each population was selected for further analysis (PlyN74: DOPE = -16,088; PlyP56: DOPE = -15,027; PlyTB40: DOPE = -16,997). The selected EAD models were postprocessed and visualized with SYBYL-X 2.1.1 (Certara USA, Inc., Princeton, NJ, USA). The models were subjected to a short energy-minimization (Tripos Force Field, Gasteiger – Hückel charges, distance-dependent dielectric constant = 4.0 D/Å, termination criteria: energy gradient cutoff = 0.05 kcal (mol × Å)-1 or 200 iterations) followed by generation of Connolly surfaces, onto which the electrostatic potential was mapped. The stereochemical quality of the final models and their corresponding PDB templates were assessed using PROCHECK (Laskowski et al., 1993). In each of the generated endolysin EAD models, >90% of the residues were located in the most favored regions, indicating good quality models.

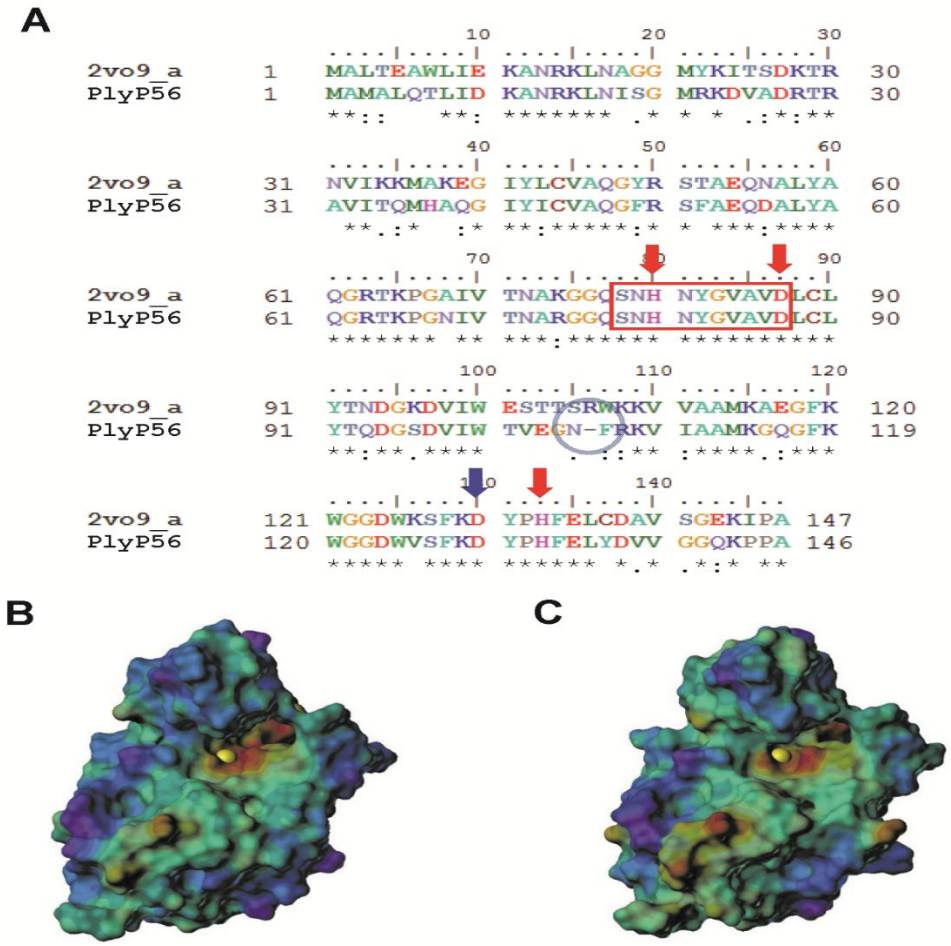

Figure 2-1. PlyP56 alignment with structural homolog Ply500. (A) Sequence alignment of *L. monocytogenes* phage A500 (Ply500) from PDB entry 2VO9 and PlyP56 EADs (Clustal X alignment symbols: asterisk = identical; colon = strongly similar; period = weakly similar; space = not similar). Overall percent identity (# identical / # total) = 70.1%; percent similarity [(# identical + # strongly similar) / # total] = 81.6%. Arrows indicate the metal-binding residues (red) and the catalytic base/acid (blue). The conserved SxHxxGxAxD zinc-binding motif is highlighted with a red rectangle. Colored ovals represent sequence insertions or deletions; see Fig. 5. **(B–C)** Connolly surfaces color-coded by electrostatic potential (blue = most positive; red = most negative) for the template Ply500 **(B)** and the modeled PlyP56 **(C)** EAD; a yellow sphere represents the Zn^{2+} ion.

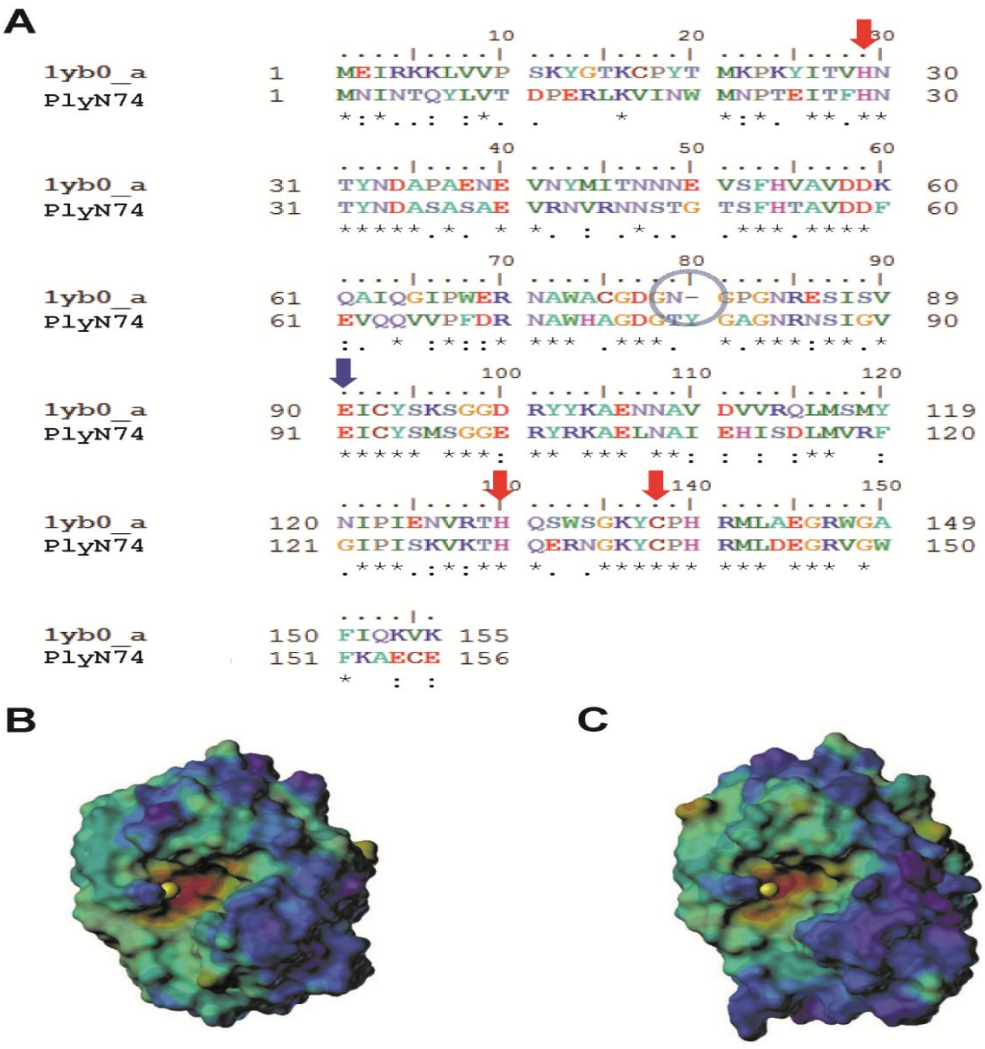

Figure 2-2. PlyN74 alignment with structural homolog PlyL. (A) Sequence alignment of *B. anthracis* λ prophage Ba02 (PlyL) from PDB entry 1YB0 and PlyN74 EADs (Clustal X alignment symbols: asterisk = identical; colon = strongly similar; period = weakly similar; space = not similar). Overall percent identity (# identical / # total) = 51.3%; percent similarity [(# identical + # strongly similar) / # total] = 64.1%. Arrows indicate the metal-binding residues (red) and the catalytic base/acid (blue). Colored ovals represent sequence insertions or deletions; see Fig. 5. **(B–C)** Connolly surfaces color-coded by electrostatic potential (blue = most positive; red = most negative) for the template PlyL **(B)** and the modeled PlyN74 **(C)** EAD; a yellow sphere represents the Zn^{2+} ion.

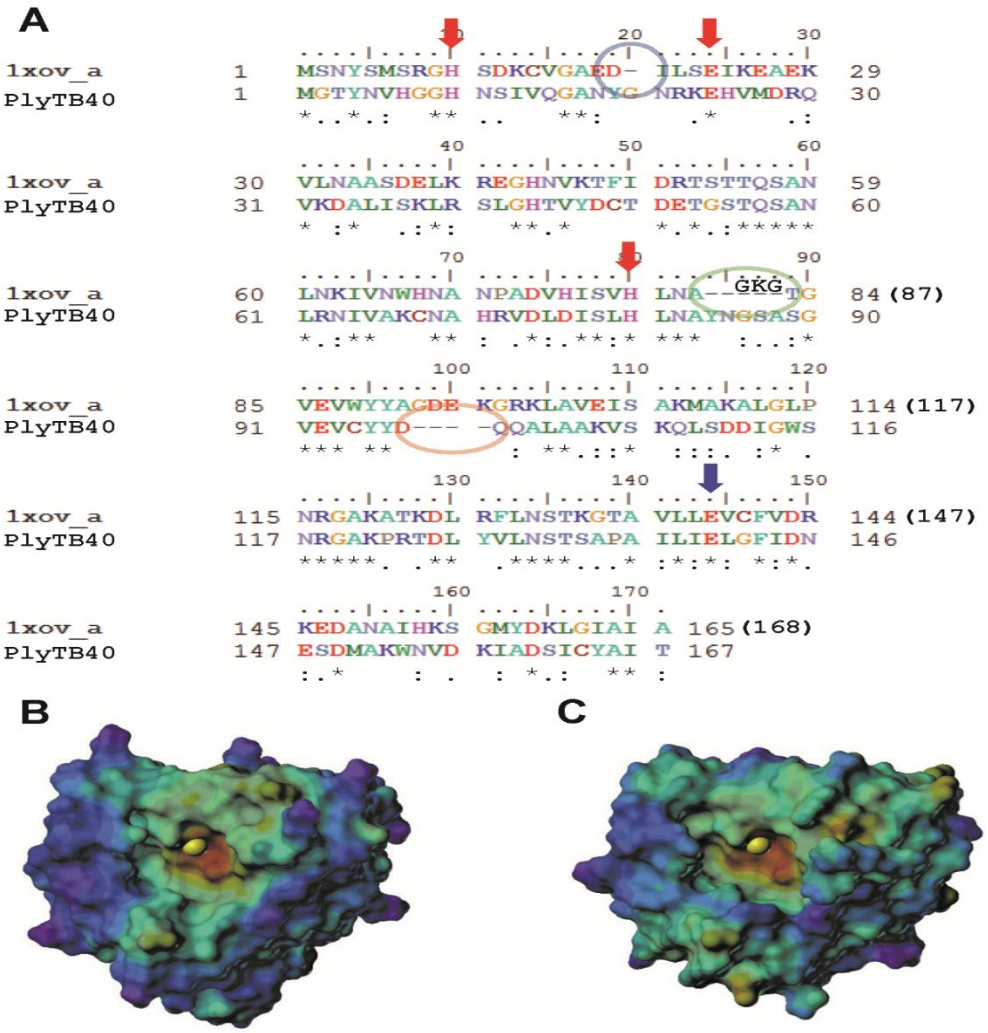

Figure 2-3. PlyTB40 alignment with structural homolog PlyPSA. (A) Sequence alignment of *L. monocytogenes* phage PSA (PlyPSA) from PDB entry 1XOV and PlyTB40 EADs (Clustal X alignment symbols: asterisk = identical; colon = strongly similar; period = weakly similar; space = not similar). Overall percent identity (# identical / # total) = 36.3%; percent similarity [(# identical + # strongly similar) / # total] = 53.2%. Arrows indicate the metal-binding residues (red) and the catalytic base/acid (blue). Colored ovals represent sequence insertions or deletions; see Fig. 5. **(B–C)** Connolly surfaces color-coded by electrostatic potential (blue = most positive; red = most negative) for the template PlyPSA **(B)** and the modeled PlyTB40 **(C)** EAD; a yellow sphere represents the Zn^{2+} ion.

2.3 Results

2.3.1 Phylogenetic Analysis

The 46 bacteriophages used in this study were originally isolated, sequenced, and annotated by undergraduate students under the SEA-PHAGES initiative (Jordan et al., 2014) and deposited in the *Bacillus* Phages Database (bacillus.phagesdb.org). All ORFs were analyzed for genes encoding putative endolysins. Sequences for six biochemically or structurally characterized homologs (LysB4, Ply500, PlyL, PlyPSA, LysBPS13, and phi29) were also included in our analysis (Korndörfer et al., 2006, 2008; Low et al., 2005b; Park et al., 2012; Saedi et al., 1987; Son et al., 2012). The 52 enzymes were grouped into nine separate phylogenetic families based on identities and architectural arrangement of the EAD and CBD domains (Table 2-3). Phylogenetic analysis of the EADs alone indicated four different enzymatic clades (Figure 2-4). The endolysins from bacteriophages Phrodo, Nigalana, and TsarBomba, called PlyP56, PlyN74, and PlyTB40, respectively, were chosen for expression and further study because they displayed EADs from separate clades but had similar CBDs.

Table 2-3. Phylogenetic analysis of 46 *Bacillus* bacteriophage endolysins.

Family	EAD	CBD	Examples
I.	G25 muramidase	Amidase02_C	Vinny ORF63
II.	G25 PlyB-like	Amidase02_C	Stitch ORF31
III.	MurNAc-LAA	2X LysM	Taylor ORF31
IV.	MurNAc-LAA	SH3	TsarBomba ORF40 (PlyTB40)
V.	VanY	2X PG_binding_1	SPO1 ORF107
VI.	Peptidase M15_4/VanY	SH3	Phrodo ORF56 (PlyP56)
VII.	GH24 muramidase	SH3	Beachbum ORF23
VIII.	PGRP	Amidase02_C	Waukesha ORF68
IX.	PGRP	SH3	Nigalana ORF74 (PlyN74)

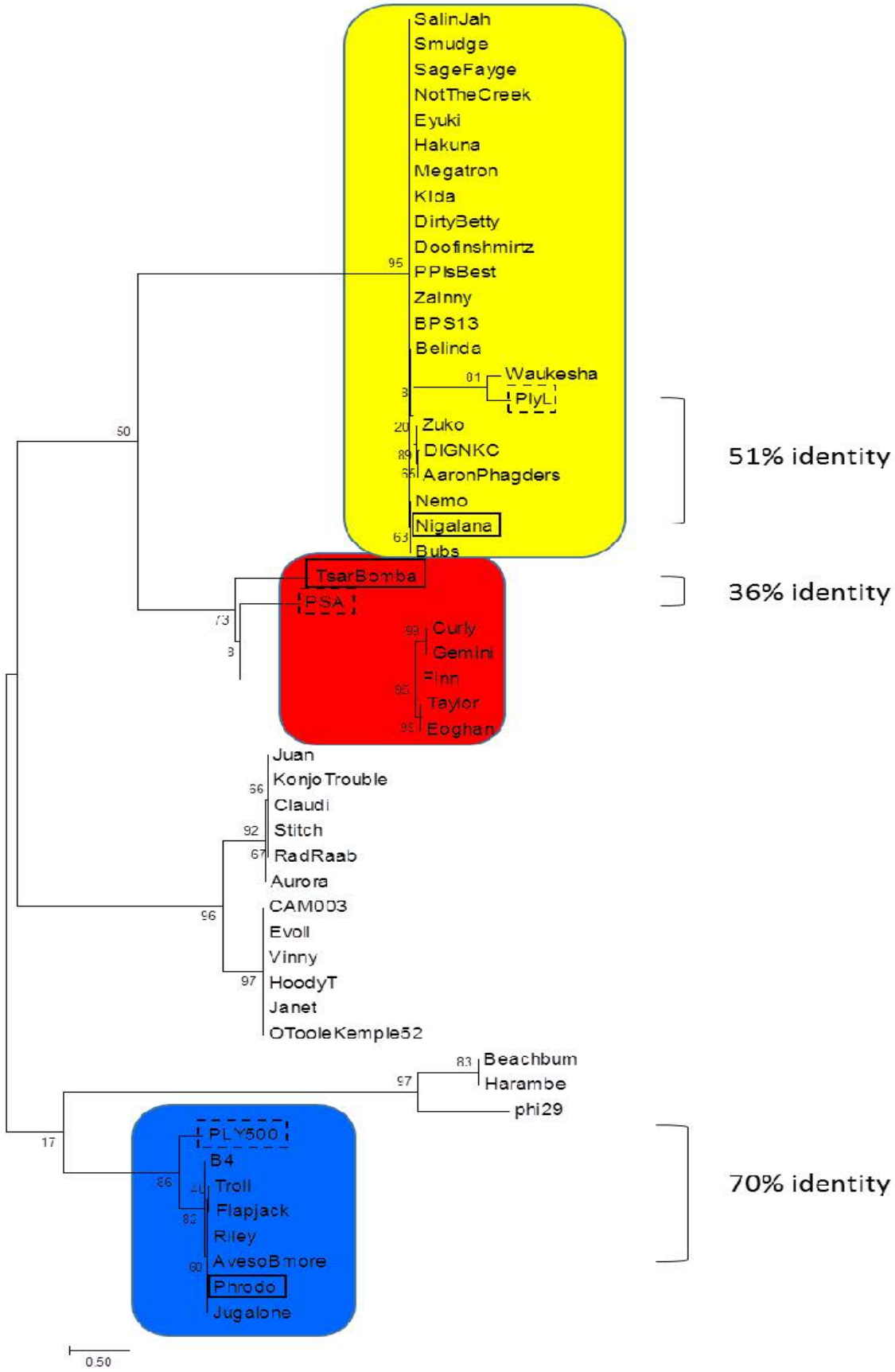
SalinJah
Smudge
SageFayge
NotTheCreek
Eyuki
Hakuna
Megatron
Klda
DirtyBetty
Doofinshmirtz
PPIsBest
Zalnny
BPS13
Belinda
Waukesha
PlyLi
Zuko
DIGNKC
AaronPhagders
Nemo
Nigalana
Bubs
TsarBomba
PSA
Curly
Gemini
Finn
Taylor
Eoghan
Juan
KonjoTrouble
Claudi
Stitch
RadRaab
Aurora
CAM003
Evoll
Vinny
HoodyT
Janet
OTooleKemple52
Beachbum
Harambe
phi29
PLY500
B4
Troll
Flapjack
Riley
AvesoBmore
Phrodo
Jugalone
0.50
51% identity
36% identity
70% identity

Figure 2-4. Molecular phylogenetic analysis of bacteriophage endolysin EADs. Sequences were obtained from *Bacillus* Phage Database (bacillus.phagesdb.org) that have also been deposited into GenBank and compared to six published phage endolysin sequences. Endolysins are represented by their phage names. The evolutionary history was inferred by using the Maximum Likelihood method. The tree is drawn to scale, with branch lengths measured in the number of substitutions per site. Endolysins tested in this manuscript are boxed in black and structurally characterized homologs are boxed in a dashed line. The scale bar represents 0.5 substitutions per amino acid site. Color coding corresponds to EAD domains in Figure 2-5.

2.3.2 Endolysin Domain Architecture and Homology

A Pfam database analysis confirmed that PlyP56, PlyN74, and PlyTB40 each contained a singular N-terminal EAD and a C-terminal CBD (Figure 2-5A). The PlyP56 EAD is predicted to be a member of the Peptidase_M15_4/VanY superfamily (Pfam 13539, Pfam 02557), which is associated with a D-alanyl-D-alanine carboxypeptidase activity. However, such an activity would not readily lead to lysis of the peptidoglycan. Furthermore, the PlyP56 EAD shares significant sequence homology (95% identity) with LysB4 (AFF27501.1), an endolysin from the *B. cereus* bacteriophage B4, which has a confirmed L-alanoyl-D-glutamate endopeptidase activity based on mass spectrometry analysis (Son et al., 2012). The PlyN74 EAD is predicted to belong to the Amidase_2/PGRP superfamily (Pfam 01510) and shares 95% identity to LysBPS13 (AEZ50187.1), a confirmed N-acetylmuramoyl-L-alanine amidase from the *B. cereus* bacteriophage BPS13 (Park et al., 2012). These enzymes cleave the amide bond between the glycan component (N-acetylmuramic acid) and the peptide component (L-alanine) of the peptidoglycan. Finally, the PlyTB40 EAD is a putative Amidase_3/MurNAc-LAA (pfam 01520). Similar to the Amidase_2 catalytic domain of the PGRP superfamily, the Amidase_3 catalytic domain also possesses an N-acetylmuramoyl-L-alanine amidase activity, although this EAD adopts a different fold (Figure 2-6) (Büttner et al., 2015). Thus, despite PlyN74 and PlyTB40 containing structurally different catalytic domains (compare Figure 2-9E,H), both endolysins share a similar enzymatic target—the amide bond between N-acetylmuramic acid and L-alanine in the peptidoglycan

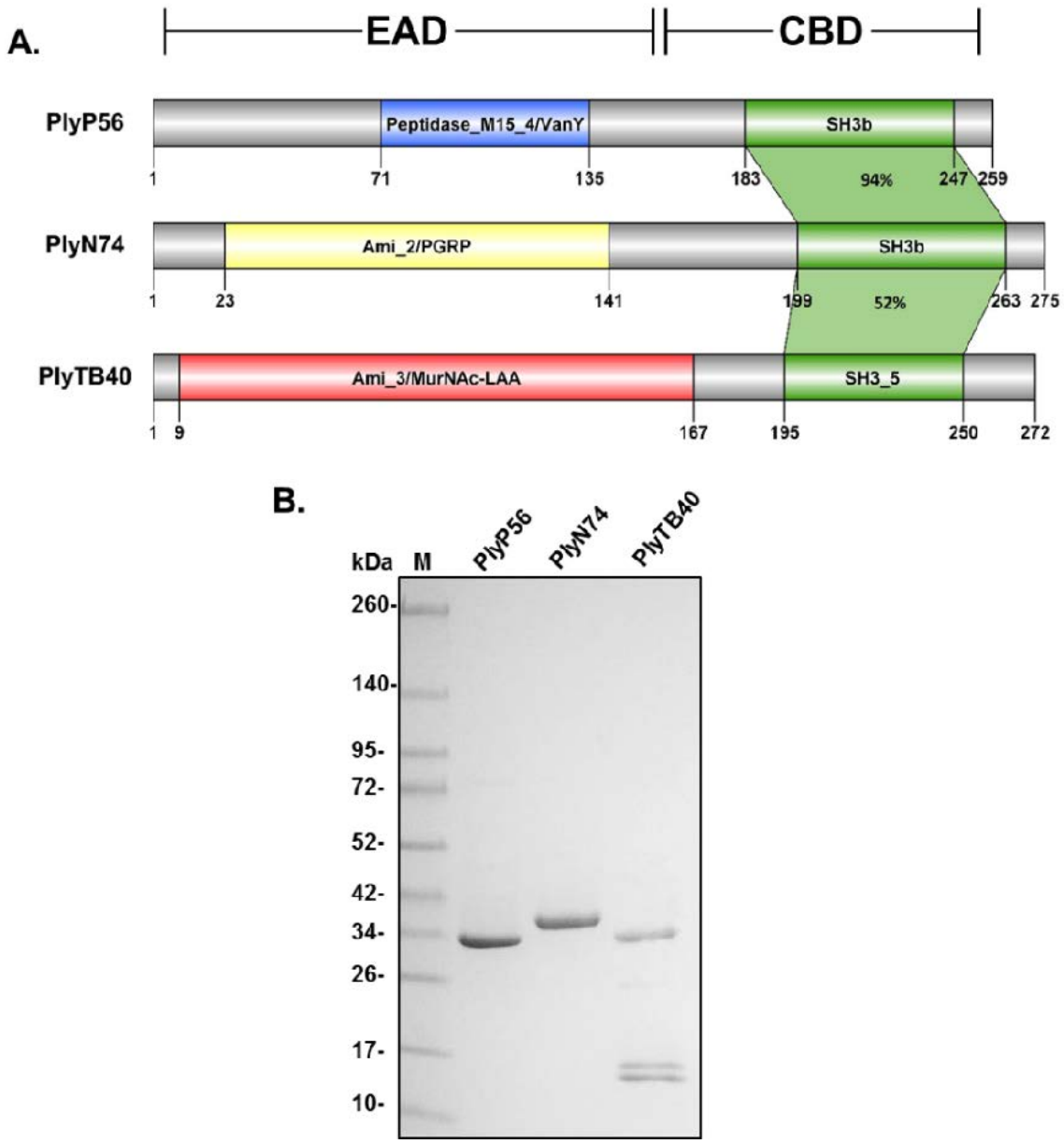

Figure 2-5. Bacillus bacteriophage endolysin structural characterization and protein profile. (**A**) PlyP56, PlyN74, and PlyTB40 contain divergent N-terminal enzymatic active domains (EADs) and conserved C-terminal cell wall binding domains (CBDs). PlyP56 has a Peptidase_M15_4 EAD domain found within the VanY superfamily. PlyN74 has an Amidase_2 EAD domain that is part of the MurNAc-LAA superfamily. PlyTB40 has an Amidase_3 EAD that is also part of the MurNAc-LAA superfamily but lacks homology with the Amidase_2 domain of

PlyN74. All three endolysins have similar SH3-family binding domains. Color coding of EADs correspond to Figure 2-4. (**B**) Purification of Bacillus phage endolysins. *E. coli* BL21-(DE3) cells were transformed with a vector encoding recombinant endolysins, grown, and induced with L-arabinose as described under Methods. The recombinant endolysins were purified to homogeneity by nickel affinity chromatography. Protein samples were analyzed for purity by SDS-PAGE with Coomassie blue staining. Lane 1, molecular mass markers as indicated; Lane 2, PlyP56; Lane 3, PlyN74; Lane 4, PlyTB40.

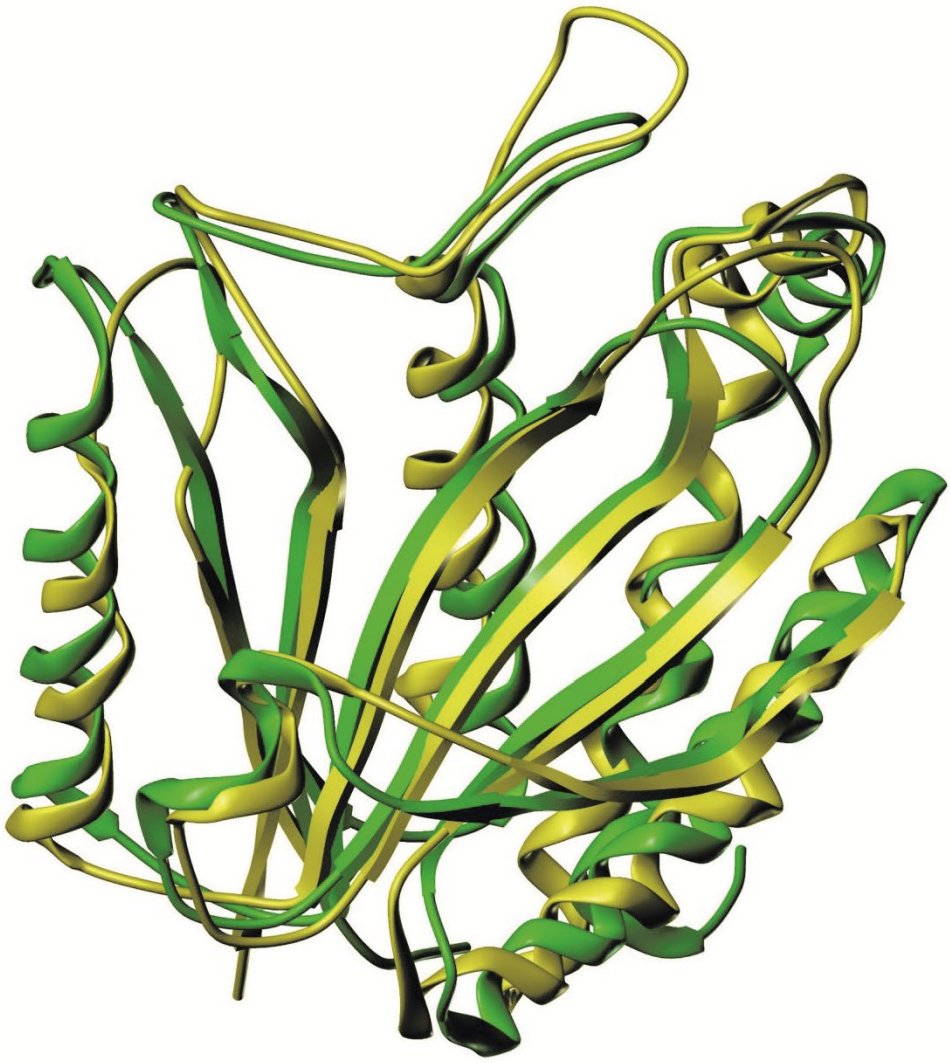

Figure 2-6. Carboxypeptidase T-type Amidase_3 fold. Ribbon diagrams of the endolysins EADs of *L. monocytogenes* bacteriophage PlyPSA (PDB ID: 1XOV; PlyTB40 homology modeling template; green) and *B. polymyxa var. colistinus* CwIV (PDB ID: 1JWQ; yellow), each exhibiting the carboxypeptidase T-type Amidase_3 fold.

In contrast to the divergent EADs, all three endolysins are predicted to have a type of src-homology 3 (SH3) domain as their C-terminal CBD (Figure 2-5A). The CBDs of PlyP56 and PlyN74 have SH3 bacterial domains, known as SH3b domains (smart 00287), which share 94% identity. The PlyTB40 CBD has a very similar SH3_5 domain (pfam 08460) that shares ~52% identity with the SH3b domains of PlyP56 and PlyN74. Notably, SH3b and SH3_5 domains are commonly found CBDs in endolysins derived from bacteriophage that infect Gram-positive bacteria (Nelson et al., 2012), including the *Bacillus*-specific endolysins Ply21 (Loessner et al., 1997) and LysB4 (Son et al., 2012).

2.3.3 Purification and Biochemical Characterization

All three endolysins and their corresponding CBDs were expressed as soluble proteins in a pBAD24 expression vector and purified to homogeneity by nickel affinity chromatography via C-terminal 6xHis tags. The size of purified PlyP56, PlyN74, and PlyTB40 bands on SDS-PAGE corresponded to 28.5 kDa, 31.4 kDa, and 30.0 kDa, respectively (Figure 2-5B). Notably, the PlyTB40 purified protein fraction resulted in a full-length ~30 kDa protein and one or two smaller bands in the ~10–15 kDa range on SDS-PAGE. It should be noted that some clostridial and enterococcal endolysins use alternate translation start sites that generate an additional CBD resulting in the formation of heterodimer enzymes, which would explain the presence of protein bands that correspond to the full-length endolysin and that of a CBD (Dunne et al., 2016; Proença et al., 2015). However, I did not detect consensus Shine–Dalgarno sequences or in-frame start codons in the region corresponding to the beginning of the PlyTB40 CBD. I believe the smaller fragment(s) represent a degradation event despite our use of protease inhibitors during purification.

2.3.4 Activity and Biochemical Characterization of Endolysins

All three endolysins exhibited a dose–response curve from 100 to 3 μg/mL when tested via the turbidity reduction assay against overnight cultures of *B. cereus* ATCC 4342, with PlyP56 being at least twice as active as PlyN74 and PlyTB40 at all tested concentrations (Figure 2-7). PlyP56-induced lysis of the bacterial peptidoglycan caused a decrease in OD from 1.0 to 0.4 (60% decrease) within the first 4 min of the turbidity assay at the highest tested dose (100 μg/mL), whereas equimolar concentrations of PlyN74 and PlyTB40 required 10–15 min to achieve the same degree of lysis.

Based on numerous studies, the enzymatic effectiveness of endolysins can often be affected by salt concentration, pH, and temperature (Fischetti, 2010; García et al., 2010; Nelson et al., 2012; Yuan et al., 2012). To determine the optimum conditions for PlyP56, PlyN74, and PlyTB40, the lytic activity of these enzymes was surveyed over a broad range of pH (3–11), NaCl concentrations (0–500 mM), and exposure to different temperatures (4–60ºC). In general, all endolysins displayed similar biochemical/biophysical profiles despite possessing different EADs (Figure 2-8). All three endolysins displayed high lytic activity (90%–100%) at pH 7 and 8, but activity rapidly dropped off outside of this range for PlyP56 and PlyN74 (Figure 2-8A,B). In contrast, PlyTB40 retained >60% activity at pH 6 and ~40% activity at pH 5 (Figure 2-8C). These findings suggest a narrower pH range than found in other *Bacillus*-specific endolysins, but nonetheless, they are consistent with a skew toward neutral to basic pH optimums. For instance, PlyPH, a bacteriolytic enzyme identified within the genome of *B. anthracis*, exhibits a relatively broad optimum from pH 5 to 9 (Yoong et al., 2006), whereas LysB4, a PlyP56 homolog, has optimal lytic activity between pH 8.0 and pH 10.5 (Son et al., 2012).

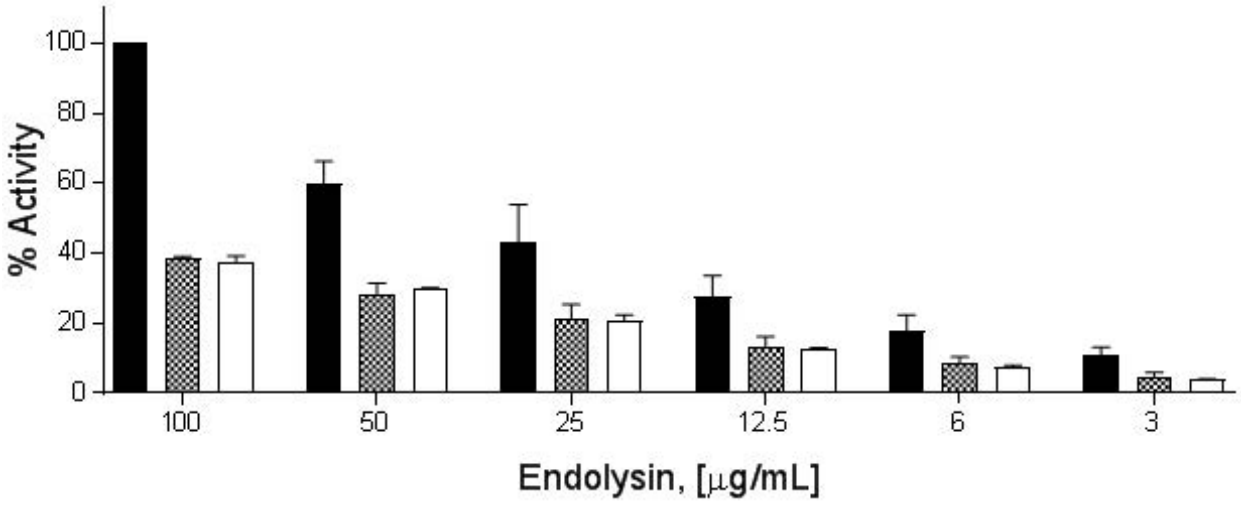

Figure 2-7. PlyP56, PlyN74, and PlyTB40 lytic activity comparison. Stationary phase *B. cereus* ATCC 4342 cells at final OD_{600} of 1.0 were treated with endolysin doses from 100 μg/mL to 3 μg/mL over 20 min. PlyP56 (black bars), PlyN74 (checker bars), and PlyTB40 (white bars) are indicated. The cell lysis was assayed by turbidity reduction as described in Methods. The % lytic activities were normalized to 100% activity of PlyP56 (black bars) at 100 μg/mL. Experiments were run in triplicates on three independent days. The error bars represent standard deviation.

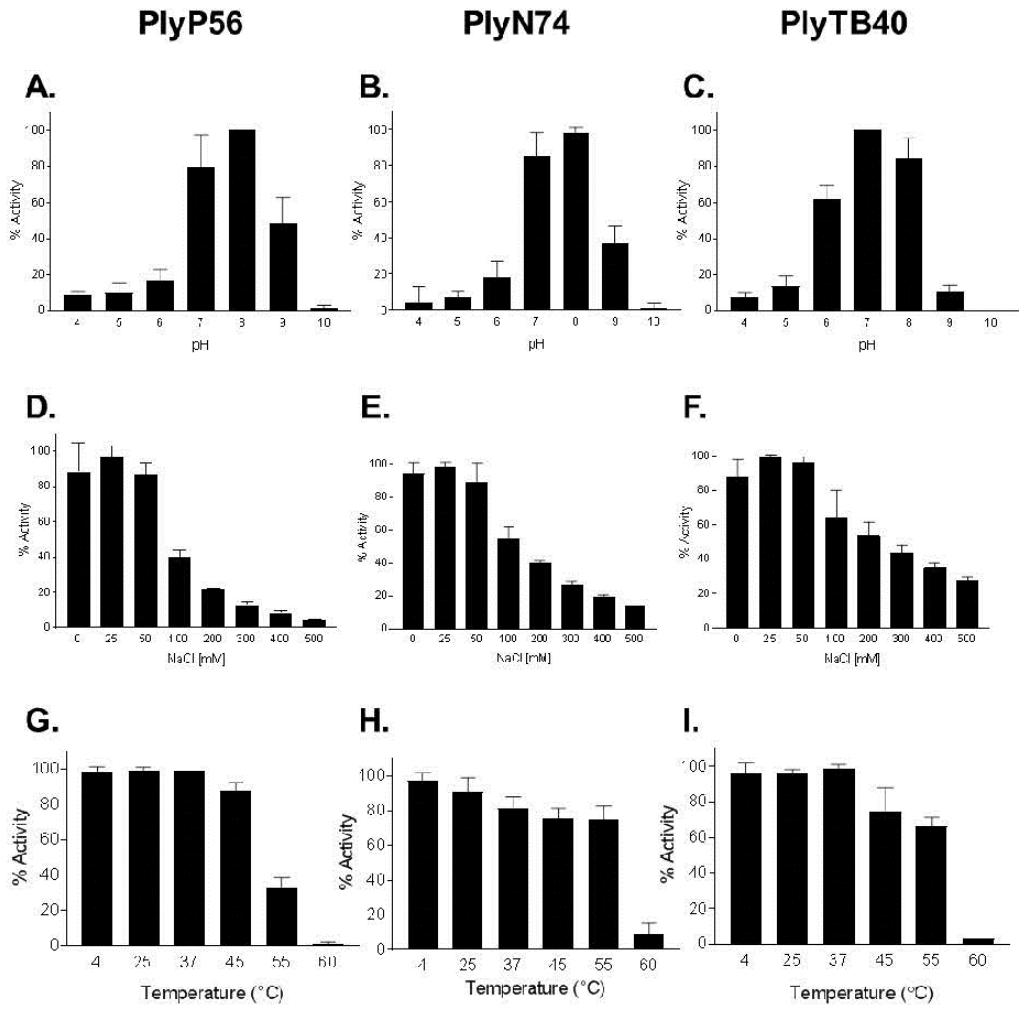

Figure 2-8. Biochemical characterization of optimal conditions for *Bacillus* bacteriophage endolysins activity. The effects of pH (**A**–**C**), NaCl dependence (**D**–**F**), stability (**G**–**I**) was evaluated for each of the three endolysins. PlyP56 (**A**,**D**,**G**), PlyN74 (**B**,**E**,**H**), and PlyTB40 (**C**,**F**,**I**) were assayed for lytic activity, each at 50 μg/mL, and tested separately via turbidity reduction assay against stationary phase *B. cereus* ATCC 4342 cells for 20 min All endolysins were preincubated at indicated temperatures for 30 min and subsequently recovered on ice for 5 min to test a temperature effect on lytic activity. Values are presented as a percentage of lytic activity in relation to highest activity observed for each tested parameter. All experiments were run in triplicates on three independent days. Error bars indicate standard deviations.

LysBPS13, a *B. cereus*-specific endolysin and a homolog of PlyN74, exhibits similar low tolerance to acidic pH below 6.0 (Park et al., 2012b). In our experiments, pH extremes not only reduced enzymatic activity of the surveyed endolysins, but it also caused a precipitation of endolysins at the acidic pH. Taken together, our findings suggest that *Bacillus* species-specific endolysins can sustain their enzymatic activity at a broad pH range but prefer physiological and slightly basic conditions.

The influence of NaCl on enzymatic activity was also studied at pH 7.4, where all the enzymes displayed maximum activity. It was reported that salt concentrations can significantly enhance enzymatic activity of many endolysins (García et al., 2010). However, NaCl concentrations up to 100 mM had little effect (<10% deviation) on the lytic activity of PlyP56, PlyN74, and PlyTB40 (Figure 2-8D–F). A similar effect was observed for staphylococcal endolysin, PlyGRCS (Linden et al., 2015), which displayed full activity up to 500 mM NaCl. On the contrary, NaCl concentrations equal to or above 100 mM significantly inhibited enzymatic activity of all three enzymes, with PlyP56 being the most sensitive, losing half of its activity at just 100 mM NaCl. PlyTB40 was the least sensitive to NaCl of the three enzymes, but still lost half of its lytic activity at 300 mM.

The thermal stability of each endolysin was determined by incubation at temperatures ranging from 4 to 60ºC, recovering on ice, and measuring residual activity by the turbidity reduction assay. It was determined that all endolysins were enzymatically active over a temperature range from 4 to 45ºC, with minor deviations in activity (±15% of maximum) (Figure 2-8G–I). At 55ºC, PlyN74 and PlyTB40 maintained >80% of maximum activity whereas PlyP56 displayed <40% of maximum activity. By 60ºC, all three endolysins had <10% lytic activity remaining. In general, the thermal stability profile of PlyP56, PlyN74, and PlyTB40 was found to

be consistent with other Bacillus endolysins. For instance, LysBPS13 and BtCS33 were inactivated after a 30 min incubation at 60ºC in the absence of thermoprotective agents (Yuan et al., 2012a)

2.3.5 Structural Modeling of Bacillus Bacteriophage Endolysin EADs

Plausible three-dimensional models of the PlyP56, PlyN74, and PlyTB40 EADs (Figure 2-9) were generated using homology modeling techniques (see Methods). Each model fit its template well, with complete conservation of catalytic residues, moderate to high conservation of noncatalytic amino acids, and only a few small insertions or deletions in loop regions. The differences in amino acid composition on the surfaces of closely related EAD family members are responsible for differences in their shape and electrostatic nature (see e.g., Figures 2-1–2-3). These factors in turn contribute to differences in the functional protein–protein interactions and catalytic specificity exhibited by members within and between the various endolysin fold families (Büttner et al., 2015; Firczuk and Bochtler, 2007; Schmelcher et al., 2012). Taken together, the 3-D structural modeling results support the functional prediction of N-acetylmuramoyl-L-alanine amidase activity for the PlyN74 and PlyTB40 endolysins, while clarifying PlyP56 as an L-alanoyl-D-glutamate peptidase.

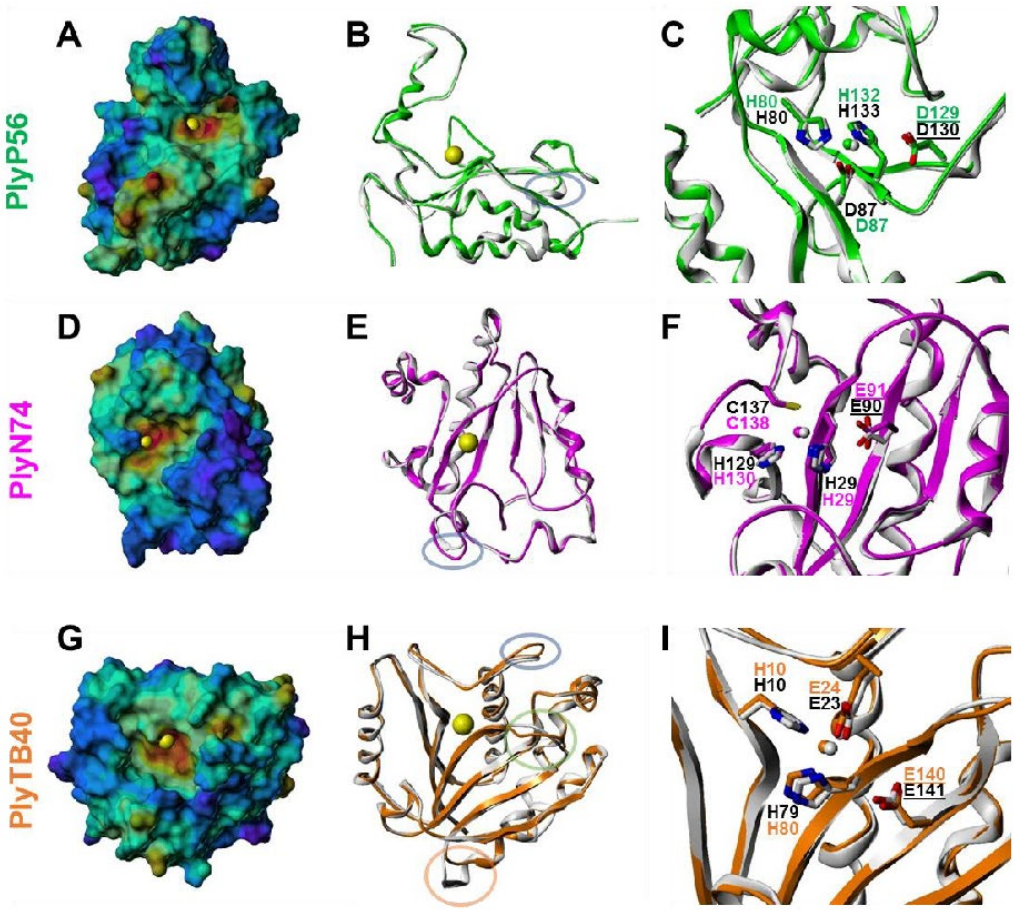

Figure 2-9. Homology models of PlyP56 (A–C), PlyN74 (D–F), and PlyTB40 (G–I) EADs. (A,D,G) Connolly surface representations color-coded by electrostatic potential (blue = most positive; red = most negative). A yellow sphere represents the Zn^{2+} ion. (B,E,H) Ribbon representations of the homology modeling template (PlyP56: PDB ID = 2VO9; PlyN74: PDB ID = 1YB0; PlyTB40: PDB ID = 1XOV; white) and target (PlyP56, green; PlyN74, magenta; PlyTB40, orange) EADs illustrating the putative protein fold conservation. Colored ovals represent sequence insertions or deletions; see Figures 2-1–2-3. (C,F,I) Catalytic active site amino acid residues. Residue label colors represent template (black) and target (PlyP56, green; PlyN74, magenta; PlyTB40, orange) EADs. An underline indicates the catalytic base/acid. Small spheres represent the Zn^{2+} ion.

2.3.6 Effect of Divalent Metal Ions

Based on 3-D modeling, all three endolysin EADs are predicted to have a characteristic monometallic metallopeptidase-like catalytic active site in which a Zn^{2+} ion is tetrahedrally coordinated by three conserved amino acid residues and a water molecule, and that also contains an adjacent catalytic base/acid, usually Asp or Glu (Cerdà-Costa and Gomis-Rüth, 2014). For PlyP56, the Zn^{2+}-coordinating residues are His80, Asp87, and His132, and the catalytic base/acid is Asp129 (Figure 2-9C). For PlyN74, the Zn^{2+}-coordinating residues are His29, His130, and Cys138, and the catalytic base/acid is Glu91 (Figure 2-9F). For PlyTB40, the Zn^{2+}-coordinating residues are His10, Glu24, and His80, and the catalytic base/acid is Glu140 (Figure 2-9I). Significantly, Ply500 contains a conserved metal binding sequence (SxHxxGxAxD) and its crystal structure revealed an ion in the active site (Korndörfer et al., 2008). Sequence alignment also detected this motif in PlyP56 (Figure 2-1A). Although not necessarily associated with a specific sequence motif, the metal binding site in Amidase_2 and Amidase_3 N-acetylmuramoyl-L-alanine amidases has been structurally characterized using X-ray crystallography, and strictly conserved metal-coordinating residues have been identified (Büttner et al., 2015). The sequence similarity of PlyN74 and PlyTB40 to Amidase_2 and Amidase_3 N-acetylmuramoyl-L-alanine amidases and the high quality of the resulting MODELLER-generated models provide strong evidence that these metal binding sites are present in these endolysin EADs as well.

To further elucidate these findings, PlyP56, PlyN74, and PlyTB40 were dialyzed overnight in buffer supplemented with 5 mM EDTA to remove residual meatal ions. Interestingly, EDTA treatment completely ablated enzymatic activity of PlyP56 but had no effect on the activities of PlyN74 or PlyTB40 (Figure 2-10). Further, EDTA-treated proteins were dialyzed overnight in TBS supplemented with an excess of metal relative to the EDTA (i.e., 6 mM Mg^{2+} or 6 mM Ca^{2+})

to restore cations in these enzymes. Lytic activity of PlyP56 was restored to 80% of the pre-EDTA levels by Mg^{2+} ions and to 70% by Ca^{2+} ions (Figure 2-10). Our EDTA results are consistent with those found for LysB4, an EAD sequence homolog of PlyP56, which had activity restored to EDTA-treated samples by the addition of Mg^{2+} or Ca^{2+} ions (Son et al., 2012). This confirms that PlyP56 requires divalent metal ions for its enzymatic activity.

In contrast to the PlyP56 results, EDTA treatment had no effect on the enzymatic activity of PlyN74 despite an ion being present in the active site of the crystal structure for PlyL, a homolog of the PlyN74 EAD (Low et al., 2005). However, EDTA-treated LysBPS13, another PlyN74 homolog, was similarly not dependent on the presence of metal ions for activity (Park et al., 2012). Finally, I found that PlyTB40 was also not affected by EDTA, even though a Zn2+ ion was identified in the crystal structure of an homologous PlyPSA (Korndörfer et al., 2006).

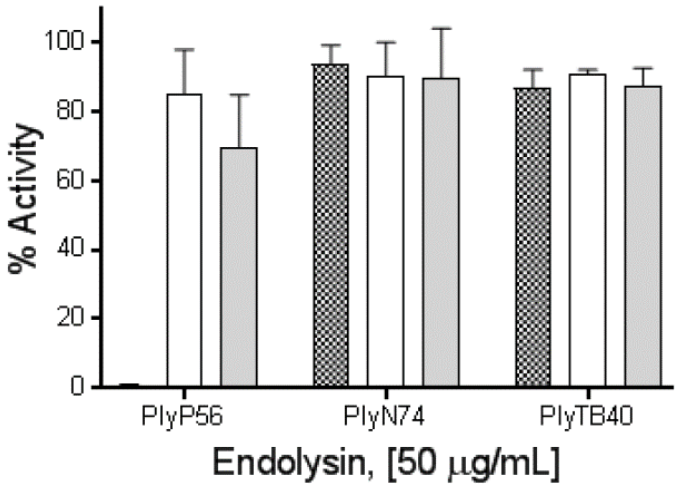

Figure 2-10. Metal binding properties of PlyP56, PlyN74, and PlyTB40. The influence of divalent cations on PlyP56, PlyN74, and PlyTB40 lytic activity against stationary phase *B. cereus* ATCC 4342 was assayed via turbidity reduction assay. Mean values from three independent experiments run in triplicate are represented as the percentage residual lytic activity relative to untreated endolysins. Endolysins treated with EDTA (checker bars), and subsequently recovered via dialysis with additions of divalent ions, Mg^{2+} (white bars), Ca^{2+} (grey bars) are shown.

2.3.7 Host Specificity

To determine the host range of PlyP56, PlyN74, and PlyTB40, lytic activity was tested via turbidity assay on a variety of *B. cereus* strains and other *Bacillaceae* (Table 2-1). Similar to the dose–response curves for *B. cereus* ATCC 4342 (Figure 2-7), PlyP56 was more effective in lysing *B. cereus sensu lato* group species than PlyN74 or PlyTB40, but all three enzymes displayed strong activity, defined as >20% lysis in the 20 min assay period, against all *sensu lato* members tested (i.e., four *B. cereus* strains and one *B. thuringiensis* strain). In addition, all three enzymes showed strong activity against *Bacillus pumilus* strain BJ0050, PlyP56 and PlyN74 both showed strong activity against *Bacillus megaterium* and *Bacillus amyloliquefaciens*, PlyN74 showed strong activity against *Bacillus licheniformis*, and PlyP56 showed strong activity against *Bacillus circulans* and *Lysinbacillus sphaericus*. Weak, but measurable, activity was noted for all three enzymes against *Bacillus coagulans*, *Bacillus subtilis*, and *Paenibacillus polymyxa*.

B. cereus ATCC 4342 is a transition state strain that is phylogenetically located between *B. cereus* and *B. anthracis* (Helgason et al., 2000), and as such, I expected these enzymes to be equally effective in cell lysis of *B. anthracis*. However, using the same set of parameters employed for assays in Table 2-1, I did not observe lytic activity in a turbidity reduction assay against biosafety level 2 *B. anthracis* strains (34F2 Sterne, Ames35, and UM23) or the biosafety level 3 *B. anthracis* Ames strain. However, lytic activity measured via a plate lysis assay, which tends to be more sensitive given longer incubation times, did reveal significant lysis of *B. anthracis* Ames35 bacilli by PlyP56 and PlyN74 with lesser activity against the *B. anthracis* UM23 strain (Table 2-4). PlyTB40, on the other hand, had very low activity against these strains. Collectively, our findings suggest PlyP56, PlyN74, and PlyTB40 have targeted lytic activity against the *B. cereus sensu lato* group and a few closely related species.

Table 2-4. Plate lysis.

Bacterial species	Strains[1]	Bacteriophage Endolysins[2]		
		PlyP56	PlyN74	PlyTB40
B. cereus	**ATCC 4342**	+++	+++	++
B. anthracis	**Ames 35**	++	+++	+
B. anthracis	**UM23**	+	+/-	+/-

[1] See Methods for source of species and strains. [2] Activity of endolysins was evaluated via plate lysis assay. 10 µL of each endolysin containing 10, 1, or 0.1 µg were spotted onto a surface of semisolid agar containing a mid-log bacterial cell suspension. The strength of lysis was defined by the presence of a clearing zone: +/-, for a partial clearing zone at 10 µg; +, for a clearing zone at 10 µg; ++, for a clearing zone at 1 µg; and +++, for a clearing zone at 0.1 µg. PBS was spotted in equal volumes and served as a negative control.

2.3.8 Cell Wall Binding

As with many endolysins, the SH3b and SH3_5 domains present in PlyP56, PlyN74, and PlyTB40 are thought to function as their CBDs. To test this hypothesis, the CBDs of these enzymes were chemically crosslinked with AlexaFluor555, purified and assessed for their binding properties by fluorescent microscopy. All three CBDs bound tightly to the peptidoglycan of *B. cereus* ATCC strains 4342, 14579, 11778, and 13061. Binding to strain 4342 is shown in Figure 2-11 (two left columns), but similar binding was observed for all *B. cereus* strains. Additionally, all three CBDs bound tightly to the peptidoglycan of the *B. anthracis* strains UM23 and Ames35, with the later depicted in Figure 2-11 (two right columns). In contrast, none of the CBDs bound non-sensu lato strains of *Bacillus*, including *B. licheniformis* ATCC 14580 and *B. coagulans* ATCC 7050. Likewise, the CBDs did not bind other representative Gram-positive bacteria, such as *Streptococcus pyogenes* D471.

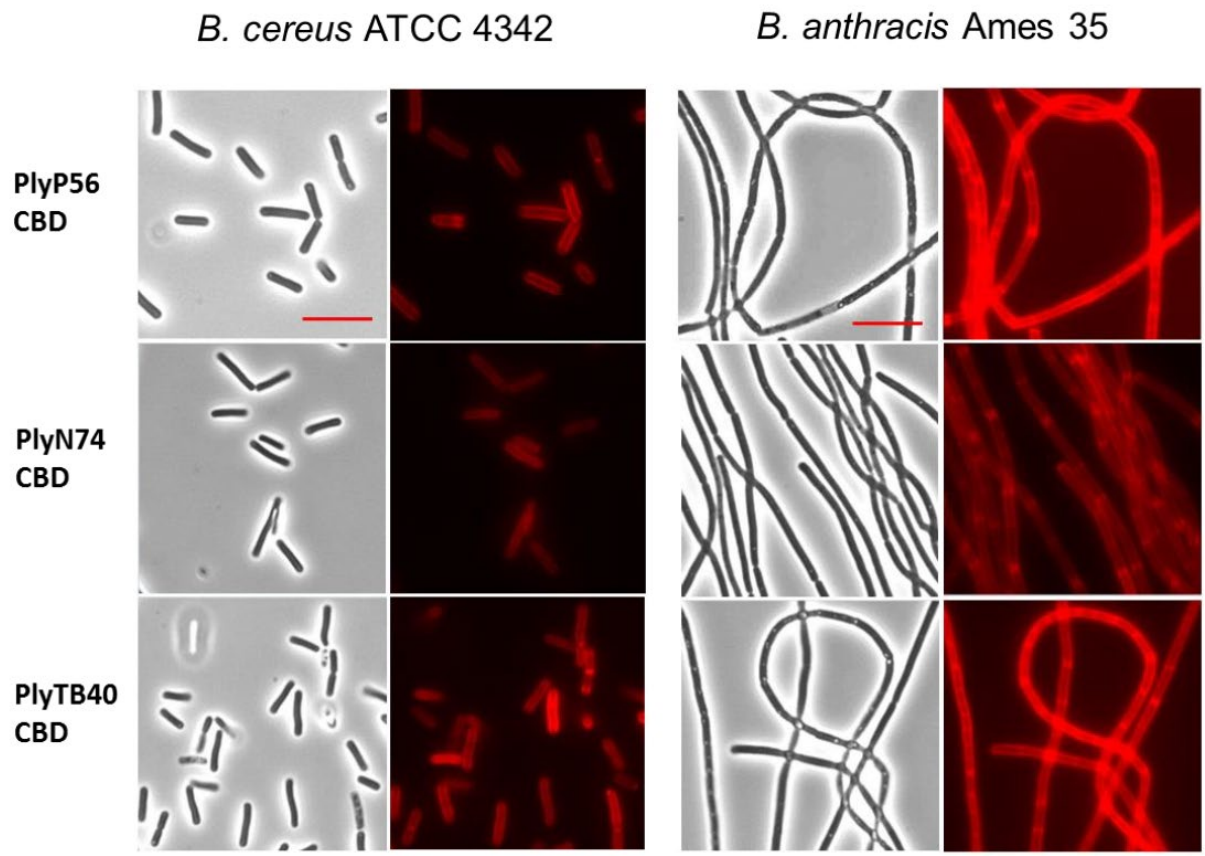

Figure 2-11. Binding of AlexaFluor-labeled CBDs to a cell wall of bacilli. Decoration of *B. cereus* ATCC 4342 (two left columns) and *B. anthracis* Ames 35 (two right columns) by fluorescently tagged CBDs of PlyP56, PlyN74, and PlyTB40. 1000× bright-field images (columns 1 and 3) are shown with their corresponding fluorescent images (columns 2 and 4). The AlexaFluor-labeled CBDs recognize and bind to an evenly distributed ligand on the surface of *B. cereus* and *B. anthracis*. Red scale bar = 5 μm.

2.4 Discussion

Bacteriophage-encoded endolysins are of great interest for their potential as antimicrobial agents useful for controlling bacterial infections and preventing biofilm formation (Schuch et al., 2013)(Pires et al., 2016; Schuch et al., 2013; 2009). They can also be used for unwanted food contamination by opportunistic or pathogenic bacteria (Schmelcher and Loessner, 2014). The three *B. cereus* specific endolysins, PlyP56, PlyN74, and PlyTB40, which share basic structural properties of an N-terminal conserved EAD and a C-terminal CBD, have been identified and characterized.

PlyP56 is predicted to have an L-alanoyl-D-glutamate peptidase activity derived from the Peptidase_M15_4/VanY superfamily EAD domain. Sequence analysis identified a conserved (SxHxxGxAxD) motif within the PlyP56 EAD that plays an active role in harboring a metal ion, as first described for VanX of *Enterococcus faecium* (McCafferty et al., 1997) and supported by the modeling studies with the Ply500 structural homolog (Figure 2-9A). As predicted, the PlyP56 lytic activity was abolished by EDTA treatment, which was subsequently restored by addition of excess Mg^{2+} or Ca^{2+} ions. The PlyN74 Amidase_2/PGRP superfamily EAD and the PlyTB40 Amidase_3/MurNAc-LAA superfamily EAD are not homologous and arise from different phylogenetic clades (Table 2-3), but they nonetheless are predicted to possess identical N-acetylmuramoyl-L-alanine amidase activities, suggesting convergent evolution of these superfamily domains. The modeling to structural homologs for both of these EADs suggested a metal binding pocket with active site residues similar to those of the PlyP56 EAD. However, I was unable to inhibit lytic activity of these two endolysins by EDTA treatment. This discovery suggests that enzymatic activity of both endolysins is independent from metal ions, as proposed by Park *et al*. (2012) for the PGRP superfamily. Alternatively, it is possible that the affinity of the metal ion

to the coordinating residues was too strong, and/or the accessibility of the metal binding pocket was too limited, to be susceptible to chelation by EDTA.

PlyP56, PlyN74, and PlyTB40 had very similar biochemical, biophysical, and binding/host range characteristics. The similar binding patterns of these endolysins were anticipated since they all had similar SH3-family CBDs and were originally selected due to high lytic activity on the same *B. cereus* ATCC 4342 indicator strain. However, all three endolysins have distinct EADs, so it is somewhat surprising that their pH, NaCl sensitivity, and temperature stability profiles overlap to a large degree. Given that PlyP56 displays twice the activity of PlyN74 and PlyTB40, it is inviting to speculate that the Peptidase_M15_4 EAD of PlyP56 is more efficient than the Amidase_2 or Amidase_3 EADs of PlyN74 and PlyTB40, respectively. This is further supported by the near-identical CBDs shared by PlyP56 and PlyN74, suggesting these enzymes are only differentiated by their EADs. However, the differences in charge of the EADs cannot be discounted as contributing to the observed differences in activity. A number of studies have reported correlation between the charge of an EAD and its enzymatic activity (Oliveira et al., 2013). Truncated, positively charged EADs of PlyL and CD27L were reported to have higher bactericidal activity and broader host spectrum than their wild-type precursors (Low et al., 2011; Mayer et al., 2011). Remarkably, at neutral pH, the PlyP56 EAD and linker sequence (residues 1–173) would have a predicted net positive charge (pI = 8.55), the PlyN74 EAD/linker (residues 1–189) would have a neutral charge (pI = 7.02), and the PlyTB40 EAD/linker (residues 1–190) would have a slight negative charge (pI = 6.28). It is possible that differences in charge of the EADs, specifically positively charged EADs, may enhance binding properties of the CBDs to negatively charged wall teichoic acids on the bacterial surface and contribute to observed lytic activity, although additional experimentation will be needed to determine if that is the case with the enzymes described here.

It is noteworthy that PlyP56, PlyN74, and PlyTB40 had higher activity against *B. cereus* ATCC 4342 than they did against any other bacilli. Significantly, *B. cereus* ATCC 4342 is a known transition state strain between *B. cereus* and *B. anthracis*, and it is the only *B. cereus* strain lysed by the PlyG endolysin, which lyses all *B. anthracis* strains. Therefore, I expected that the newly discovered endolysins presented here would also be active against *B. anthracis* strains. Although I observed strong binding to *B. anthracis* via all three endolysin CBDs (Figure 2-11, right two columns) as well as activity against *B. anthracis* in a spot lysis assay for the full-length proteins (Table 2-4), the overall lytic activity of PlyP56, PlyN74, and PlyTB40 against *B. anthracis* species is considered quite weak since I never observed activity in a liquid turbidity reduction assay. At present, I do know if this diminished activity is related to assay conditions, the strains I chose for study, differences in the peptidoglycan between members of the *sensu lato* group, or the SH3-based CBDs present in these enzymes. Additionally, PlyG is not homologous to any of our endolysins, and PlyL, another well-characterized endolysin with high activity against B. anthracis (Low et al., 2005), shares only 53% identity with the EAD of PlyTB40. Moreover, the absence of homology between the CBDs of our enzymes and that of characterized *B. anthracis* endolysins suggests they do not share common epitopes. Further work is needed to fully elucidate the interactions between *Bacillus*-specific endolysin EADs and their CBDs.

This study contributes three new *Bacillus*-specific endolysins to the growing toolbox of EADs and CBDs that can be evolved, modified, or shuffled through chimeragenesis to create new enzymes. Despite similar biochemical profiles acquired for PlyP56, PlyN74, and PlyTB40, PlyP56 is the most enzymatically active and has a broader host range than PlyN74 and PlyTB40, which makes it a good lead candidate for further antimicrobial development and bioengineering studies.

Acknowledgements

I.E. served as a military service member over the course of this work, which was prepared as part of her official duties. Title 17 USC. §105 provides that 'Copyright protection under this title is not available for any work of the United States Government'. The views expressed in this article are those of the authors and do not necessarily reflect the official policy or position of the Department of the Navy, Department of Defense, nor the U.S. Government.

3 Diversity Engineering and Screening for Functional Chimerism of ClyBC1, ClyBC2, ClyBC3, ClyBC4, and ClyBCBA1 Chimeric Lysins

This chapter is being edited and formatted for imminent submission.

Abstract

Four *B. cereus*-specific chimeric lysins, named ClyBC1, ClyBC2, ClyBC3, and ClyBC4, were engineered by domain shuffling of divergent EADs and similar SH3-family CBDs of the previously identified *B. cereus* bacteriophage-derived endolysins, PlyP56, PlyN74, and PlyTB40. Chimeric lysins ClyBC1 and ClyBC2 share the Peptidase_M15_4/VanY superfamily EAD of PlyP56 and have SH3-family PlyN74 and PlyTB40 CBDs, respectfully. In contrast, ClyBC3 and ClyBC4 share the SH3-family PlyP56 CBD and have divergent PlyN74 T7 lysozyme-type Amidase_2 and PlyTB40 carboxypeptidase T-type Amidase_3 EADs, respectively. Lytic activity of all chimeric lysins, except for ClyBC2 (SH3-family CBD of PlyTB40), was comparable to their most active PlyP56 predecessor tested against *B. cereus* ATCC 4342 cells, which suggests interchangeable nature of the Peptidase_M15_4, Amidase_2, and Amidase_3 EADs in conjunction to 94% identical SH3-family CBDs of PlyP56 and PlyN74. All chimeric lysins retained their host specificity to *B. cereus* species efficiently lysing mid-log cultures bacilli at concentrations 10 µg/mL. Additionally, I made chimera between PlyP56 and PlyG, a *B. anthracis* specific endolysin, which I named ClyBCBA1 that contained the PlyP56 EAD and the PlyG Amidase02_C CBD. I extended host specificity of the ClyBCBA1 chimera to *B. anthracis* species, yet, the activity was only one third of the activity of the parental PlyG endolysin. ClyBCBA1 retained PlyG lytic pattern with the most effective lysis of *B. anthracis* Ames 35 strain compare to the UM23 strain. Low enzymatic activity of ClyBCBA1 suggests that its L-alanoyl-D-glutamate peptidase originated from the PlyP56 lysin does not efficiently cleave the covalent bonds in peptidoglycan substrate of *B. anthracis* in comparison with the N-acetylmuramoyl-L-alanine EAD of PlyG fused with the PlyG Amidase02_C CBD. The CBD sequence alignments showed a conserved motif in all CBDs originating from *B. cereus*- specific lysins that was different from the known PlyG biding peptide

motif, yet, it shared conserved amino acids elucidating a binding of these CBDs to both the stationary and mid-log bacilli of *B. cereus* and *B. anthracis* species that might occur via distinct to PlyG ligand. These results demonstrate that rational design of functional modular lysins with desired lytic properties against the *B. cereus sensu lato* group of bacilli requires not only knowledge of the enzymatic properties of candidate EADs, but also the binding properties of CBDs in addition to the knowledge of divergent in *Bacillus* species secondary cell wall structures that may or may not obstruct enzymatic units from lysing its PG substrate.

3.1 Introduction

Bactericidal properties of phage-encoded enzymes, endolysins, have been researched with high interest for over past two decades (Fischetti, 2018; Moak and Molineux, 2004). This interest has recently been revived due to emergence of highly volatile pathogenic bacteria with broad-range antibiotic resistance across different bacterial families (Ventola, 2015; Zaman et al., 2017). Since treatment of such pathogens is limited due to their antibiotic resistance pattern, an application of phage-encoded enzymes to alternate or enhance the therapeutic effect of antibiotics is highly desirable (Alisky et al., 1998; Haddad Kashani et al., 2017; Kutsuna et al., 2017). Endolysins from phages infecting Gram-positive bacteria have a modular structure typically composed of divergent N-terminal EADs and species-specific C-terminal CBDs (Fischetti, 2010; López and García, 2004). CBDs enable proper localization of the endolysins to the PG substrate by binding conserved secondary cell wall structures on the cellular surface of their bacterial host, while divergent EADs have evolved to cleave conserved covalent bonds in the PG substrate of their host bacteria (Schmelcher et al., 2012).

The modular organization of endolysins enables interchange of these domains between different endolysins with the aim to enhance their lytic capabilities via addition of EADs with known lytic properties (Gerstmans et al., 2018; Low et al., 2011) or redirecting their host preferences by interchanging species-specific CBDs (Lopez et al., 1997). Additionally, since EADs target different bonds in the PG substrate, creating chimeras by adding multiple EADs to target different bonds within the PG substrate (Becker et al., 2016) or enhancing endolysin binding affinity with the addition of CBDs in tandem repeats (Schmelcher et al., 2011) is rationally possible. These engineering strategies have been employed with some success to date to create effective antibacterial recombinant lysins (Croux et al., 1993; São-José, 2018).

Moreover, it has been experimentally proven that purified recombinant endolysins can be effectively utilized to control contamination in food with *B. cereus* (Kong and Ryu, 2015; Na et al., 2016) and other Gram-positive bacilli like *Listeria* (Callewaert et al., 2011). The benefits of using endolysins instead of the antibiotics are noteworthy. Since endolysins target evolutionarily conserved bonds in the PG substrate of the bacterial cell wall, resistance to endolysins have not yet been observed (Nelson et al., 2012). On the contrary, multiple reports describe alarming resistance of bacteria to broad-range antibiotics, which brings up the necessity to look for alternative antibacterials.

Previously, I identified and characterized the PlyP56, PlyN74 and PlyTB40 endolysins from *Bacillus* – specific bacteriophages (bacillus.phagesdb.org) and have shown that PlyP56 possesses the highest bacteriolytic activity against *B. cereus* strains. In this study, I created chimeric lysins, which I called ClyBC1, ClyBC2, ClyBC3, and ClyBC4, by fusion of divergent EADs with the CBDs from three wild type endolysins. I was able to rescue lytic activity of all chimeras except for ClyBC2 to the level of PlyP56 activity against *B. cereus* ATCC 4342 strain. ClyBC2 has 52% homology in its CBD sequences to other chimeric lysins. Additionally, I fused the most enzymatically active PlyP56 EAD with the PlyG CBD of a known *B. anthracis* – specific endolysin, and called it ClyBCBA1. This study demonstrated that ClyBCBA1 did not obtain enhanced lytic activity against tested *B. anthracis* species, reaching only to one-third of the activity of parental PlyG on *B anthracis* Ames 35 strain. This suggests that EADs similarly to CBDs might retain specificity to bacterial species, particularly, to the distinct peptidoglycan substrate and the secondary cell wall associated structures that are divergent among different *B. cereus* and *B. anthracis* strains.

3.2 Materials and Methods

3.2.1 Bacterial Strains and Culture Conditions

Bacterial strains *B. cereus* ATCC 4342, *B. cereus* ATCC 11778, *B. cereus* ATCC 13061, *B. thuringiensis* ATCC 10792, and *B. subtilis* ATCC 6051 were purchased from the American Type Culture Collection (ATCC), and the BSL2 *B. anthracis* strains, Ames 35 and UM23, were obtained from the Biodefense and Emerging Infections Research Resources (BEI Resources). Chemically competent DH5α and BL21 (DE3) *E. coli* strains for cloning purposes and protein expression were propagated in Luria–Bertani (LB) broth or LB agar plates (BD Biosciences, Franklin Lakes, NJ, USA) supplemented with 100 µg/ml ampicillin as described previously (Etobayeva et al., 2018). The bacterial strains were stored frozen at -80ºC in 20% (v:v) glycerol and propagated as needed. All chemicals and culture media were acquired from Sigma (St. Louis, MO, USA) unless otherwise stated.

3.2.2 Bioinformatic analysis

Protein sequences were searched with the BLASTP, Pfam, CDD, and SMART databases to map EADs, CBDs, and linker peptides for PCR amplification (Letunic and Bork, 2018; Marchler-Bauer et al., 2017). The net charge at pH 7.4 for peptides was calculated via the Protein calculator (version number 3.4, Scripps Research, La Jolla, CA, USA). Multiple alignments were created with CLUSTALW (Larkin et al., 2007) and BoxShade (version number 3.2, Lausanne, Switzerland) (Hofmann and Baron, 1996). DNA sequences were manipulated to create fusion proteins using the ApE-A plasmid editor (version number 2.0.47, University of Utah, Salt Lake City, UT, USA).

3.2.3 Cloning of Vector Constructs

Standard DNA cloning procedures (Sambrook et al., 1989) have been used for design and cloning of EADs and chimeric fusion proteins. The plasmids, pBAD24::*plyP56*, pBAD24::*plyN74*, pBAD24::*plyTB40* (Etobayeva et al., 2018), and pBAD24::*plyG* (Heselpoth et al., 2015), were used as the templates for PCR amplification of CBD and EAD coding regions of the endolysins PlyP56, PlyN74, PlyTB40, and PlyG, respectfully (see Table 3-1 for a list of primers used in this study). Briefly, EADs with their native linkers and CBDs with C-terminal His-tags were amplified by PCR and purified with the Thermo Scientific™ GeneJET™ PCR Purification Kit following manufacturer's instructions in the first step. DNA fragments in PCR reactions were created with Thermo Scientific™ Phusion High-Fidelity DNA Polymerase. Then, PCR fragments from first two reactions were assembled by second step PCR using overlapping pairs of primers. Fusion constructs with a C-terminal hexahistidine tag (6xHis tag) sequence or EAD sequences with an N-terminal 6xHis tag were separated on 1% Agarose gel. The bands with DNA fragments of the right size were purified from gel with the Thermo Scientific™ GeneJET™ Gel Extraction Kit. Purified constructs were digested with *EcoRI/ XbaI* restriction enzymes and cloned into a pBAD24 backbone vector using *EcoRI-XbaI* restriction sites. T4 DNA ligase and *EcoRI/ XbaI* restriction enzymes were purchased from Thermo Fisher Scientific (Waltham, MA USA). Plasmids with fusion constructs were transformed into the DH5α and BL21 (DE3) competent *E. coli*. Plasmids from ampicillin-resistant colonies were purified with Invitrogen™ PureLink™ Quick Plasmid Miniprep Kit (Thersmo Fisher Scientific, Waltham, MA USA) and sequenced (Macrogen, Seoul, South Korea) to inspect quality of the construct.

3.2.4 Expression and Purification of Chimeric Lysins and EADs

Fusion proteins were expressed and purified in a similar fashion as described previously with some minor modifications (Etobayeva et al., 2018). Briefly, overnight cultures of BL21 (DE3) *E. coli* cells were subcultured at 1:100 ratio (v:v) in LB – ampicillin (100 µg/ml) selective media and propagated at 37ºC until the OD_{600} reached 0.8. The protein expression was induced with L-arabinose (0.25%) and bacterial cultures were returned to incubator for overnight expression at 18°C. The next morning, bacterial cells were pelleted at 5,000 rpm for 10 min. The cell pellets were frozen for 15-20 min at -80ºC. After a freeze-thaw cycle, cell pellets were resuspended in purification buffer (10 mM imidazole and 1 mM phenylmethylsulfonyl fluoride (PMSF)), and then sonicated for 14 min in 3 sec bursts at 20% power output using a Branson Sonifier 450 (VWR Scientific, Radnor, PA, USA). Cellular debris was removed by centrifugation at 12,000 rpm followed by filtration of the supernatant through a 0.45 µm filter (Whatman, Maidstone, UK). Fusion proteins and EAD proteins were purified via the Ni-affinity chromatography using the 5 mL Mini Profinity™ IMAC Cartridges (Bio-Rad, Hercules, CA, USA). Bound proteins were eluted in 10 mL fractions of 20, 50, 100, 250, and 500 mM imidazole and tested for purity by SDS-polyacrylamide gel electrophoresis (SDS-PAGE). Fractions that contained homogenous (% purity) proteins were pooled together and subjected to a buffer exchange against phosphate buffered saline (PBS) at pH 7.4 in 10 kDa molecular weight cut-off Amicon® Ultra centrifugal filter devices (MilliporeSigma, Burlington, MA, USA). Protein concentrations were determined spectrophotometrically (NanoDrop ND-1000) and proteins was stored in 15% glycerol stocks at –80°C.

Table 3-1. Primers used in this study.

Template	Primer pair	Sequence (5' → 3')*	Application
pBAD24::*plyP56*	F'	CGTGAATTCATGCATCATCATCATCATCATG CAATGGCACTGCAGACC	Amplification of *plyP56* EAD with N-terminal 6xHIS tag
	R'	CGTTCTAGATTAATTATCAACGGCACCACC	
pBAD24::*plyN74*	F'	GGTGAATTCATGCATCATCATCATCATCATA ACATCAACACCCAGTAT	Amplification of *plyN74* EAD with N-terminal 6xHIS tag
	R'	CGTTCTAGATTAATTACGTTTTTCATTTGCAC GACG	
pBAD24::*plyTB40*	F'	CGTGAATTCATGCATCATCATCATCATCATG GCACCTATAATGTTCATGGTGGC	Amplification of *plyTB40* EAD with N-terminal 6xHIS tag
	R'	CGTTCTAGATTAGGTACGCTGACCGGTAATT GCATA	
pBAD24::*plyP56*	F'	CGTGAATTCATGGCAATGGCACTGCAGACC	Amplification of *plyP56* EAD for fusion with *plyN74* CBD
	R'	CTGCTATCATAATCGCCACCTGTGCTGCCA	
pBAD24::*plyP56*	F'	CGTGAATTCATGGCAATGGCACTGCAGACC	Amplification of *plyP56* EAD for fusion with *plyTB40* CBD
	R'	CAGCTGCTATCATAGCCACCTGTGCTGCCA	
pBAD24::*plyP56*	F'	CGTGAATTCATGGCAATGGCACTGCAGACC	Amplification of *plyP56* EAD for fusion with *plyG* CBD
	R'	GTTCTGCTTGGTCGGGCCACCTGTGCTGCC	
pBAD24::*plyP56*	F'	AAACCTCCGAGCGGTGATTATGATAGCAGC	Amplification of *plyP56* CBD for fusion with *plyN74* EAD
	R'	CGTTCTAGATTAATGATGATGATGATGATGT TTAAACGTGCCCCAATA	
pBAD24::*plyP56*	F'	GGCAGCACAGGTGGCGATTATGATAGCAGC	Amplification of *plyP56* CBD for fusion with *plyTB40* EAD
	R'	CGTTCTAGATTAATGATGATGATGATGATGT TTAAACGTGCCCCAATA	
pBAD24::*plyN74*	F'	GGTGAATTCATGAACATCAACACCCAGTAT	Amplification of *plyN74* EAD for fusion with *plyP56* CBD
	R'	GCTGCTATCATAATCACCGCTCGGAGGTTT	
pBAD24::*plyN74*	F'	TGGCAGCACAGGTGGCGATTATGATAGCAG	Amplification of *plyN74* CBD for fusion with *plyP56* EAD
	R'	CGTTCTAGATTAATGATGATGATGATGATGT TTAAAGGTGCCCCAATAATTCAC	

pBAD24::*plyTB40*	F’	GGTGAATTCATGGGCACCTATAATGTTCATGGTGGC	Amplification of *plyTB40* EAD for fusion with *plyP56* CBD
	R’	GCTGCTATCATAATCGCCACCTGTGCTGCC	
pBAD24::*plyTB40*	F’	GGCAGCACAGGTGGCGATTATGATAGCAGC	Amplification of *plyTB40* CBD for fusion with *plyP56* EAD
	R’	CGTTCTAGATTAATGATGATGATGATGATGCTGAAAGGTGCCCCAATAGCTAAT	
pBAD24::*plyG*	F’	GGCAGCACAGGTGGCCCGACCAAGCAGAAC	Amplification of *plyG* CBD for fusion with *plyP56* EAD
	R’	CGTTCTAGATTAATGATGATGATGATGATGTTTCACTTCGTACCA	

* Restriction sites underlined

3.2.5 Turbidity Reduction Assay and Host Spectrum

Bacterial lysis was measured as previously described in a dose-dependent fashion (Etobayeva et al., 2018). Subcultures of bacteria in mid-log growth phase and in stationary phase were used for all bacteriolytic assays. The EADs were tested at 10, 25, and 50 µg/mL and fusion proteins were tested for bacterial lysis in final concentrations of 10 µg/mL with a starting OD_{600} of bacterial cell suspensions adjusted in PBS (pH 7.4) to 0.50-0.68. The lysis of bacteria was represented using two approaches. At first, it was quantified as the percentage of lysis (% activity) relative to activity of the PlyP56 or PlyG endolysins at a concentration of 25 µg/mL (Nelson et al., 2012). In the second approach, the change in OD_{600} (ΔOD_{600}) was recorded after incubation of bacteria for 20 min with each fusion protein or EAD. The OD values were normalized against a PBS group, a the ΔOD_{600} in the PBS control group with bacteria was subtracted from the values reported (Loessner et al., 1996).

The host spectrum of activity (see Methods for list of strains) for EADs was tested at 25-50 µg/mL using the turbidity reduction assay as described above. All tested bacteria were subcultured and tested via turbidity reduction during their mid-log phase of growth as well as at their stationary phase. Each experiment was repeated in triplicate on three consecutive days.

3.2.6 Cell wall binding assays and fluorescence microscopy

The binding of single CBDs to bacilli was examined on a variety of *Bacillus* species as described before (Etobayeva et al., 2018). In brief, bacteria in stationary and mid-log phases were incubated with AlexaFluor® 555 labelled CBDs (AlexaFluor® 555 fluorescent dye, ThermoFisher Scientific). Cells were washed twice in PBS and visualized. Images were obtained with an Eclipse 80i epifluorescent microscope (Nikon, Tokyo, Japan) and analyzed with the NIS-Elements software (version number 3.22.15, Nikon).

3.3 Results

3.3.1 Chimera Engineering and Purification

The four *B. cereus* specific chimeric lysins, ClyBC1, ClyBC2, ClyBC3, and ClyBC4, were engineered by domain shuffling of the divergent EADs including native linkers with similar SH3-family CBDs. Chimeric fusion lysins, ClyBC1 and ClyBC2, share the PlyP56 EAD, a L – alanoyl-D–glutamate endopeptidase of the Peptidase_M15_4/VanY superfamily, and each have SH3-family PlyN74 and PlyTB40 CBDs that are 52% homologous in their amino acid (AA) sequence. In contrast, ClyBC3 and ClyBC4 share the SH3-family PlyP56 CBD, but have divergent EADs considting of the PlyN74 T7 lysozyme-type Amidase_2 EAD and the PlyTB40 carboxypeptidase T-type Amidase_3 EAD, respectfully. Additionally, I made a chimera between PlyP56 and PlyG, a *B. anthracis*-specific endolysin, and named it, ClyBCBA1. It comprises the PlyP56 EAD and the PlyG CBD of Amidase02_C origin. Separately, I amplified all EADs with N-terminal 6xHis tags and without the corresponding linker. All DNA fragments were amplified from the native *B. cereus* bacteriophage-derived endolysins, PlyP56, PlyN74, and PlyTB40 (Fig. 3-1A) that have been previously identified and characterized (Etobayeva et al., 2018)

EADs and chimera constructs were subcloned into the pBAD24 vector and transformed into BL21 *E. coli* for protein expression. Following overexpression and purification, fractions with soluble fusion proteins and EAD proteins were purified by nickel affinity chromatography and run on SDS-PAGE for purity confirmation. The size of PlyP56, ClyBC1, ClyBC2, ClyBC3, ClyBC4, and ClyBCBA1 bands on SDS-PAGE corresponds to 28.5 kDa, 28.5 kDa, 28.1 kDa, 31.4 kDa, 30.4 kDa, and 26.9 kDa, respectively (Figure 3-1B), and the size of corresponding EADs from P56, N74, and TB40 correspond to 17.6 kDa, 19.7 kDa, and 19.7 kDa, respectfully (Figure 3-1C).

A

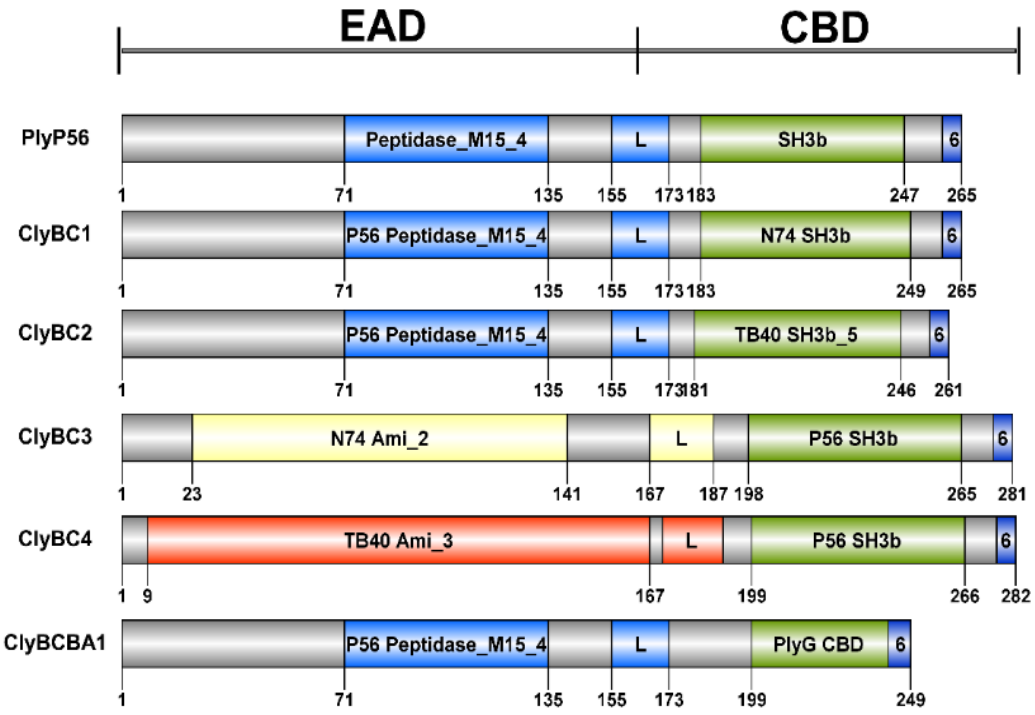
EAD
CBD
PlyP56
Peptidase_M15_4
L
SH3b
6
1 71 135 155 173 183 247 265
ClyBC1
P56 Peptidase_M15_4
L
N74 SH3b
6
1 71 135 155 173 183 249 265
ClyBC2
P56 Peptidase_M15_4
L
TB40 SH3b_5
6
1 71 135 155 173 181 246 261
ClyBC3
N74 Ami_2
L
P56 SH3b
6
1 23 141 167 187 198 265 281
ClyBC4
TB40 Ami_3
L
P56 SH3b
6
1 9 167 199 266 282
ClyBCBA1
P56 Peptidase_M15_4
L
PlyG CBD
6
1 71 135 155 173 199 249

B

.

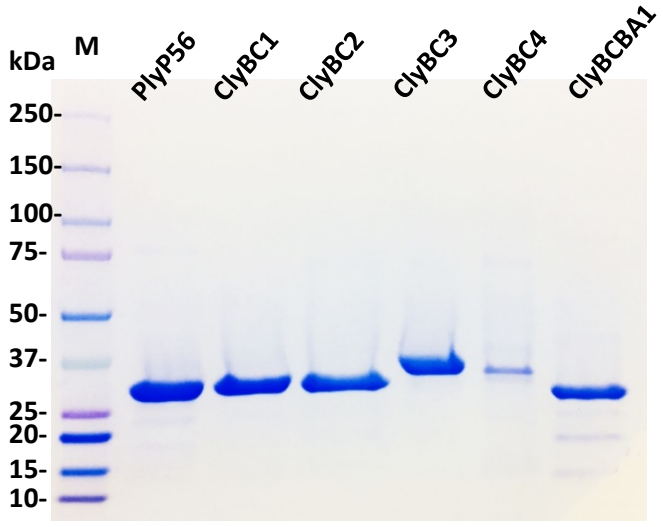
kDa
M
PlyP56
ClyBC1
ClyBC2
ClyBC3
ClyBC4
ClyBCBA1
250-
150-
100-
75-
50-
37-
25-
20-
15-
10-

C

.

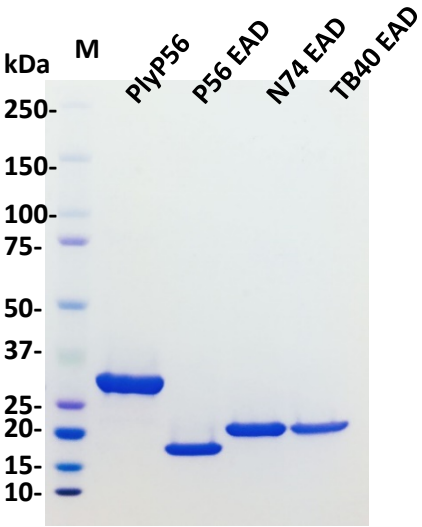
kDa
M
PlyP56
P56 EAD
N74 EAD
TB40 EAD
250-
150-
100-
75-
50-
37-
25-
20-
15-
10-

Figure 3-1. Engineered fusion proteins and SDS-PAGE protein profiles. (**A**) Schematic representation of different constructs. EADs and CBDs are color coded according to their wild type predecessors, PlyP56, PlyN74, and PlyTB40: Blue - Peptidase_M15_4 EAD of PlyP56; Yellow - an Amidase_2 EAD of PlyN74; Red - an Amidase_3 EAD of PlyTB40; Green – CBDs; (L) – linker peptide color coded to match native lysins; (6) – C-terminal His tag. All three EADs are divergent. All CBDs are SH3-family binding domains. The P56 CBD has 94% homology to the N74 CBD, and 52% homology to the TB40 CBD. The PlyG CBD belongs to the Amidase02 C family and is not homologous to SH3-family CBDs. (**B**) SDS-PAGE of engineered chimeras stained with Coomassie blue. Lane 1, molecular mass markers as indicated; Lane 2, wild-type PlyP56; Lane 3, ClyBC1; Lane 4, ClyBC2; Lane 5, ClyBC3; Lane 6, ClyBC4; Lane 7, ClyBCBA1. (**C**) EAD protein samples were analyzed for purity by SDS-PAGE and Coomassie blue staining. Lane 1, molecular mass markers as indicated; Lane 2, wild-type PlyP56; Lane 3, P56 EAD; Lane 4, N74 EAD; Lane 5, TB40 EAD.

3.3.2 EADs Lytic Activity

To determine whether truncated EADs sustained their enzymatic activity in the absence of CBDs, I tested their activity at physiological pH 7.4 at the concentrations ranging from 10 µg/mL to 50 µg/mL using mid-log cell suspensions of a variety of *B. cereus* strains from our collection (see our previous work for list of strains) (Etobayeva et al., 2018). The native full-length PlyP56 endolysin served as the control. I was unable to detect lytic activity conferred by the P56, N74, or TB40 EADs at tested concentrations on any of the tested strains. It was a surprising finding, since I expected that the P56 EAD would show enhanced lytic activity due an overall positive net charge carried by this EAD domain. Previously, it was shown that the subset of EADs with positive net-charge on their catalytic domain from the *B. anthracis* specific endolysins, PlyL, PlyG, and PlyBa04, displays strong lytic activity to *B. anthracis* compare to full-length enzymes. For some of these EADs, truncation also broadened their host range activity beyond *B. anthracis* species expending it to *B. cereus* or *B. subtilis* species (Low et al., 2011).

To further elucidate this findings, I calculated net charge for EADs, CBDs, and adjacent peptides for native PlyP56 and all chimeras (Table 3-2). I discovered that despite the overall net positive charge on the P56 EAD, the majority of the net charge (+4.8) is due to the leader peptide adjacent to the EAD, but not on the EAD itself. The charge of the P56 EAD on its own was actually negative (-1.1) as well as the net charges on the N74 EAD (-0.7) and TB40 EAD (-3.0). In comparison, net charge on PlyG EAD (+0.9) was positive in addition to positively charged leader peptide (+1.8). This finding might explain why our truncated EADs do not show lytic activity at the given concentrations.

Table 3-2. Correlation between domain architecture and net charge

Lysin	EAD domain architecture	Net charge, Z[1]						
		Leader peptide	EAD	EAD C-term peptide	Linker	CBD	CBD C-term peptide	Total charge
PlyP56	Peptidaze_M15_4/VanY	4.8	-1.1	-2.2	-0.2	1.8	2.8[2]	5.9
PlyG	Ami_2/PGRP	1.8[2]	0.9	-	-0.2	-0.2	0.8	3.1
ClyBC1	Peptidaze_M15_4/VanY	4.8	-1.1	-2.2	-0.2	0.8	2.8[2]	4.9
ClyBC2	Peptidaze_M15_4/VanY	4.8	-1.1	-2.2	-0.2	-0.1	0.8[2]	2.0
ClyBC3	Ami_2/PGRP	-0.2	-0.7	1.8	-0.2	1.8	2.8[2]	5.3
ClyBC4	Ami_3/MurNAc-LAA	-0.1	-3.0	0.8	-0.2	1.8	2.8[2]	2.1
ClyBCBA1	Peptidaze_M15_4/VanY	4.8	-1.1	-2.2	-0.2	-0.2	0.8[2]	1.9

[1]The net charge of peptides was estimated at physiological pH 7.4 using the Protein calculator version number 3.4 (The Scripps Research Institute, La Jolla, CA, USA).

[2]The positive charge (+0.7) of 6xHis tag was excluded from this table.

3.3.3 Combination of Divergent EADs with Homologous CBDs Rescues Lytic Activity of Chimeras to the Level of Native PlyP56 Endolysin

Lytic activity of all chimeric lysins was assayed via turbidity reduction assay against mid-log and stationary phase bacterial cultures of *B. cereus* ATCC 11778 and *B. cereus* ATCC 13061 at a final concentration 10 μg/mL. Results were interpreted as an overall decrease in OD of the bacterial cell suspension and the % activity normalized to 100% activity of the native PlyP56 lysin to determine the rate of PG lysis. I was able to rescue activity of all chimeras to the level of the wild-type PlyP56 lysin against mid-log cultures of *B. cereus* ATCC 11778 (Figure 3-2C). In contrast, only ClyBC1 was equally effective in lysing mid-log cultures of *B. cereus* ATCC 13061 (Figure 3-2D). Stationary phase cultures of both *B. cereus* strains were also effectively lysed only by PlyP56 and ClyBC1, which shared the L–alanoyl-D–glutamate peptidase EAD of PlyP56, in addition to the N74 CBD, which shares 94% homology to the PlyP56 CBD (Figure 3-2E,F). Although, lytic activity of both enzymes was four times lower in *B. cereus* ATCC 13061 than in *B. cereus* ATCC 11778 (Figure 3-2A,B), despite low rate of PG hydrolysis both lysins at the end of 20 min assays effectively lysed both mid-log and stationary bacterial cultures. (Figure 3-2C-F).

The ClyBC4 chimera with the Ami_3 TB40 EAD fused with the P56 CBD caused approximately ~50% lysis in both strains in stationary phase cultures, while ClyBC3 with the Ami_2 N74 EAD fused with TB40 CBD was less effective in lysis of stationary bacilli and mid-log bacilli of *B. cereus* ATCC 13061 (Figure3-2D). Surprisingly, ClyBC2 also possesses the L–alanoyl-D–glutamate peptidase EAD of PlyP56 fused with TB40 CBD, but it was not effective in lysing any stationary bacterial cultures or mid-log bacterial cells of *B. cereus* ATCC 13061.

Here I confirmed the interchangeable nature of divergent L–alanoyl-D–glutamate peptidase, Ami_2, or Ami_3, which are both N-acetylmuramoyl–L–alanine amidases. These EAD

architectures are not unusual among *Bacillus* specific endolysins. It appears that amidases are often found in the *B. cereus* and *B. anthracis* specific endolysins. An Ami_2 enzymatic domain was discovered and characterized in the *B. cereus* specific LysPBS13 lysin (Park et al., 2012). The Ami_3 domain has been found more often in endolysins of the phages infecting *B. cereus* species, such as LysPBC1 and LysPBC4, which contain this domain architectures (Kong and Ryu, 2015; Na et al., 2016). However, the L–alanoyl-D–glutamate peptidase of PlyP56 has only one endolysin with similar architecture, LysB4, that was previously characterized (Son et al., 2012).

All chimeric lysins retained their host specificity to *B. cereus* species efficiently lysing mid-log cell suspensions at a concentration 10 μg/mL. This is not surprising since all of them where amplified from the endolysins specific to *B. cereus* species. The ClyBC1, ClyBC3, and ClyBC4 chimeras generated with the P56 and N74 CBDs that shared 94% identity in their AA sequence were more enzymatically active in combination with the L–alanoyl-D–glutamate peptidase and Ami_3 TB40 EADs, and less effective with the Ami_2 N74 EAD on stationary cultures of the *B. cereus* strains. ClyBC2, the chimera with an L–alanoyl-D–glutamate peptidase fused to the SH3-family TB40 CBD that was only 52% homologous to the P56 and N74 CBDs rendered itself less effective in lysis of stationary *B. cereus* cultures.

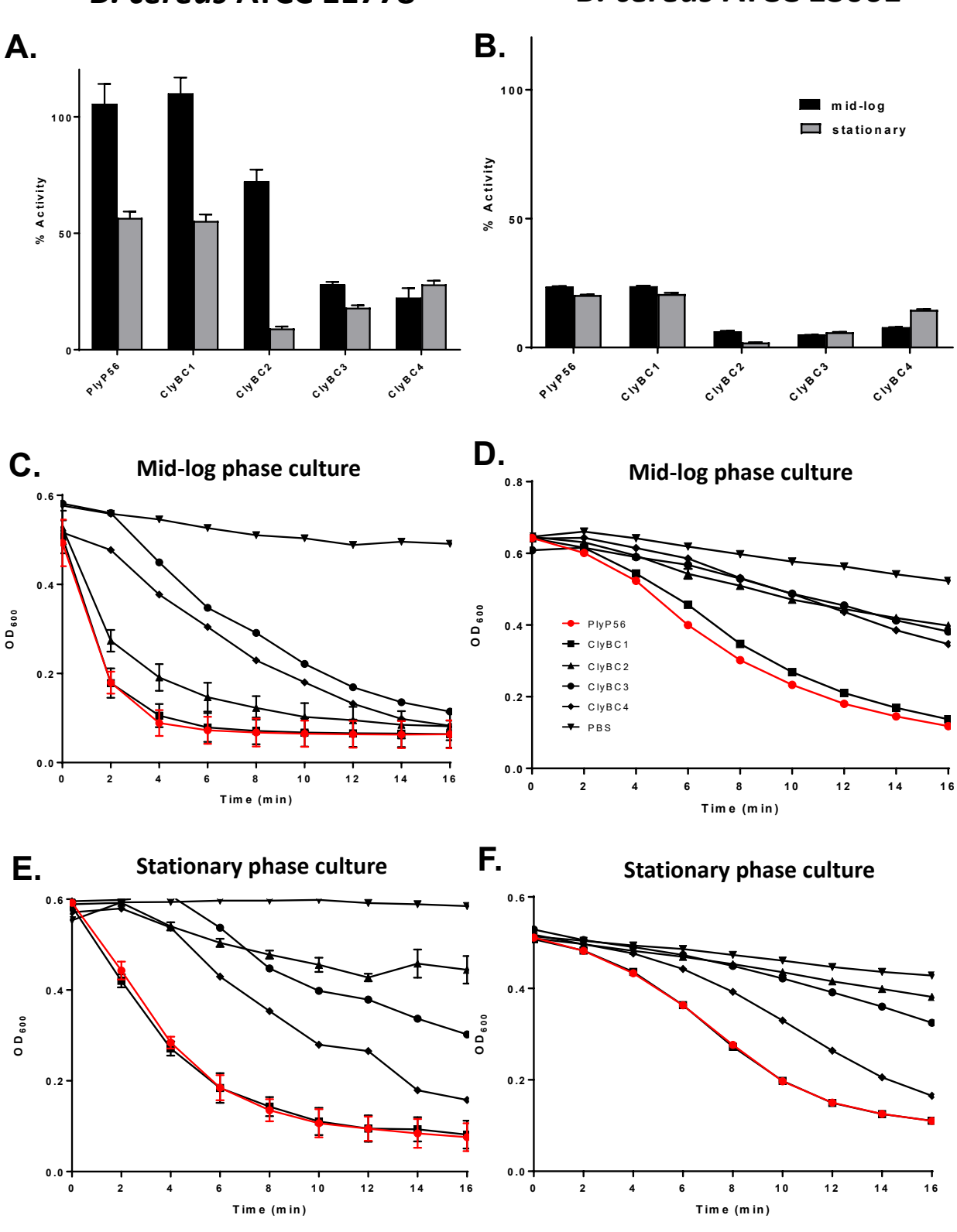
B. cereus ATCC 11778
B. cereus ATCC 13061
A.
B.
% Activity
100
50
0
PlyP56
ClyBC1
ClyBC2
ClyBC3
ClyBC4
mid-log
stationary
C.
Mid-log phase culture
D.
Mid-log phase culture
OD600
Time (min)
PlyP56
ClyBC1
ClyBC2
ClyBC3
ClyBC4
PBS
E.
Stationary phase culture
F.
Stationary phase culture

Figure 3-2. Lytic activities of native PlyP56 endolysin and chimeric lysins against mid-log and stationary cultures of *B. cereus* ATCC 11778 (A, C, E) and *B. cereus* ATCC 13061 (B, D, F). (**A**, **B**) PlyP56, ClyBC1, ClyBC2, ClyBC3, and ClyBC4 lytic activity comparison. Mid-log bacterial cultures (black bars) and stationary bacterial cultures (grey bars) at their final OD ranging from 0.50 to 0.68 were incubated with chimeric lysins at a concertation 10 μg/mL for 20 min. duration of the turbidity reduction assay as described in Methods. The lytic activity was normalized to 100% activity of native PlyP56 (control). (**C**, **D**) Lysis curves represent the changes in optical density of mid-log phase bacterial cultures over a period of 20 min after addition of PlyP56, ClyBC1, ClyBC2, ClyBC3, and ClyBC4 to cell suspensions. (**E**, **F**) Lysis curves represent the changes in optical density of stationary phase bacterial cultures for 20 min period after addition of PlyP56, ClyBC1, ClyBC2, ClyBC3, and ClyBC4 to cell suspensions. All experiments were run in triplicates. The error bars represent standard deviations.

3.3.4 Fusion ClyBCBA1 chimera gains moderate B. anthracis lytic activity

Because all three native endolysins, PlyP56, PlyN74, and PlyTB40, that I used as the templates to amplify EADs and CBDs have been down selected from the phages infecting *B. cereus* species, I engineered the ClyBCBA1 chimera by fusion of most active L-alanoyl–D–glutamate EAD of PlyP56 with the Amidase02_C CBD originating from the *B. anthracis* specific endolysin, PlyG. Moreover, despite the fact that the P56, N74, and TB40 CBDs bound to *B. anthracis* Ames 35 and *B. anthracis* UM23 bacilli (Figure 3-3A), I did not observed lysis in turbidity reduction assays of *B. anthracis* bacilli using our native endolysins (Etobayeva et al., 2018).

ClyBCBA1, a combination of the P56 EAD with the Amidase02_C CBD of PlyG was able to lyse *B. cereus* ATCC 4342 cells almost as efficiently as the native PlyG lysin (Figure 3-3B). ClyBCBA1 showed minor lysis of *B. cereus* ATCC 13061 cells in comparison to PlyG, which to our surprise caused decrease in OD about 1/3 of the lysis of *B. cereus* ATCC 4342 cells. Both lysins were inactive or had very minor effect on the cells of *B. thuringiensis* ATCC 10792 and *B. subtilis* ATCC 6051. Additionally, ClyBCBA1 had acquired an extended to *B. anthracis* species host range, yet, the OD decrease caused by ClyBCBA1 was comparable to only one third of the activity observed for the PlyG endolysin tested in both *B. anthracis* Ames 35 and UM23 strains. ClyBCBA1 retained the PlyG lytic pattern with the most effective lysis of the *B. anthracis* Ames 35 strain compared to the UM23 strain.

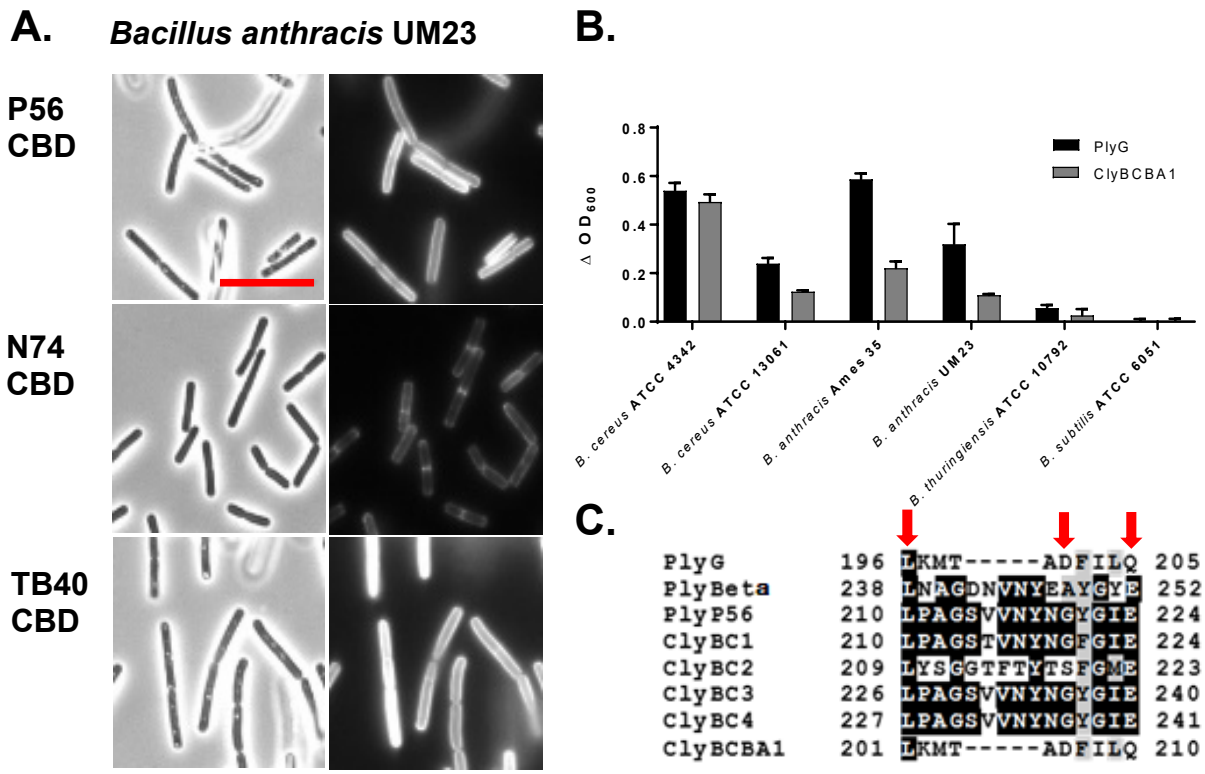

Figure 3-3. CBDs binding, lytic activities and sequence alignment. (**A**) Binding of AlexaFluor-labeled CBDs, P56, N74, and TB40, to the cell walls of *B. anthracis* UM23 bacilli. Bright field images (column 1) are shown next to their corresponding fluorescent images (column 2). Images were taken using epifluorescent microscopy. Red scale bar = 5µm. (**B**) Lytic activity of PlyG (black bars) and ClyBCBA1 (grey bars). The turbidity reduction assay was done with mid-log cultures. Bacterial cells were resuspended to OD 0.50 - 0.68 and treated with 25 µg/mL final concentration of PlyG or ClyBCBA1. All experiments were done in triplicate. The error bars represent standard deviations. (**C**) Sequence alignment of PlyG, Plyβ, PlyP56, ClyBC1, ClyBC2, ClyBC3, ClyBC4, and ClyBCBA1. Shown here is the homologous region alignment with the PlyG binding peptide (Kikkawa et al., 2007). AA residues critical for binding marked with red arrow. Identical residues shaded in black.

3.3.5 CBD alignment reveled conserved motif

It was unanticipated to discover that ClyBCBA1, chimeric lysin with the L-alanoyl–D–glutamate of PlyP56 EAD fused with PlyG CBD showed low lytic activity against mid-log bacilli of *B. anthracis* species in comparison to PlyG, even though it had identical activity to PlyG in lysing *B. cereus* ATCC 4342, a known *B. cereus* transition to *B. anthracis* strain. The Amidase02_C CBD of PlyG is known to confer a high degree of specificity to the PG of *B. anthracis* species (Schuch et al., 2002). I aligned the AA sequences of native PlyP56 and the chimeric lysins to PlyG and Plyβ, another *B. anthracis* specific endolysin that can bind and lyse both mid-log and stationary bacterial cultures (Paskaleva et al., 2015). I discovered that all three *B. cereus* specific CBDs, P56 of PlyP56, ClyBC3, and ClyBC4; N74 of ClyBC1; and TB40 of ClyBC2, had a high degree of homology with the CBD of Plyβ (Figure 3-3C).

An alignment shows a highly conserved (LxxGxxxxYxx[Y]Gx[E]) motif between Plyβ and all three *B. cereus* specific CBDs, where Tyr [Y] and Glu [E] AA residues can be substituted with Phe [F] and Gln [Q] in the PlyG CBD, respectfully. Negatively charged Glu and uncharged Gln side chains (R-groups) share a similar stereo spatial configuration, as well as R-groups of aromatic AAs, uncharged Tyr, and nonpolar Phe, respectfully, so the substitution of these AAs in the alignment is reasonable at tested neutral pH 7.4. These are hydrophobic AAs, commonly found on the outside of proteins that frequently engage in hydrogen bonds (Gln, Tyr), ionic bonds (Glu) or Vander Waals interactions (Phe) (Nelson and Cox, 2013).

Alignment of the PlyG binding peptide (Figure 3-3C) shows three conserved key AA residues, nonpolar Leu_{196} [L], negatively charged Asp_{201} [D], and uncharged Gln_{205} [Q], which are marked with the red arrows. These three AAs facilitate binding of the PlyG peptide to a ligand expressed on the surface of *B. anthracis*. "Loss of function" mutations revealed that either Leu_{196}

or Gln_{205} on their own can facilitate binging of the peptide in absence of other two AAs (Kikkawa et al., 2007). The numbering of AAs is slightly skewed in this alignments in account for the N-terminal 6xHis tag in PlyG clone. Based on the alignment, I identified a highly conserved Leu_{196} residue in all CBDs, corresponding to Leu_{210} in PlyP56 and ClyBC1, Leu_{209} in ClyBC2, Lue_{226} in ClyBC3, and Leu_{227} in ClyBC4. A second residue, $Gln_{205,}$ was substituted to Glu_{252} in Plyβ as well as in all our chimeras, Glu_{224} in PlyP56 and ClyBC1, Glu_{223} in ClyBC2, Glu_{240} in ClyBC3, and Glu_{241} in ClyBC4, which is an acceptable substitution as described earlier.

Additionally, I discovered that the P56 CBD of PlyP56 and the N74 CBD of ClyBC1 amplified from PlyN74 had only two point mutations in their binding motifs, (Val $[V]_{215}$→Thr $[T]_{215}$) and (Tyr$[Y]_{221}$→Phe$[F]_{221}$) that might have affected binding affinity of CBDs. I tested binding of equal concentrations of the P56, N74, and TB40 CBDs to bacilli of *B. anthracis* UM23 (Figure 3-3A), and *B. anthracis* Ames 35 (Etobayeva et al., 2018) and noticed that AlexaFluor labeled N74 CBDs uniformly bound the ligand expressed on the surface of *B. anthracis* UM23 bacilli, albeit, less effectively than the P56 TB40 CBDs. I made similar observations for the CBD binding to the *B. anthracis* Ames 35 cells (Etobayeva et al., 2018).

3.4 Discussion

Bacteriophage-encoded endolysins are alternative antimicrobials with targeted specificity to pathogenic species. They can enhance antibiotic action by synergistic effects (Becker et al., 2008; García et al., 2010), and, in some applications, perhaps, can even replace failing conventional antibiotics. Phage have been studied for about a century now (Twort, 1915), however, the lytic potential of their endolysins was not subject of research until the late 20th century (Loeffler et al., 2001; Lopez et al., 1997; Schuch et al., 2002). There are a number of publically accessible

databases that contain sequences of phage encoded endolysins (Wu et al., 2014). Since phage endolysins have proven to be highly specific to the host bacteria, this feature can be enhanced by molecular engineering to render desirable host specificity (Schmelcher et al., 2011). Lytic properties of the enzymatic domains can also be modified via active site mutagenesis (Mayer et al., 2011). Furthermore, biochemical and biophysical characteristics of endolysins can be enhanced to render them more desirable as stable recombinant proteins (Heselpoth et al., 2015). Despite these extensive investigations, today only a limited number of endolysins have been characterized in detail, and none of them have been approved yet for use in human therapy.

The chimeric *Bacillus*-specific lysins engineered in this study have demonstrated the interchangeable nature of the three divergent EADs, an L–alanoyl-D–glutamate endopeptidase of the Peptidase_M15_4/VanY superfamily, a T7 lysozyme-type Amidase_2 of the PGRP superfamily, and a carboxypeptidase T-type Amidase_3 of the MurNAc-LAA superfamily in combination with SH3-family CBDs. The resulting chimeric lysins were named ClyBC1, ClyBC2, ClyBC3, and ClyBC4. A comprehensive study on the modular recombination of endolysins has previously been investigated for *Listeria* phage endolysins (Schmelcher et al., 2010) and pneumococcal/clostridial lysins (Croux et al., 1993).

The EAD architectures of the T7 lysozyme-type Amidase_2 domain of the PGRP superfamily (Etobayeva et al., 2018; Park et al., 2012) and the carboxypeptidase T-type Amidase_3 of the MurNAc-LAA superfamily (Etobayeva et al., 2018; Kong and Ryu, 2015; Na et al., 2016) are often found in *B. cereus* and *B. anthracis*-specific phage endolysins (Low et al., 2005; Park et al., 2018). It is noteworthy that the L–alanoyl-D–glutamate peptidase of the Peptidase_M15_4/VanY superfamily is only the second endopeptidase discovered to date in *B. cereus*-specific phages and none have been discovered in *B. anthracis*-specific phages (Son et al.,

2012). This type of EAD may be specific to the PG substrate of *B. cereus* and *Listeria* species. Ply500, an endolysin from a *Listeria* phage, is a structural homolog to the PlyP56 EAD, which suggests that this architecture can also occur in *Listeria*-specific phages (Korndörfer et al., 2008).

To test the L-alanoyl-D-glutamate endopeptidase lytic activity on *B. anthracis* cells, I made the ClyBCBA1chimera by fusion of the PlyP56 the EAD with the Amidase02_C CBD of PlyG, a *B. anthracis*-specific endolysin. Based on this combination, the PlyG CBD would confer specificity to the chimera for recognition of the *B. anthracis* cell wall (Schuch et al., 2002). However, upon testing, this combination had low lytic activity (~1/3 that of PlyG) against *B. anthracis* Ames 35 and *B. anthracis* UM23 strains. It is possible that the L-alanoyl-D-glutamate endopeptidase of PlyP56 was not as effective as the Ami_2 or Ami_3 amidases in lysis of PG substrate of *B. anthracis* species, although, the CBD of PlyG bound *B. anthracis* bacilli in both mid-log and stationary bacterial cultures (Paskaleva et al., 2015).

The Amidase_2 (Kikkawa et al., 2008; Schuch et al., 2002), Amidase_3 (Park et al., 2018), and GH25 (Paskaleva et al., 2015; Yoong et al., 2006) domain architectures have been discovered in endolysins of phages infecting *B. anthracis* species. The Ami_2 domain of PlyG and the Ami_3 domain of the AP50-31 lysins are both associated with N-acetylmuramoyl-L-alanine enzymatic activity, and the GH25 domain is reported to have PlyB-like muramidase activity. Based on this information, I believe the L-alanoyl–D–glutamate of PlyP56,a *B. cereus*-specific endolysin, is more effective in hydrolysis of the *B. cereus* PG, which is divergent in its secondary cell wall polymers (Schaffer & Messner, 2005) and in many cases lacks an S-layer (Mesnage et al., 1999), than its hydrolysis of the *B. anthracis* PG, although, both have similar DAP-type PG of the Gram-positive species. Since the L–alanoyl-D–glutamate peptidase has not been discovered in phages infecting *B. anthracis* species, I think it has been limited to *B. cereus* species only. This specificity

might be very useful in speciation of these two species apart from one another. Another explanation could be that the combination of the L–alanoyl-D–glutamate peptidase with the Amidase02_C CBD in contrast to the SH3-family CBD of the native PlyP56 lysin might have conferred improper conformation of the recombinant lysin that affected the orientation of the EAD relative to the position of its PG substrate (Schmelcher et al., 2011).

On the contrary, *B. cereus*-specific chimeric lysins created by domain shuffling of either the L–alanoyl-D–glutamate peptidase, the Ami_2 PGRP EAD, or the Ami_3 MurNAc-LAA with SH3-family CBDs of homologous P56, N74, and TB40 CBDs, were equally effective in lysing mid-log culture cells of *B. cereus* ATCC 11778. In contrast, only ClyBC1, a combination of the P56 L–alanoyl-D–glutamate peptidase fused with the N74 CBD, efficiently lysed mid-log culture cells of *B. cereus* ATCC 13061, and additionally lysed stationary phase cultures of both strains. I also observed loss of function in the ClyBC2 chimera, a combination of the L–alanoyl-D–glutamate peptidase fused with the TB40 CBD that shared only 52% identity with the P56 and N74 CBDs. It was not effective in lysis of either mid-log cultures of *B. cereus* ATCC 13061 or the stationary cultures of both strains. My observation confirms that switching CBDs, even in highly related endolysins, swapped their binding and lytic activities, yet, their host range driven by CBDs, remained limited to *B. cereus* species. Similar findings were observed for chimeric constructs of pneumococcal phage lysins and pneumococcal-lactococcal lysins (Díaz et al., 1990; Sheehan et al., 1996)

It has been reported in the literature that lysins truncated to just their EADs can retain strong bacteriolytic activity in the absence of CBD (Cheng and Fischetti, 2007). Despite that the N-terminal EADs that I studied here did not lyse PG in absence of their CBDs. An activity independent of the CBDs is speculated to be associated with the net positive charge on it's EAD.

However, I discovered that the L–alanoyl-D–glutamate peptidase of the Peptidase_M15_4 VanY superfamily, the T7 lysozyme-type Amidase_2 of the PGRP superfamily, and the carboxypeptidase T-type Amidase_3 of MurNAc-LAA superfamily tested here, actually, had net negative charge on the globular domain of their EADs, even if the leader or linker sequences had a strong positive charge. In fact, the majority of the net charge for the L–alanoyl-D–glutamate peptidase, the most efficient at lysis of *B. cereus* bacilli, was on the N-terminal peptide adjacent to EAD. It has been reported that truncation of PlyG and PlyL to EADs with a net positive charge on their EAD retained lytic activity, although it was much lower in comparison to the full-length native endolysins. Additionally, the truncated EADs, lacking the specificity of the CBDs, displayed a broadened host range that included other *Bacillus* species (Low et al., 2011). Since studied here EADs had a net negative charge and lacked independent activity, obtained data supports the "charge" hypothesis for EAD activity in the absence of CBDs.

Modular CBDs confer targeted specificity to endolysins by binding conserved ligands on the surface of the bacteria (Fischetti, 2010). In general, CBD swapping has proven to be effective in expanding or completely changing the host range of chimeras (Schmelcher et al., 2011). According to this, an Amidase02_C CBD of PlyG would have conferred a high degree of specificity to the chimeras by recognition of a conserved ligand on the cell wall of *B. anthracis* species (Schuch et al., 2002). Since lytic activity of PlyG was primarily directed towards mid-log bacteria, I aligned CBD AA sequences to Plyβ, an endolysin that lyses stationary *B. anthracis* cells, and the PlyG peptide that facilitates binding to *B. anthracis* cell wall (Kikkawa et al., 2007).

I discovered conserved AA motif (LxxGxxxxYxx[Y]Gx[E]) in all three *B. cereus*-specific CBDs with high degree of conservation to Plyβ sequence that recognizes a ligand on the cell wall of stationary bacilli (Paskaleva et al., 2015). All three CBDs had conserved AAs similar to a key

AA, Leu [L], of the binding peptide identified in the PlyG CBD, where Leu_{196} [L] and Gln_{205} [Q], each on their own could facilitate binding of PlyG peptide to the cell wall of *B. anthracis* (Kikkawa et al., 2007). I observed that Tyr [Y] and Glu [E] AA residues in this motif could be substituted with Phe [F] and Gln [Q], respectfully. All AA substitutions were possible due to similar stereo special configuration of their R-groups. These hydrophobic AAs commonly found on the outside of proteins are frequently engage in hydrogen bonds (Gln, Tyr), ionic bonds (Glu) or Vander Waals interactions (Phe) (Nelson and Cox, 2013). Additionally, I found two point mutations in this motif in *B. cereus*-specific P56 and N74 CBDs, ($V_{215}\rightarrow T_{215}$) and ($Y_{221}\rightarrow F_{221}$), respectfully, that might have effect on binding affinity of these CBDs to different *Bacillus* species. I have not established yet if all these CBDs bind a similar ligand or whether they bind the same ligand as Plyβ. Taken together, these findings suggest that the CBDs have diverged by acquiring point-mutations in their binding peptides, which allowed for altered specificity to match the target ligand expressed on cell wall of different *Bacillus* species.

In conclusion, this work provides novel chimeric lysins that can be used for control of *B. cereus* pathogens. It identifies potential *B. cereus* specific binding peptides that can be further tuned to discover binding ligands and utilized to expand the host range activity of these enzymes. Finally, this work shows that modular engineering of chimeras by domain shuffling requires knowledge of the structural variation in the glucan strands of PG and associated secondary cell wall polymers that can be species-specific in *Bacillus* genus.

4 Discussion

The emergence of antibiotic-resistant species originating from *Bacillus cereus* group of organisms is a significant concern (Ikeda et al., 2015). *Bacillus* species are ubiquitous spore forming bacilli that are highly abundant in the soil, vegetation, and natural water bodies. They range in their virulence types and phenotypes (Stenfors Arnesen et al., 2008). From soil, bacilli and spores easily disseminate to food and cause diseases in animals. Cases of food contamination with antibiotic-resistant *B. cereus* isolates have been reported worldwide (Arslan et al., 2014; Kim et al., 2015; Merzougui et al., 2014; Yim et al., 2015). Within the *Bacillus* genus the *B. cereus sensu lato* group stands out with *B. cereus*, *B. anthracis*, and *B. thuringiensis* being representative members of this group (Aronson, 2002; Han et al., 2006).

B. cereus is a common foodborne pathogen (Bottone, 2010; Guinebretière et al., 2002; Stenfors Arnesen et al., 2008), which can also cause permanent blindness (Drobniewski, 1993), and forms biofilms on vegetables (Elhariry, 2011), industry equipment (Andersson et al., 1995), and on the surface of orthopedic implanted devices (Gallo et al., 2011). It can cause catheter associated infections (Koch and Arvand, 2005) and disease resembling inhalational anthrax (Hoffmaster et al., 2004, 2006) similar to *B. anthracis* species, which was weaponized during the Cold War (Abramova et al., 1993). *B. thuringiensis* is an insect pathogen and forms parasporal crystals toxic to insects. It is currently being used as an insecticide (Ghribi et al., 2004).

B. cereus species are considered an ancestral species within the *sensu lato* group (Helgason et al., 2000b). All distinguishing features of the other two species, *B. anthracis* and *B. thuringiensis*, have been encoded by the genes located on highly mobile plasmids (Rasko et al., 2004; Thomas et al., 2000). Additionally, the *B. cereus* group of genetically related organisms evokes high concern by their ability to exchange these mobile plasmids among each other. Because

of this trait, *B. anthracis* has been described as a clone of *B. cereus* difficult to speciate one from another (Hill et al., 2004; Keim et al., 2000). Since emetic *B. cereus* strains can be involved in a conjugative plasmid transfer between *B. cereus* and *B. thuringiensis* in food (Van der Auwera et al., 2007), the threat of antibiotic-resistance gene transfer across these *Bacillus* species is real. Multiple studies have demonstrated that bacteriophage endolysins can effectively lyse viable bacilli of different *Bacillus* species (Etobayeva et al., 2018; Low et al., 2005; Park et al., 2018; Schuch et al., 2002b).

In this study, the PlyP56, PlyN74, and PlyTB40 endolysins of *B. cereus* phages Phrodo, Nigalana and TsarBomba have been identified, characterized, and engineered into chimeric lysins to enhance their lytic potential and expand host specificity. All three endolysins, PlyP56, PlyN74, and PlyTB40, have been identified to share a basic modular organization, with an N-terminal EAD and a C-terminal CBD common to Gram-positive phage endolysins (Fischetti, 2010). EADs have been identified with an enzymatic activity and CBDs are used for attachment to the cell surface by binding conserved ligands, usually cell wall associated proteins (Dramsi et al., 2008) or wall teichoic acids (Neuhaus and Baddiley, 2003).

PlyP56 has been predicted to have an L-alanoyl-D-glutamate endopeptidase activity in its EAD derived from the Peptidase_M15_4 of the VanY superfamily with a conserved (SxHxxGxAxD) metal binding motif (McCafferty et al., 1997). At first, this motif was described in the zinc catalytic site architecture of the D-alanyl-D-alanine dipeptidase of the vancomycin-resistant Gram-negative *Enterococcus faecium*. The structural homology between PlyP56 and Ply500 of the *Listeria* phage A500 (Korndörfer et al., 2008) has revealed strictly conserved metal binding residues in the PlyP56 EAD depended on the metal ion for enzymatic function. In our experiments, EDTA chelation abolished the PlyP56's N-alanoyl-D-glutamate peptidase activity,

and it was subsequently restored by addition of divalent metal ions. This finding suggests equivalent mechanisms for dipeptide hydrolysis of the *Listeria* and *Bacillus* PG polymer by the N-alanoyl-D-glutamate peptidase dependent on the presence of a divalent metal ion within the groove of the enzymatic pocket in order to hydrolyze the PG substrate, which I confirmed for PlyP56 by ETDA chelation.

The EAD of PlyN74, a T-7 lysozyme-type Amidase_2 of the PGRP superfamily, and the EAD of PlyTB40, a carboxypeptidase T-type Amidase_3 of the MurNAc-LAA superfamily, both have been predicted to have an N-acetylmuramoyl-L-alanine amidase activity. Despite the same lytic activity, these two EADs do not share similar protein folds. The Amidase_2 of PlyN74 has 51% identity with PlyL of the *B. anthracis* Ba-02 prophage γ (Low et al., 2005). In turn, an Amidase_3 of PlyTB40 has 36% identity with PlyPSA of the *Listeria* phage PSA (Korndörfer et al., 2006). Modeling to structural homologs for both of these EADs suggested a metal binding pocket and active-site residues. However, these enzymes were found to be capable of hydrolyzing PG substrate independent of metal ions, since their enzymatic activity was not abolished by EDTA chelation. Similar observations have been made in the homologous LysBPS13 of the *B. cereus* phage BPS13 (Park et al., 2012). Presence of both amidase architectures in *B. cereus*, *B. anthracis,* and *Listeria* phage endolysins indicates similarity of the covalent bonds in the PG substrate that have been attacked by these enzymes, which further underscores the likeness of their general PG structure (Vollmer et al., 2008).

The EAD architectures identified in the *Bacillus* phages in this study have been grouped into five distinct families, GH25, GH24, MurNAc_LAA, VanY, and PGRP. Out of these five families, only four, the GH25, MurNAc_LAA, VanY, and PGRP EAD architectures have been expressed and biochemically studied in the *Bacillus* specific endolysins. The GH25 EAD

architecture has been found in phages infecting all three species, *B. cereus*, *B. anthracis*, and *B. thuringiensis* (Paskaleva et al., 2015; Porter et al., 2007; Yuan et al., 2012). The PGRP family Amidase_2 EAD and the MurNAc_LAA Amidase_3 EAD that I discovered in *B. cereus* phage lysins, PlyN74 and PlyTB40, have been identified in multiple *B. cereus* and *B. anthracis* phage lysins (Etobayeva et al., 2018; Kong and Ryu, 2015; Loessner et al., 1997; Low et al., 2005; Na et al., 2016; Park et al., 2012; Park et al., 2018; Peng and Yuan, 2018; Schuch et al., 2002c). To this day, only two VanY EAD architectures with N-alanoyl-D-glutamate peptidase activity have been found in *B. cereus* lysins, LysB4 (Son et al., 2012) and PlyP56 which I described in this work. This finding suggests that EADs with amidase enzymatic activity are the predominant enzymes associated with endolysins specific to both bacterial hosts, *B. cereus* and *B. anthracis*.

PlyP56, PlyN74, and PlyTB40 showed similar biochemical characteristics with optimal conditions at physiological pH (7.0-8.0), over a broad temperature range (4-55ºC), and at low salt concentrations (NaCl, <50mM). These are much narrower parameters from what have been previously reported for other *B. cereus* lysins. For instance, LysBPS13 isolated from phage in food sewage, South Korea, has been found more enzymatically active at basic pH (9.0-9.5), high salt concertation (NaCl, 150-250 mM), plus, it retained full enzymatic activity at high temperatures (42-45ºC) (Park et al., 2012). LysB4, another *B. cereus* phage lysin isolated from the forest mud, has showed remarkable stability at extreme basic pH conditions with nearly full lytic activity observed at pH ranging from (8.0) to (10.5). LysB4 has sustained its activity at high temperatures (45-55ºC), yet, lost more than half of its activity at 37ºC, and at 25ºC retaining only one fourth of its activity. LysB4 has showed quite similar response to an effect of salt concentrations in comparison to our lysins with an optimum at (0-50mM) (Son et al., 2012). Since phages in this study, Prodo, Nigalana, and TsarBomba, have been identified from the environmental samples

they have adapted, and, so, their endolyins, to function at low temperatures, neutral to slightly basic pH and low concentrations of salts. The high tolerance of LysBPS13 to extreme conditions is likely a consequence of traits that evolved in an evolutionary arms race of the *Bacillus* phage with its host bacteria in the food sewage that have been observed between bacteria and its phage (Poullain et al., 2007). This selective pressure on phage to evolve and adapt to keep infecting its host bacteria has also pushed its endolysin to evolve and keep its functions in decomposing food.

Endolysins in this study have been selected due to their high lytic activity on the *B. cereus* ATCC 4342 strain, a known transition state strain between *B. cereus* and *B. anthracis* species. All three endolysins have been predicted to have a type of src-homology 3 (SH3) domain as their C-terminal CBD. The CBDs of PlyP56 and PlyN74 have very similar SH3b domains that share 94% identity, while the CBD of PlyTB40 has a SH3_5 domain with less than 52% identity in its AA sequence with the other two. The SH3b and SH3_5 family CBDs have been commonly found in endolysins derived from *Bacillus* phages (Nelson et al., 2012) including *B. cereus* specific lysins, Ply21 (Loessner et al., 1997) and LysB4 (Son et al., 2012).

The CBDs usually define the lytic range and preposition for species specificity. In some known cases, like in *Listeria* phage endolysins, the CBDs bind the teichoic acid molecules achieving not only species specificity, but the serovar and strain specificity (Schmelcher and Loessner, 2014). All three AlexaFluor® labeled truncated CBDs in this study have showed similar binding patterns with each other, limited to *B. cereus* strains, and their lytic activities have correlated with this trend. To our surprise, CBDs also bound bacilli of two *B. anthracis* strains, Ames35 and UM 23, but the lytic activity on these strains was not observed at the tested concentrations via turbidity reduction assay. However, it is noteworthy that lytic activity tested via the plate lysis assay was positive for lysis of imbedded in the semisolid agar *B. anthracis* bacilli.

The strain of *B. anthracis* Ames 35 has appeared to be more sensitive to the lysis by PlyP56 and PlyN74, yet, less by PlyTB40 despite apparent CBD binding facilitated by all three. The plate lysis method is much more sensitive than the turbidity reduction assay. Thus, I conclude that the enzymes do work on *B. anthracis*, but at a significantly diminished capacity compared to their activity on *B. cereus* species. I anticipate that *B. anthracis* strains have specific modifications in their PG structure that render their cell wall different from the *B. cereus* cell wall, and, hence, tolerant to the lytic action of our enzymes.

Unmodified PG polymer consists of glucan strands with alternating -1,4-linked Glc*N*Ac and Mur*N*Ac residues (Vollmer et al., 2008). Interestingly, this unmodified PG structure has been rarely preserved in bacteria due to secondary modifications that occur right after PG polymer synthesis. In fact, Gram-positive species attach other cell wall polymers such as the teichoic acids and capsular polysaccharides via the phosphodiester bonds to their Glc*N*Ac or Mur*N*Ac residues. In different *Bacillus* species, secondary glucan strand modifications have effects on interactions with the elements of the host immune system, and these modifications have been commonly observed in pathogenic species. For example, *O*-acetylation of Mur*N*Ac with an extra acetyl group linked to the C6-OH position to form a 2,6-*N*,*O*-diacetyl muramic acid residue, is more prevalent in *B. cereus* strains than the *N*-deacetylation (Vollmer, 2008). The *N*-deacetylation of Glc*N*Ac to Glc*N* residues in *B. cereus* strains has rendered these organisms resistant to host lysozyme (Araki et al., 1971) as well as the N-deacetylation of Mur*N*Ac to Mur*N* residues, which was first discovered in *B. anthracis* (Zipperle Jr. et al., 1984). In general, the *N*-deacetylation of either Glc*N*Ac or Mur*N*Ac residue has been discovered in *B. cereus*, *B. anthracis* and *B. thuringiencis* with different percentages of modifications in the glucan strands based on the species (Araki et al., 1971; Zipperle Jr. et al., 1984), while *O*-acetylation tends to be more specific to *B. cereus* strains.

Additionally, there are secondary modifications the PG structure of *Bacillus* strains. Secondary cell wall polysaccharides (SCWPs) covalently attached to the PG through a phosphate group at the reducing end of the polysaccharide (Leoff et al., 2008). There is a clear evidence that the *B. cereus* group of organism is highly divergent in the expression of the SCWPs in a species specific manner (Ganguly et al., 2013). Lytic activity of lysins also has been proven to be highly dependent on the presence of these polysaccharides. For instance, the SCWP structures of *B. anthracis* and pathogenic *B. cereus* G9241 are comprised of a similar →4)-β-D-Man*pN*Ac-(1→4)-β-D-Glc*pN*Ac-(1→6)-α-D-Glc*pN*Ac-(1→ backbone, where the α-Glc*N*Ac residue has been substituted with α-Gal and β-Gal at O3 and O4 positions, respectively, and the β-Glc*N*Ac substituted with α-Gal at O3 position (Choudhury et al., 2006). In a non-pathogenic strain, *B. cereus* ATCC 10987, the α-Gal*N*Ac has been substituted at O3 with a β-Gal residue and the β-Man*N*Ac has been acetylated at O3 position (Leoff et al., 2008). Recent studies have identified that SCWPs can also serve as the functional binding ligands to CBDs of PlyL and PlyG, *B. anthracis* phage lysins (Ganguly et al., 2013). I hypothesize that the divergent nature of the SCWPs might obstruct lysis of the vegetative bacilli, explaining the species to species or strain to strain variability in our results. I think the SCWPs may obstruct the lytic activity by blocking covalent bonds in PG structure that would have been normally hydrolyzed by the lysis.

Phages, like any viruses, evolve by homologous and non-homologous recombination events with other viruses and prophage genomes adding point mutations and new genes with novel functions to their genome in the process. The comparative analysis of AA sequences suggest that novel genes in phages can be assembled from the parts of the genes and via horizontal exchange of the sequences between related phages (Hendrix, 2002). To test that CBDs and EADs from *B. cereus* phages can be assembled from different domains, I created fusion lysins by domain

shuffling of the divergent EADs and CBDs identified in this study. I demonstrated the interchangeable nature of three divergent EADs, the L–alanoyl-D–glutamate endopeptidase of PlyP56, the T7 lysozyme-type Amidase_2 of PlyN74, and the carboxypeptidase T-type Amidase_3 of PlyTB40 in combination with the *B. cereus* specific SH3-family CBDs. I named these constructs ClyBC1, ClyBC2, ClyBC3, ClyBC4 as defined for chimeric (C) lysin (ly) of *B. cereus* (BC). ClyBC1 and ClyBC2 have a shared PlyP56 EAD, and each have the SH3-family CBD of PlyN74 or PlyTB40 with 52% homology in their CBD AA sequence. ClyBC3 and ClyBC4 have a similar SH3-family CBD of PlyP56, and a divergent Amidase_2 EAD of PlyN74 or Amidase_3 EAD of PlyTB40, respectfully. Previously, successful recombination of EADs and CBDs was observed in two *Listeria* phage endolysins, PlyPSA and Ply118 (Schmelcher et al., 2010), which supports our findings that modular domains in related phages can be recombined. A chimeric lysin created by recombination of EAD of the bacterial autolysin with the muramidase activity from the *Clostridium acetobutylicum* ATCC 824 and cholin-dependent CBD of pneumococcal lysin Cpl1 (Croux et al., 1993), has provided experimental support to a theory that murein hydrolases are likely to share their ancestral origin with their bacterial host.

I identified that amidases of PlyN74 and PlyTB40, the T7 lysozyme-type Amidase_2 of the PGRP superfamily and the carboxypeptidase T-type Amidase_3 of the MurNAc-LAA superfamily, respectfully, have been commonly identified in endolysins of phages infecting *B. cereus* and *B. anthracis* species (Kong and Ryu, 2015; Na et al., 2016; Park et al., 2012). The *B. anthracis* prophage lysin, PlyL, with the PGRP family architecture (Low et al., 2005) has similar activity to both PlyN74 and PlyTB40, and additionally, shares 53% identity with the PlyTB40 EAD. Both amidases in this study have the N-acetylmuramoyl-L-alanine amidase activity and cleave an amide bond between the glycan Mur*N*Ac residue and first AA of the stem peptide, L-

Ala. Since it separates glucan strand from the peptide stem, it has been considered highly destabilizing to the PG structure causing fast lysis of bacilli. The enzymatically active L-alanoyl-D-glutamate peptidase of PlyP56 identified in this work has a broad specificity to *B. cereus* strains. I found similar EAD architecture in published *B. cereus* specific lysin, LysB4 (Son et al., 2012), but I was not successful in finding similar architectures in the *B. anthracis* phage lysins. The L–alanoyl-D–glutamate peptidase cleaves peptide bonds between two peptides in the peptide stem, L-Alanine and D-Glutamic acid. Similar endopeptidase activity has been described in the listerial lysin, Ply500 (Korndörfer et al., 2008), a structural homolog to the PlyP56 EAD, and in the Ply118 endolysin (Loessner et al., 1995). Presence of similar enzymes with an endopeptidase enzymatic activity in the phages that infect distant Gram-positive species suggests a high degree of conservation of the targeted covalent bonds in the PG substrate in both species.

In addition to the lytic activity of the full-length lysins, fusion of EAD and CBD subunits, I studied lytic activity of the truncated EADs amplified from the PlyP56, PlyN74, and PlyTB40 endolysins. Contradictory to the classical behavior of native lysin, whereas the EADs possess enzymatic activity and the CBDs contribute to binding, it has been reported that lytic activity of some EADs can be independent of the CBDs, such as in the streptococcal phage endolysin, PlyGBS (Cheng and Fischetti, 2007). Nevertheless, the N-terminal EADs in this study did not possess lytic activity independently from their C-terminal CBDs. Recent studies have provided enough evidence that this non-classical behavior might be related to a positive charge on the EAD subunit (Low et al., 2011). Both, positively charged EADs of PlyL and PlyG, had enzymatic activity, albeit, lower than their native full-length endolysins, however, without the restrictions imposed by the CBDs, they have acquired a broader host range to *Bacillus* species. Although EADs appeared to have overall net positive charge, I discovered that single EADs actually had net

negative charge. A positive charge on the PlyP56 EAD was due to the cationic leader peptide that preceded the globular structure of the EAD. The correlation between the positive net charge on the EAD and the lytic activity of the truncated EADs, perhaps, is related to the negatively charged wall teichoic acids and lipoteichoic acids that decorate the cell surface of bacilli and create a polyanionic network (Neuhaus and Baddiley, 2003). Given this information, it is possible that the positively charged EAD could have an affinity for the bacterial cell wall via this polyanionic network that also serves as the binging ligand strong enough for the EAD to attach to and hydrolyze the PG substrate.

Additionally, I tested purified chimeric lysins for lysis of both mid-log and stationary cultures of *B. cereus* strains and found that all our chimeras retained their host range with the *B. cereus* group of species with slightly different lysis rates for different *B. cereus* strains. All constructs with either the L-alanoyl-D-glutamate peptidase, Amidase_2, or Amidase_3 domains with N-acetylmuramoyl-L-alanine amidase activity combined with the SH3-family CBDs of PlyP56, PlyN74, and PlyTB40 have effectively lysed bacilli of *B. cereus* ATCC 11778 from the mid-log culture at a concentration 10 µg/mL. However, only the ClyBC1 chimera, a combination of the L-alanoyl-D-glutamate peptidase of PlyP56 fused with the SH3-family CBD of PlyN74 has efficiently lysed both bacilli from the mid-log and stationary cultures of *B. cereus* ATCC 11778 and *B. cereus* ATCC 13061 strains. Additionally, I discovered that ClyBC2 chimera, a combination of the L-alanoyl-D-glutamate peptidase fused with the SH3-family CBD of PlyTB40, effectively lysed mid-log bacilli of *B. cereus* ATCC 11778, but could not lyse mid-log bacilli of *B. cereus* ATCC 13061 or the stationary cultures of both strains at tested concentrations. This study confirms that switching CBDs even in highly related endolysins has swapped their binding

and lytic activities; yet, their host range remained limited by their CBDs, and retained specificity to the *B. cereus* species.

The L-alanoyl-D-glutamate peptidase of the PlyP56 EAD has clearly showed potential for engineering studies. I found that in its natural state, it had no activity against *B. anthracis* strains in the liquid turbidity assay. To identify whether I could harnessed its lytic potential and apply it against bacilli of *B. anthracis,* I made a construct, ClyBCBA1, as defined for chimeric (C) lysin (ly) of *B. cereus* (BC) and *B. anthracis* (BA), where I fused the EAD of PlyP56 with the Amidase02_C CBD of PlyG, a *B. anthracis*-specific endolysin (Schuch et al., 2002b). Although this chimera was not more enzymatically active than the native PlyG endolysin, I was able to expand the host range of the PlyP56 EAD to include *B. anthracis* strains, Ames 35 and UM23. The CBD usually confers species specificity and facilitates binding of the lysin to a surface of target bacteria (Fischetti, 2010). In general, the CBD swapping technique has proven to facilitate swapped specificity in the *Listeria* lysins, PlyPSA and Ply118 (Schmelcher et al., 2011). I observed similar trend in *B. cereus* lysins, PlyP56, PlyN74, and PlyTB40 and in the *B. cereus*-*B. anthracis* chimeric lysin, ClyBCBA1. However, our interspecies chimera, ClyBCBA1, has not showed stronger lytic activity compared to the activity of PlyG against *B. anthracis* species despite that it bound to both mid-log and stationary bacilli via the PlyG CBD (Paskaleva et al., 2015). Despite the expanded host range, ClyBCBA1 also had a slightly diminished lytic activity against *B. cereus* species regardless having enzymatically active L-alanoyl-D-glutamate peptidase of PlyP56. I believe that PG modifications caused by *O*-acetylation and *N*-deamination (Vollmer, 2008), divergent secondary cell wall polymers (Schaffer and Messner, 2005) and the presence of S-layer in *B. anthracis* species (Mesnage et al., 1999), all features that cause differences in PG structures

between *B. cereus* and *B. anthracis* species, could be responsible for the lower lytic activity of ClyBCBA1 in *B. anthracis* species.

All three *B. cereus*-specific CBDs that I studied here had a high degree of conservation with the Plyβ CBD of the *B. anthracis* phage lysin (Paskaleva et al., 2015) in the region that I believe facilitates binding of CBDs to the ligand on bacterial cell wall of both *B. cereus* and *B. anthracis* species. In this conserved motif (LxxGxxxxYxx[Y]Gx[E]) I noticed that Tyr [Y] has been also substituted with a Phe [F] residue in our *B. cereus*-specific CBDs, and Glu [E] residue similar to residues in Plyβ CBD substituted to Gln [Q] residue in the PlyG CBD. The *B. cereus*-specific CBDs of PlyP56, PlyN74, PlyTB40, and *B. anthracis* specific CBD of Plyβ have had a conserved Leu [L] residue similar to Leu_{196} [L] in PlyG peptide, which on its own could facilitate binding of the PlyG peptide to the cell wall of *B. anthracis* (Kikkawa et al., 2007). In this situation, three possibilities are suggested: first, that all three *B. cereus*-specific CBDs in this work bind a similar ligand with Plyβ; second, this ligand is divergent from the ligand of PlyG; and third, all five CBDs bind similar ligand but with different affinities. Additionally, the (V_{215}→T_{215}) and (Y_{221}→F_{221}) point mutations have been found in CBDs of PlyP56 and PlyN74 that might have an effect on the binding affinity of these CBDs to different *Bacillus* species. Altogether, these findings suggest that over time, CBDs have diverged by acquiring point mutations in their binding peptides, which acquired specificity to ligands expressed on cell wall of different *Bacillus* species.

In conclusion, our work provides new *Bacillus*-specific phage endolysins that have high potentials to be developed into the therapeutic products to control infections and remediate contaminations caused by the *B. cereus* pathogens. I have identified the optimum temperature, salt concentration, and pH environment for the activity of these endolysins. Additionally, I created chimeric lysins with swapped specificity that can be further tailored to improve their lytic potential

or stability profiles. I, also discovered a conserved motif in the CBD sequences that I believe facilitates binding to bacilli. These binding peptides can be further tuned to discover binding ligands and utilized for diagnostic applications. Lastly, this work gives insights on a rational engineering of chimeric lysins that require knowledge of the target bacteria PG modifications and secondary wall structures in addition to EAD architectures and CBD specificity.

5 Future Directions

5.1 *Engineering Multimodular Chimeric Lysins*

An exponential amount of studies on Gram-positive endolysins with a majority of data on staphylococcal and streptococcal phage endolysins have been consolidated in a number of excellent reviews (Fischetti, 2010; Hermoso et al., 2007; Nelson et al., 2012). Just a limited number of phage endolysins from a huge pool of (meta)genomic data have been experimentally characterized. There are less than 20 endolysins of *Bacillus* origin that were expressed and tested for their antibacterial properties. In this work, I identified and experimentally characterized three new *Bacillus*-specific endolysins expanding the pool of Gram-positive experimentally studied phage lysins. All three discovered endolysins have a modular structure that allowed us to create chimeric lysins by swapping EAD and CBD domains. Here, I propose that next-generation of endolysins can be further engineered by addition of the multiple EAD domains to create multimodular enzymes with divergent enzymatic activity.

A major advantage of mutlimodular lysins is their superior lytic activities over the single-EAD endolysins. The multimodular endolysins are rare, but reported in nature. A streptococcal phage derived PlyC is one of the most active lysins reported (Nelson et al., 2006). It is composed of eight CBD subunits for each two EADs that possess divergent lytic activities. Each EAD independently has only 1/100 of the 100% activity of the full lysin, suggesting synergistic effect of its EAD subunits. In a recent report, the successful engineering of a triple-acting lytic enzyme has been achieved by fusion of the lysostaphin EAD with the staphylococcal lysin LysK, which contains two EADs of its own (Becker et al., 2016). This construct has proven be very effective in clearing *Staphylococcus aureus* infection. Besides the benefit of a synergistic effect between

multiple EADs, the resistance development against such chimeras, where the EADs cleave different covalent bonds in the PG substrate, is less likely to appear (Donovan et al., 2009).

I propose to engineer chimeric multimodular lysins with the EADs and CBDs selected in this work. Our in depth, three-dimensional structural analysis and biochemical characterization suggests that all three EADs belong to distant EAD architectures, MurNAc_LAA, PGRP, and VanY super families with different protein folds. Until now, I created modular lysins via domain shuffling of the divergent EAD and SH3-family CBDs. Here, I propose to amplify these domains and fuse them together in tandem repeats with the overlapping PCR primers (Figure 5-1,A1-3). I also anticipate to harness the synergistic effect of their distant EADs. It is possible that the L-alanoyl-D-glutamate endopeptidase of PlyP56 and the N-alanoyl-D-glutamate peptidase of PlyN74 and PlyTB40 would enhance each other's lytic activity by cleaving different bonds in the peptide stem. For the first step, I suggest to make constructs by combining distant EADs and fusing them together in tandem repeats at the N-terminus of the enzyme, leaving their native linker for proper folding. At the C-terminus, I will place the SH3-family CBD of the most active endolysin selected in this work. In the second step, the other three remaining constructs will have EADs on each N-terminus and C-terminus separated by single CBD and linked to each other via their native linkers (Figure 5-1,B1-3). The constructs A1 and B1 should serve as a control for determination of the lytic activity.

Additionally, there is concern that EADs assembled in tandem repeats in the first step might have limited movement ability necessary for conformational changes of the EAD and PG substrate recognition due to constriction of the movement by short or inflexible linker. To solve this issue, I propose to adjust the length of the adjacent linkers in the chimeras by adding or cleaving out non-essential AAs as necessary. The other proposed solution would be to use a linker from chimeras

that have sustained or improved their lytic activity. Another issue that should be considered, is the C-terminal location of the 6xHis-tag adjacent to the second EAD. Its position might affect folding of the second EAD domain, and render it enzymatically inactive. This location has proven to be functionally effective, while expressing relatively small 25-45 kDa recombinant proteins with C-terminal CBDs rather than C-terminal EADs. In this case, when chimeras with C-terminal EAD and adjacent 6xHis tag have low lytic activity, I propose to move the 6xHis tag to the N-terminus since this strategy has worked for other lysins.

The work on endolysins of Gram-positive origin has now reached a stage of the ready-to-use tailored enzymes against a wide range of Gram-positive bacteria, where several of them have been advanced all the way to the Phase III clinical trials (Gerstmans et al., 2018). In this work, I propose to engineer multimodular chimeric lysins with enhanced tailored lytic activities that can be commercialized for application in agriculture, food industry, and medicine.

Figure 5-1. Engineering chimeric lysins with mutliple EAD subunits. Schematic representation of different constructs. (A1-3) N-terminal EADs in tandem repeats fused with a C-terminal CBD. (B1-3) N-terminal EAD fused with CBD and C-terminal EAD via native linker (L). Each EAD will be amplified together with its native linker.

Appendix: Non-Thesis Co-Authored Manuscripts

ClyJ, a novel pneumococcal chimeric lysin with a unique CHAP catalytic domain.

*Submitted

Hang Yang, Yujing Gong, Huaidong Zhang, Irina Etobayeva, Paulina Miernikiewicz, Dehua Luo, Xiaohong Li, Xiaoxu Zhang, Krystyna Dabrowska, Daniel C. Nelson, Jin He, Hongping Wei.

Abstract

Streptococcus pneumoniae is one of the leading pathogens that cause a variety of mucosal and invasive infections. With the increased emergence of multidrug-resistant *S. pneumoniae*, new antimicrobials with mechanisms of action different from conventional antibiotics are urgently needed. In this study, we identified a putative lysin (gp20) coded by the *Streptococcus* phage SPSL1 using autolysin LytA as template. Molecular dissection of gp20 revealed a binding domain (GPC) containing choline-binding repeats (CBRs) that are high specificity for *S. pneumoniae*. By fusing GPC to the CHAP (cysteine, histidine-dependent amidohydrolases/peptidases) domain of PlyCA, we constructed a novel chimeric lysin, ClyJ, with comparable activity to the pneumococcal Cpl-1 lysin. Structural modeling combined with site-directed mutagenesis revealed that the CHAP domain of ClyJ contains a unique Cys-His-Glu-Asn proteolytic relay. No resistance was observed in *S. pneumoniae* strains after exposure to incrementally doubling concentrations of ClyJ for 8 continuous days in vitro. In a mouse bacteremia model, a single intraperitoneal injection of ClyJ improved the survival rate of lethal *S. pneumoniae* infected mice in a dose-dependent manner, much better than Penicillin G. Giving its high lytic activity and good safety profile, ClyJ may represent a promising alternative to combat pneumococcal infections.

Characterization of LysBC17, a lytic endopeptidase from *Bacillus cereus*.

*In preparation

Steven M. Swift, Irina V. Etobayeva, Kevin P. Reid, Jerel J. Waters, Brian B. Oakley, David M. Donovan, and Daniel C. Nelson.

Abstract

Bacillus cereus, a Gram-positive bacterium, is a food poisoning agent. A bioinformatic search for bacteriolytic enzymes, led to the discovery of an endolysin-like endopeptidase gene which was cloned from the genome of *B. cereus*. Recombinant endopeptidase was expressed and purified from *E.coli*. The endopeptidase had lytic activity against *B. cereus* species. Optimal lytic activity occurred between pH 7.0 and 8.0, in the absence of NaCl. The endopeptidase enzyme also had lytic activity against strains of *B. pumilus* and *B. anthracis.*

Bibliography

Abedon, S. T. (2011). Lysis from without. *Bacteriophage*, *1*(1), 46–49. https://doi.org/10.4161/bact.1.1.13980

Abramova, F. A., Grinberg, L. M., Yampolskaya, O. V, & Walker, D. H. (1993). Pathology of inhalational anthrax in 42 cases from the Sverdlovsk outbreak of 1979. *Proceedings of the National Academy of Sciences of the United States of America*, *90*(6), 2291–4. https://doi.org/10.1073/PNAS.90.6.2291

Adão, R., Seixas, R., Gomes, P., Pessoa, J. C., & Bastos, M. (2008). Membrane structure and interactions of a short Lycotoxin I analogue. *Journal of Peptide Science*, *14*(4), 528–534. https://doi.org/10.1002/psc.993

Alisky, J., Iczkowski, K., Rapoport, A., & Troitsky, N. (1998). Bacteriophages show promise as antimicrobial agents. *The Journal of Infection*, *36*(1), 5–15. https://doi.org/10.1016/S0163-4453(98)92874-2

Andersson, A., Ronner, U., & Granum, P. E. (1995). What problems does the food industry have with the spore-forming pathogens *Bacillus cereus* and *Clostridium perfringens*? *International Journal of Food Microbiology*, *28*(2), 145–55. https://doi.org/10.1016/0168-1605(95)00053-4

Araki, Y., Nakatani, T., Hayashi, H., & Ito, E. (1971). Occurrence of non-N-substituted glucosamine residues in lysozyme-resistant peptidoglycan from *Bacillus cereus* cell walls. *Biochemical and Biophysical Research Communications*, *42*(4), 691–697. https://doi.org/10.1016/0006-291X(71)90543-2

Aronson, A. (2002). Sporulation and δ-endotoxin synthesis by *Bacillus thuringiensis*. *Cellular and Molecular Life Sciences (CMLS)*, *59*(3), 417–425. https://doi.org/10.1007/s00018-002-8434-6

Aronson, A. I. (1993). *Bacillus subtilis* and Other Gram-Positive Bacteria. In R. Sonenshein, A.L., Hoch, J.A., Losick (Ed.), *Insecticidal toxins* (pp. 953–963). Washington, DC, USA: American Society for Microbiology. Retrieved from http://www.asmscience.org/content/book/10.1128/9781555818388.chap64

Arslan, S., Eyi, A., & Küçüksarı, R. (2014). Toxigenic genes, spoilage potential, and antimicrobial resistance of *Bacillus cereus* group strains from ice cream. *Anaerobe*, *25*, 42–46. https://doi.org/10.1016/J.ANAEROBE.2013.11.006

Bagaeva, V. V., Popova, V. M., Pashkova, G. S., Isadzhanyan, K. E., Nikitin, V. V., & Zhilenkov, E. L. (2015). The study of the efficacy and safety of antimicrobial agents. *Research and Practical Medicine Journal*, *2*(3), 35–42. Retrieved from http://vitabio.ru/images/НАУЧНО-ПРАКТИЧЕСКИЙ_ЖУРНАЛ_ИССЛЕДОВАНИЯ_И_ПРАКТИКА_В_МЕДИЦИНЕ.pdf

Bardell, D. (1982). *An 1898 Report by Gamaleya for a Lytic Agent Specific for Bacillus anthracis. Journal of the History of Medicine and Allied Sciences*, *XXXVII*(2), 222–225. https://doi.org/10.1093/jhmas/XXXVII.2.222

Becker, S. C., Foster-Frey, J., & Donovan, D. M. (2008). The phage K lytic enzyme LysK and lysostaphin act synergistically to kill MRSA. *FEMS Microbiology Letters*, *287*(2), 185–191. https://doi.org/10.1111/j.1574-6968.2008.01308.x

Becker, S. C., Roach, D. R., Chauhan, V. S., Shen, Y., Foster-Frey, J., Powell, A. M., … Donovan, D. M. (2016). Triple-acting Lytic Enzyme Treatment of Drug-Resistant and Intracellular *Staphylococcus aureus*. *Scientific Reports*, *6*(1), 25063. https://doi.org/10.1038/srep25063

Berman, H. M., Westbrook, J., Feng, Z., Gilliland, G., Bhat, T. N., Weissig, H., … Bourne, P. E. (2000). The Protein Data Bank. *Nucleic Acids Research*, *28*(1), 235–42. Retrieved from http://www.ncbi.nlm.nih.gov/pubmed/10592235

Borysowski, J., Weber-Dąbrowska, B., & Górski, A. (2006). Bacteriophage Endolysins as a Novel Class of Antibacterial Agents. *Experimental Biology and Medicine*, *231*(4), 366–377. https://doi.org/10.1177/153537020623100402

Bottone, E. J. (2010). *Bacillus cereus*, a volatile human pathogen. *Clinical Microbiology Reviews*, *23*(2), 382–98. https://doi.org/10.1128/CMR.00073-09

Briers, Y., & Lavigne, R. (2015). Breaking barriers: expansion of the use of endolysins as novel antibacterials against Gram-negative bacteria. *Future Microbiology*, *10*(3), 377–90. https://doi.org/10.2217/fmb.15.8

Bruynoghe, R. A. J. M., & Maisin, J. (1921). Essais de thérapeutique au moyen du bacteriophage. *CR Soc. Biol*, (85), 1120–1121.

Büttner, F. M., Renner-Schneck, M., & Stehle, T. (2015). X-ray crystallography and its impact on understanding bacterial cell wall remodeling processes. *International Journal of Medical Microbiology*, *305*(2), 209–216. https://doi.org/10.1016/j.ijmm.2014.12.018

Callewaert, L., Walmagh, M., Michiels, C. W., & Lavigne, R. (2011). Food applications of bacterial cell wall hydrolases. *Current Opinion in Biotechnology*, *22*(2), 164–171. https://doi.org/10.1016/J.COPBIO.2010.10.012

Carlson, C. R., Caugant, D. A., & Kolstø, A. B. (1994). Genotypic Diversity among Bacillus cereus and *Bacillus thuringiensis* Strains. *Applied and Environmental Microbiology*, *60*(6), 1719–25. Retrieved from http://www.ncbi.nlm.nih.gov/pubmed/16349267

Cerdà-Costa, N., & Gomis-Rüth, F. X. (2014). Architecture and function of metallopeptidase catalytic domains. *Protein Science : A Publication of the Protein Society*, *23*(2), 123–44. Retrieved from http://www.ncbi.nlm.nih.gov/pubmed/24596965

Ceuppens, S., Boon, N., & Uyttendaele, M. (2013). Diversity of *Bacillus cereus* group strains is reflected in their broad range of pathogenicity and diverse ecological lifestyles. *FEMS Microbiology Ecology*, *84*(3), 433–450. https://doi.org/10.1111/1574-6941.12110

Chanishvili, N. (2012). Phage Therapy—History from Twort and d'Herelle Through Soviet Experience to Current Approaches (Vol. 83, pp. 3–40). https://doi.org/10.1016/B978-0-12-

394438-2.00001-3

Cheng, Q., & Fischetti, V. A. (2007). Mutagenesis of a bacteriophage lytic enzyme PlyGBS significantly increases its antibacterial activity against group B streptococci. *Applied Microbiology and Biotechnology*, *74*(6), 1284–91. https://doi.org/10.1007/s00253-006-0771-1

Choma, C., & Granum, P. E. (2002). The enterotoxin T (BcET) from *Bacillus cereus* can probably not contribute to food poisoning. *FEMS Microbiology Letters*, *217*(1), 115–119. https://doi.org/10.1111/j.1574-6968.2002.tb11464.x

Choudhury, B., Leoff, C., Saile, E., Wilkins, P., Quinn, C. P., Kannenberg, E. L., & Carlson, R. W. (2006). The Structure of the Major Cell Wall Polysaccharide of *Bacillus anthracis* Is Species-specific. *Journal of Biological Chemistry*, *281*(38), 27932–27941. https://doi.org/10.1074/jbc.M605768200

Clokie, M. R. J., Millard, A. D., Letarov, A. V., & Heaphy, S. (2011). Phages in nature. *Bacteriophage*, *1*(1), 31–45. https://doi.org/10.4161/bact.1.1.14942

Comeau, A. M., Hatfull, G. F., Krisch, H. M., Lindell, D., Mann, N. H., & Prangishvili, D. (2008). Exploring the prokaryotic virosphere. *Research in Microbiology*, *159*(5), 306–313. https://doi.org/10.1016/J.RESMIC.2008.05.001

Croux, C., Ronda, C., Lopez, R., & Garcia, J. L. (1993). Interchange of functional domains switches enzyme specificity: construction of a chimeric pneumococcal-clostridial cell wall lytic enzyme. *Molecular Microbiology*, *9*(5), 1019–1025. https://doi.org/10.1111/j.1365-2958.1993.tb01231.x

d'Herelle, F., & Smith, G. H. (1926). *The bacteriophage and its behavior*. Baltimore. MD: Williams & Wilkins.

d'Herelle, F. (1917). Sur un microbe invisible antagoniste des bacilles dysentériques. *CR Acad. Sci. Paris*, (165), 373–375.

da Silva Fernandes, M., Fujimoto, G., Schneid, I., Kabuki, D. Y., & Kuaye, A. Y. (2014). Enterotoxigenic profile, antimicrobial susceptibility, and biofilm formation of *Bacillus cereus* isolated from ricotta processing. *International Dairy Journal*, *38*(1), 16–23. https://doi.org/10.1016/j.idairyj.2014.03.009

Díaz, E., López, R., & García, J. L. (1990). Chimeric phage-bacterial enzymes: a clue to the modular evolution of genes. *Proceedings of the National Academy of Sciences of the United States of America*, *87*(20), 8125–9. Retrieved from http://www.ncbi.nlm.nih.gov/pubmed/1978320

Domingo-Calap, P., & Delgado-Martínez, J. (2018). Bacteriophages: Protagonists of a Post-Antibiotic Era. *Antibiotics*, *7*(3), 66. https://doi.org/10.3390/antibiotics7030066

Donovan, D. M., Becker, S. C., Dong, S., Baker, J. R., Foster-Frey, J., & Pritchard, D. G. (2009). Peptidoglycan hydrolase enzyme fusions for treating multi-drug resistant pathogens. *Biotech*, *21*(2), 6–10.

Dramsi, S., Magnet, S., Davison, S., & Arthur, M. (2008). Covalent attachment of proteins to peptidoglycan. *FEMS Microbiology Reviews*, *32*(2), 307–320. https://doi.org/10.1111/j.1574-6976.2008.00102.x

Drobniewski, F. A. (1993). *Bacillus cereus* and related species. *Clinical Microbiology Reviews*, *6*(4), 324–38. https://doi.org/10.1128/CMR.6.4.324

Dunne, M., Leicht, S., Krichel, B., Mertens, H. D. T., Thompson, A., Krijgsveld, J., … Meijers, R. (2016). Crystal Structure of the CTP1L Endolysin Reveals How Its Activity Is Regulated by a Secondary Translation Product. *Journal of Biological Chemistry*, *291*(10), 4882–4893. https://doi.org/10.1074/jbc.M115.671172

During, K., Porsch, P., Mahn, A., Brinkmann, O., & Gie¡ers, W. (1999). The non-enzymatic microbicidal activity of lysozymes. *FEBS Letters*, *449*(2–3), 93–100. Retrieved from https://febs.onlinelibrary.wiley.com/doi/pdf/10.1016/S0014-5793%2899%2900405-6

Elhariry, H. M. (2011). Attachment strength and biofilm forming ability of *Bacillus cereus* on green-leafy vegetables: Cabbage and lettuce. *Food Microbiology*, *28*(7), 1266–1274. https://doi.org/10.1016/j.fm.2011.05.004

Entenza, J. M., Loeffler, J. M., Grandgirard, D., Fischetti, V. A., & Moreillon, P. (2005). Therapeutic Effects of Bacteriophage Cpl-1 Lysin against *Streptococcus pneumoniae* Endocarditis in Rats. *Antimicrobial Agents and Chemotherapy*, *49*(11), 4789–4792. https://doi.org/10.1128/AAC.49.11.4789-4792.2005

Etobayeva, I., Linden, S., Alem, F., Harb, L., Rizkalla, L., Mosier, P., … Nelson, D. C. (2018). Discovery and Biochemical Characterization of PlyP56, PlyN74, and PlyTB40—*Bacillus* Specific Endolysins. *Viruses*, *10*(5), 276. https://doi.org/10.3390/v10050276

Firczuk, M., & Bochtler, M. (2007). Folds and activities of peptidoglycan amidases. *FEMS Microbiology Reviews*, *31*(6), 676–691. https://doi.org/10.1111/j.1574-6976.2007.00084.x

Fischetti, V. (2018). Development of Phage Lysins as Novel Therapeutics: A Historical Perspective. *Viruses*, *10*(6), 310. https://doi.org/10.3390/v10060310

Fischetti, V. A. (2005). Bacteriophage lytic enzymes: novel anti-infectives. *Trends in Microbiology*, *13*(10), 491–496. https://doi.org/10.1016/J.TIM.2005.08.007

Fischetti, V. A. (2008, October). Bacteriophage lysins as effective antibacterials. *Current Opinion in Microbiology*. https://doi.org/10.1016/j.mib.2008.09.012

Fischetti, V. A. (2010). Bacteriophage endolysins: A novel anti-infective to control Gram-positive pathogens. *International Journal of Medical Microbiology*, *300*(6), 357–362. https://doi.org/10.1016/j.ijmm.2010.04.002

Fiser, A., Do, R. K. G., & Šali, A. (2000). Modeling of loops in protein structures. *Protein Science*, *9*(9), 1753–1773. https://doi.org/10.1110/ps.9.9.1753

Forsberg, L. S., Choudhury, B., Leoff, C., Marston, C. K., Hoffmaster, A. R., Saile, E., … Carlson, R. W. (2011). Secondary cell wall polysaccharides from *Bacillus cereus* strains G9241, 03BB87 and 03BB102 causing fatal pneumonia share similar glycosyl structures with the polysaccharides from Bacillus anthracis. *Glycobiology*, *21*(7), 934–948. https://doi.org/10.1093/glycob/cwr026

Gallo, P. H., Melton-Kreft, R., Nistico, L., Sotereanos, N. G., Sewecke, J. J., Stoodley, P., … Kathju, S. (2011). Demonstration of *Bacillus cereus* in Orthopaedic-Implant-Related Infection with Use of a Multi-Primer Polymerase Chain Reaction-Mass Spectrometric Assay. *The Journal of Bone and Joint Surgery-American Volume*, *93*(15), e85(1)-e85(6). https://doi.org/10.2106/JBJS.J.01181

Ganguly, J., Low, L. Y., Kamal, N., Saile, E., Forsberg, L. S., Gutierrez-Sanchez, G., … Kannenberg, E. L. (2013). The secondary cell wall polysaccharide of *Bacillus anthracis* provides the specific binding ligand for the C-terminal cell wall-binding domain of two phage endolysins, PlyL and PlyG. *Glycobiology*, *23*(7), 820–832. https://doi.org/10.1093/glycob/cwt019

García, P., Martínez, B., Rodríguez, L., & Rodríguez, A. (2010). Synergy between the phage endolysin LysH5 and nisin to kill *Staphylococcus aureus* in pasteurized milk. *International Journal of Food Microbiology*, *141*(3), 151–155. https://doi.org/10.1016/j.ijfoodmicro.2010.04.029

Gerstmans, H., Criel, B., & Briers, Y. (2018). Synthetic biology of modular endolysins. *Biotechnology Advances*, *36*(3), 624–640. https://doi.org/10.1016/j.biotechadv.2017.12.009

Gherardi, G. (2016). *Bacillus cereus* disease other than food-borne poisoning. In V. Savini (Ed.), *The diverse faces of Bacillus cereus* (pp. 93–106). London, UK: Elsevier Inc. Retrieved from https://www.sciencedirect.com/science/article/pii/B9780128014745000086

Ghribi, D., Zouari, N., & Jaoua, S. (2004). Improvement of bioinsecticides production through mutagenesis of *Bacillus thuringiensis* by u.v. and nitrous acid affecting metabolic pathways and/or delta-endotoxin synthesis. *Journal of Applied Microbiology*, *97*(2), 338–346. https://doi.org/10.1111/j.1365-2672.2004.02323.x

Gonzalez, J., & Carlton, B. C. (1980). Patterns of plasmid DNA in crystalliferous and acrystalliferous strains of *Bacillus thuringiensis*. *Plasmid*, *3*(1), 92–98. https://doi.org/10.1016/S0147-619X(80)90038-4

Granum, P. E., & Lund, T. (2006). *Bacillus cereus* and its food poisoning toxins. *FEMS Microbiology Letters*, *157*(2), 223–228. https://doi.org/10.1111/j.1574-6968.1997.tb12776.x

Guinebretière, M.-H., Broussolle, V., & Nguyen-The, C. (2002). Enterotoxigenic profiles of food-poisoning and food-borne *Bacillus cereus* strains. *Journal of Clinical Microbiology*, *40*(8), 3053–6. https://doi.org/10.1128/JCM.40.8.3053-3056.2002

Haddad Kashani, H., Schmelcher, M., Sabzalipoor, H., Seyed Hosseini, E., & Moniri, R. (2017). Recombinant Endolysins as Potential Therapeutics against Antibiotic-Resistant *Staphylococcus aureus* : Current Status of Research and Novel Delivery Strategies. *Clinical Microbiology Reviews*, *31*(1). https://doi.org/10.1128/CMR.00071-17

Han, C. S., Xie, G., Challacombe, J. F., Altherr, M. R., Bhotika, S. S., Bruce, D., … Gilna, P. (2006). Pathogenomic Sequence Analysis of *Bacillus cereus* and *Bacillus thuringiensis* Isolates Closely Related to *Bacillus anthracis* †. *Journal of Bacteriology*, *188*(9), 3382–3390. https://doi.org/10.1128/JB.188.9.3382-3390.2006

Hancock, R. E. W., Farmer, S. W., Li, Z., & Poolet, K. (1991). Interaction of Aminoglycosides with the Outer Membranes and Purified Lipopolysaccharide and OmpF Porin of *Escherichia coli* Downloaded from. *Antimicrobial Agents and Chemotherapy*, *35*(7), 1309–1314. Retrieved from http://aac.asm.org/

Helgason, E., Okstad, O. A., Caugant, D. A., Johansen, H. A., Fouet, A., Mock, M., … Kolstø, A. B. (2000). *Bacillus anthracis*, *Bacillus cereus*, and *Bacillus thuringiensis*--one species on the basis of genetic evidence. *Applied and Environmental Microbiology*, *66*(6), 2627–30. https://doi.org/10.1128/AEM.66.6.2627-2630.2000

Hendrix, R. W. (2002). Bacteriophages: Evolution of the Majority. *Theoretical Population Biology*, *61*(4), 471–480. https://doi.org/10.1006/tpbi.2002.1590

Hermoso, J. A., García, J. L., & García, P. (2007). Taking aim on bacterial pathogens: from phage therapy to enzybiotics. *Current Opinion in Microbiology*, *10*(5), 461–472. https://doi.org/10.1016/j.mib.2007.08.002

Hermoso, J. A., Monterroso, B., Albert, A., Galán, B., Ahrazem, O., García, P., … Menéndez, M. (2003). Structural Basis for Selective Recognition of Pneumococcal Cell Wall by Modular Endolysin from Phage Cp-1. *Structure*, *11*(10), 1239–1249. https://doi.org/10.1016/j.str.2003.09.005

Heselpoth, R. D., Owens, J. M., & Nelson, D. C. (2015). Quantitative analysis of the thermal stability of the gamma phage endolysin PlyG: A biophysical and kinetic approach to assaying therapeutic potential. *Virology*, *477*, 125–132. https://doi.org/10.1016/j.virol.2014.11.003

Heselpoth, R. D., Swift, S. M., Linden, S. B., Mitchell, M. S., & Nelson, D. C. (2018). Enzybiotics: Endolysins and Bacteriocins. In *Bacteriophages* (pp. 1–42). Cham: Springer International Publishing. https://doi.org/10.1007/978-3-319-40598-8_34-1

Heselpoth, R. D., Yin, Y., Moult, J., & Nelson, D. C. (2015). Increasing the stability of the bacteriophage endolysin PlyC using rationale-based FoldX computational modeling. *Protein Engineering, Design & Selection : PEDS*, *28*(4), 85–92. https://doi.org/10.1093/protein/gzv004

Hill, K. K., Ticknor, L. O., Okinaka, R. T., Asay, M., Blair, H., Bliss, K. A., … Jackson, P. J. (2004). Fluorescent amplified fragment length polymorphism analysis of *Bacillus anthracis*, *Bacillus cereus*, and *Bacillus thuringiensis* isolates. *Applied and Environmental Microbiology*, *70*(2), 1068–80. https://doi.org/10.1128/AEM.70.2.1068-1080.2004

Hoffmaster, A. R., Hill, K. K., Gee, J. E., Marston, C. K., De, B. K., Popovic, T., … Jackson, P. J. (2006). Characterization of *Bacillus cereus* Isolates Associated with Fatal Pneumonias: Strains Are Closely Related to *Bacillus anthracis* and Harbor *B. anthracis* Virulence Genes. *Journal of Clinical Microbiology*, *44*(9), 3352–3360. https://doi.org/10.1128/JCM.00561-06

Hoffmaster, A. R., Ravel, J., Rasko, D. A., Chapman, G. D., Chute, M. D., Marston, C. K., … Fraser, C. M. (2004). Identification of anthrax toxin genes in a *Bacillus cereus* associated with an illness resembling inhalation anthrax. *Proceedings of the National Academy of Sciences of the United States of America*, *101*(22), 8449–54. https://doi.org/10.1073/pnas.0402414101

Hofmann, K., & Baron, M. D. (1996). Boxshade 3.21. Pretty printing and shading of multiple-alignment files. Lausanne, Switzerland: Kay Hofmann ISREC Bioinformatics Group.

Hoopes, J. T., Stark, C. J., Kim, H. A., Sussman, D. J., Donovan, D. M., & Nelson, D. C. (2009). Use of a bacteriophage lysin, PlyC, as an enzyme disinfectant against *Streptococcus equi*. *Applied and Environmental Microbiology*. https://doi.org/10.1128/AEM.02195-08

Ibrahim, H. R., Yamada, M., Matsushita, K., Kobayashi, K., & Kato, K. (1994). Enhanced bactericidal action of lysozyme to *Escherichia coli* by inserting a hydrophobic pentapeptide into its C terminus. *The Journal of Biological Chemistry*, *269*(7), 5059–5063. Retrieved from http://www.jbc.org/content/269/7/5059.short

Ikeda, M., Yagihara, Y., Tatsuno, K., Okazaki, M., Okugawa, S., & Moriya, K. (2015). Clinical characteristics and antimicrobial susceptibility of *Bacillus cereus* blood stream infections. *Annals of Clinical Microbiology and Antimicrobials*, *14*(1), 43. https://doi.org/10.1186/s12941-015-0104-2

Jones, D. T., Taylor, W. R., & Thornton, J. M. (1992). The rapid generation of mutation data matrices from protein sequences. *Computer Applications in the Biosciences : CABIOS*, *8*(3), 275–82. Retrieved from http://www.ncbi.nlm.nih.gov/pubmed/1633570

Jordan, T. C., Burnett, S. H., Carson, S., Caruso, S. M., Clase, K., DeJong, R. J., … Hatfull, G. F. (2014). A Broadly Implementable Research Course in Phage Discovery and Genomics for First-Year Undergraduate Students. *MBio*, *5*(1), e01051-13. https://doi.org/10.1128/mBio.01051-13

Keim, P., Price, L. B., Klevytska, A. M., Smith, K. L., Schupp, J. M., Okinaka, R., … Hugh-Jones, M. E. (2000). Multiple-Locus Variable-Number Tandem Repeat Analysis Reveals Genetic Relationships within *Bacillus anthracis*. *Journal of Bacteriology*, *182*(10), 2928–2936. https://doi.org/10.1128/JB.182.10.2928-2936.2000

Khasnabis, J., Adhikari, P., Chowdhury, D., Rai, C., & Roy, A. (2017). Incidence of multiple drug resistant *Bacillus cereus* in some popular snacks and sweets sold in Kolkata city, India. *Indian J. Microbiol Res*, *4(1)*, 14–19. Retrieved from https://www.researchgate.net/profile/Arindam_Roy17/publication/315543918_Incidence_of_multiple_drug_resistant_Bacillus_cereus_in_some_popular_snacks_and_sweets_sold_in_Kolkata_city_India/links/58d3edad92851c44d441528c/Incidence-of-multiple-drug-resistant-

Kikkawa, H., Fujinami, Y., Suzuki, S., & Yasuda, J. (2007). Identification of the amino acid residues critical for specific binding of the bacteriolytic enzyme of γ-phage, PlyG, to *Bacillus anthracis*. *Biochemical and Biophysical Research Communications*, *363*(3), 531–535. https://doi.org/10.1016/J.BBRC.2007.09.002

Kikkawa, H. S., Ueda, T., Suzuki, S., & Yasuda, J. (2008). Characterization of the catalytic activity

of the Î³-phage lysin, PlyG, specific for *Bacillus anthracis*. *FEMS Microbiology Letters*, *286*(2), 236–240. https://doi.org/10.1111/j.1574-6968.2008.01280.x

Kim, C.-W., Cho, S.-H., Kang, S.-H., Park, Y.-B., Yoon, M.-H., Lee, J.-B., … Kim, J.-B. (2015). Prevalence, Genetic Diversity, and Antibiotic Resistance of *Bacillus cereus* Isolated from Korean Fermented Soybean Products. *Journal of Food Science*, *80*(1), M123-128. https://doi.org/10.1111/1750-3841.12720

Koch, A., & Arvand, M. (2005). Recurrent bacteraemia by 2 different *Bacillus cereus* strains related to 2 distinct central venous catheters. *Scandinavian Journal of Infectious Diseases*, *37*(10), 772–774. https://doi.org/10.1080/00365540510012116

Kong, M., & Ryu, S. (2015). Bacteriophage PBC1 and Its Endolysin as an Antimicrobial Agent against Bacillus cereus. *Applied and Environmental Microbiology*, *81*(7), 2274–2283. https://doi.org/10.1128/AEM.03485-14

Koo, Y. S., Kim, J. M., Park, I. Y., Yu, B. J., Jang, S. A., Kim, K.-S., … Kim, S. C. (2008). Structure–activity relations of parasin I, a histone H2A-derived antimicrobial peptide. *Peptides*, *29*(7), 1102–1108. https://doi.org/10.1016/J.PEPTIDES.2008.02.019

Korndörfer, I. P., Danzer, J., Schmelcher, M., Zimmer, M., Skerra, A., & Loessner, M. J. (2006). The Crystal Structure of the Bacteriophage PSA Endolysin Reveals a Unique Fold Responsible for Specific Recognition of *Listeria* Cell Walls. *Journal of Molecular Biology*, *364*(4), 678–689. https://doi.org/10.1016/j.jmb.2006.08.069

Korndörfer, I. P., Kanitz, A., Danzer, J., Zimmer, M., Loessner, M. J., & Skerra, A. (2008). Structural analysis of the L-alanoyl-D-glutamate endopeptidase domain of *Listeria* bacteriophage endolysin Ply500 reveals a new member of the LAS peptidase family. *Acta Crystallographica Section D: Biological Crystallography*, *64*(6), 644–650. https://doi.org/10.1107/S0907444908007890

Kramer, J. M., & Gilbert, R. J. (1989). *Bacillus cereus* and other *Bacillus* species. In M. P. Doyle (Ed.), *Foodborne bacterial pathogens* (pp. 21–70). New York, NY: Marcel Dekker, INC.

Kumar, S., Stecher, G., & Tamura, K. (2016). MEGA7: Molecular Evolutionary Genetics Analysis Version 7.0 for Bigger Datasets. *Molecular Biology and Evolution*, *33*(7), 1870–1874. https://doi.org/10.1093/molbev/msw054

Kutsuna, S., Hayakawa, K., Kita, K., … Y. K.-A. journal of, & 2017, U. (2017). Risk factors of catheter-related bloodstream infection caused by *Bacillus cereus*: Case-control study in 8 teaching hospitals in Japan. *American Journal of Infection Control*, *45(11)*, pp.1281-1283. Retrieved from https://www.sciencedirect.com/science/article/pii/S0196655317305990

Larkin, M. A., Blackshields, G., Brown, N. P., Chenna, R., McGettigan, P. A., McWilliam, H., … Higgins, D. G. (2007). Clustal W and Clustal X version 2.0. *Bioinformatics*, *23*(21), 2947–2948. https://doi.org/10.1093/bioinformatics/btm404

Laskowski, R. A., MacArthur, M. W., Moss, D. S., Thornton, J. M., & IUCr. (1993). PROCHECK:

a program to check the stereochemical quality of protein structures. *Journal of Applied Crystallography*, *26*(2), 283–291. https://doi.org/10.1107/S0021889892009944

Leggett, M. J., McDonnell, G., Denyer, S. P., Setlow, P., & Maillard, J.-Y. (2012). Bacterial spore structures and their protective role in biocide resistance. *Journal of Applied Microbiology*, *113*(3), 485–498. https://doi.org/10.1111/j.1365-2672.2012.05336.x

Leggett, M. J., Schwarz, J. S., Burke, P. A., Mcdonnell, G., Denyer, S. P., & Maillard, J.-Y. (2015). Resistance to and killing by the sporicidal microbicide peracetic acid. *Journal of Antimicrobial Chemotherapy*, *70*(3), 773–779. https://doi.org/10.1093/jac/dku445

Leoff, C., Choudhury, B., Saile, E., Quinn, C. P., Carlson, R. W., & Kannenberg, E. L. (2008). Structural Elucidation of the Nonclassical Secondary Cell Wall Polysaccharide from *Bacillus cereus* ATCC 10987. *Journal of Biological Chemistry*, *283*(44), 29812–29821. https://doi.org/10.1074/jbc.M803234200

Letunic, I., & Bork, P. (2018). 20 years of the SMART protein domain annotation resource. *Nucleic Acids Research*, *46*(D1), D493–D496. https://doi.org/10.1093/nar/gkx922

Linden, S. B., Zhang, H., Heselpoth, R. D., Shen, Y., Schmelcher, M., Eichenseher, F., & Nelson, D. C. (2015). Biochemical and biophysical characterization of PlyGRCS, a bacteriophage endolysin active against methicillin-resistant *Staphylococcus aureus*. *Applied Microbiology and Biotechnology*, *99*(2), 741–752. https://doi.org/10.1007/s00253-014-5930-1

Loeffler, J. M., Nelson, D., & Fischetti, V. A. (2001). Rapid Killing of *Streptococcus pneumoniae* with a Bacteriophage Cell Wall Hydrolase. *Science*, *294*(5549), 2170–2172. https://doi.org/10.1126/science.1066869

Loessner, M. J. (2005). Bacteriophage endolysins — current state of research and applications. *Current Opinion in Microbiology*, *8*(4), 480–487. https://doi.org/10.1016/j.mib.2005.06.002

Loessner, M. J., Maier, S. K., Daubek-Puza, H., Wendlinger, G., & Scherer, S. (1997). Three *Bacillus cereus* bacteriophage endolysins are unrelated but reveal high homology to cell wall hydrolases from different bacilli. *Journal of Bacteriology*, *179*(9), 2845–51. Retrieved from http://www.ncbi.nlm.nih.gov/pubmed/9139898

Loessner, M. J., Schneider, A., & Scherer, S. (1996). Modified *Listeria* bacteriophage lysin genes (ply) allow efficient overexpression and one-step purification of biochemically active fusion proteins. *Applied and Environmental Microbiology*, *62*(8), 3057–60. Retrieved from http://www.ncbi.nlm.nih.gov/pubmed/8702301

Loessner, M. J., Wendlinger, G., & Scherer, S. (1995). Heterogeneous endolysins in *Listeria monocytogenes* bacteriophages: a new class of enzymes and evidence for conserved holin genes within the siphoviral lysis cassettes. *Molecular Microbiology*, *16*(6), 1231–1241. https://doi.org/10.1111/j.1365-2958.1995.tb02345.x

López, R., & García, E. (2004). Recent trends on the molecular biology of pneumococcal capsules, lytic enzymes, and bacteriophage. *FEMS Microbiology Reviews*, *28*(5), 553–580.

https://doi.org/10.1016/j.femsre.2004.05.002

Lopez, R., Garcia, E., Garcia, P., & Garcia, J. L. (1997). The Pneumococcal Cell Wall Degrading Enzymes: A Modular Design to Create New Lysins? *Microbial Drug Resistance*, *3*(2), 199–211. https://doi.org/10.1089/mdr.1997.3.199

Low, L. Y., Yang, C., Perego, M., Osterman, A., & Liddington, R. (2011). Role of Net Charge on Catalytic Domain and Influence of Cell Wall Binding Domain on Bactericidal Activity, Specificity, and Host Range of Phage Lysins. *Journal of Biological Chemistry*, *286*(39), 34391–34403. https://doi.org/10.1074/jbc.M111.244160

Low, L. Y., Yang, C., Perego, M., Osterman, A., & Liddington, R. C. (2005). Structure and lytic activity of a *Bacillus anthracis* prophage endolysin. *The Journal of Biological Chemistry*, *280*(42), 35433–9. https://doi.org/10.1074/jbc.M502723200

Lund, T., De Buyser, M.-L., & Granum, P. E. (2000). A new cytotoxin from *Bacillus cereus* that may cause necrotic enteritis. *Molecular Microbiology*, *38*(2), 254–261. https://doi.org/10.1046/j.1365-2958.2000.02147.x

Luxananil, P., Tanapongpipat, S., Promdonkoy, B., Atomi, H., Imanaka, T., & Panyim, S. (2003). Expression of Binary Toxin Genes in the Mosquito-Colonizable Bacteria, *Bacillus cereus*, Leads to High Toxicity Against Culex quinquefasciatus Larvae. *Current Microbiology*, *47*(5), 372–375. https://doi.org/10.1007/s00284-002-4026-9

Makino, S., Uchida, I., Terakado, N., Sasakawa, C., & Yoshikawa, M. (1989). Molecular characterization and protein analysis of the cap region, which is essential for encapsulation in *Bacillus anthracis*. *Journal of Bacteriology*, *171*(2), 722–30. https://doi.org/10.1128/JB.171.2.722-730.1989

Marchler-Bauer, A., Bo, Y., Han, L., He, J., Lanczycki, C. J., Lu, S., … Bryant, S. H. (2017). CDD/SPARCLE: functional classification of proteins via subfamily domain architectures. *Nucleic Acids Research*, *45*(D1), D200–D203. https://doi.org/10.1093/nar/gkw1129

Mayer, M. J., Garefalaki, V., Spoerl, R., Narbad, A., & Meijers, R. (2011). Structure-Based Modification of a *Clostridium difficile*-Targeting Endolysin Affects Activity and Host Range. *Journal of Bacteriology*, *193*(19), 5477–5486. https://doi.org/10.1128/JB.00439-11

Mayer, M. J., Payne, J., Gasson, M. J., & Narbad, A. (2010). Genomic sequence and characterization of the virulent bacteriophage phiCTP1 from *Clostridium tyrobutyricum* and heterologous expression of its endolysin. *Applied and Environmental Microbiology*, *76*(16), 5415–22. https://doi.org/10.1128/AEM.00989-10

McCafferty, D. G., Lessard, I. A. D., & Walsh, C. T. (1997). Mutational Analysis of Potential Zinc-Binding Residues in the Active Site of the Enterococcal d -Ala- d -Ala Dipeptidase VanX †. *Biochemistry*, *36*(34), 10498–10505. https://doi.org/10.1021/bi970543u

Merril, C. R., Scholl, D., & Adhya, S. L. (2003). The prospect for bacteriophage therapy in Western medicine. *Nature Reviews Drug Discovery*, *2*(6), 489–497.

https://doi.org/10.1038/nrd1111

Merzougui, S., Lkhider, M., Grosset, N., Gautier, M., & Cohen, N. (2014). Prevalence, PFGE Typing, and Antibiotic Resistance of *Bacillus cereus* Group Isolated from Food in Morocco. *Foodborne Pathogens and Disease*, *11*(2), 145–149. https://doi.org/10.1089/fpd.2013.1615

Mesnage, S., Tosi-Couture, E., & Fouet, A. (1999). Production and cell surface anchoring of functional fusions between the SLH motifs of the *Bacillus anthracis* S-layer proteins and the Bacillus subtilis levansucrase. *Molecular Microbiology*, *31*(3), 927–936. https://doi.org/10.1046/j.1365-2958.1999.01232.x

Mesnage, S., Tosi-Couture, E., Mock, M., Gounon, P., & Fouet, A. (1997). Molecular characterization of the *Bacillus anthracis* main S-layer component: evidence that it is the major cell-associated antigen. *Molecular Microbiology*, *23*(6), 1147–1155. https://doi.org/10.1046/j.1365-2958.1997.2941659.x

Moak, M., & Molineux, I. J. (2004). Peptidoglycan hydrolytic activities associated with bacteriophage virions. *Molecular Microbiology*, *51*(4), 1169–1183. https://doi.org/10.1046/j.1365-2958.2003.03894.x

Mock, M., & Fouet, A. (2001). Anthrax. *Annual Review of Microbiology*, *55*(1), 647–671. https://doi.org/10.1146/annurev.micro.55.1.647

Montville, T. J., & Matthews, K. R. (2005). *Food microbiology: an introduction.* Washington, D.C.: ASM Press. Retrieved from https://trove.nla.gov.au/work/17206533?q&versionId=46533632

Na, H., Kong, M., & Ryu, S. (2016). Characterization of LysPBC4, a novel *Bacillus cereus* -specific endolysin of bacteriophage PBC4. *FEMS Microbiology Letters*, *363*(12), fnw092. https://doi.org/10.1093/femsle/fnw092

Nelson, D. C., Schmelcher, M., Rodriguez-Rubio, L., Klumpp, J., Pritchard, D. G., Dong, S., & Donovan, D. M. (2012). Endolysins as antimicrobials. *Advances in Virus Research*, *83*, 299–365. https://doi.org/10.1016/B978-0-12-394438-2.00007-4

Nelson, D. L., & Cox, M. M. (2013). Amino Acids, Peptides, and Proteins. In *Lehninger Principles of Biochemistry* (6ht editio). New-York, NY: W.H. Freeman and Company.

Nelson, D., Schuch, R., Chahales, P., Zhu, S., & Fischetti, V. A. (2006). PlyC: a multimeric bacteriophage lysin. *Proceedings of the National Academy of Sciences of the United States of America*, *103*(28), 10765–70. https://doi.org/10.1073/pnas.0604521103

Neuhaus, F. C., & Baddiley, J. (2003). A continuum of anionic charge: structures and functions of D-alanyl-teichoic acids in gram-positive bacteria. *Microbiology and Molecular Biology Reviews : MMBR*, *67*(4), 686–723. Retrieved from http://www.ncbi.nlm.nih.gov/pubmed/14665680

Nikaido, H. (2003). Molecular Basis of Bacterial Outer Membrane Permeability Revisited. *Microbiology and Molecular Biology Reviews : MMBR*, *67*(4), 593–656.

https://doi.org/10.1128/MMBR.67.4.593-656.2003

Okinaka, R. T., & Keim, P. (2016). The Phylogeny of *Bacillus cereus sensu lato*. *Microbiology Spectrum*, *4*(1). https://doi.org/10.1128/microbiolspec.TBS-0012-2012

Oldham, E. R., & Daley, M. J. (1991). Lysostaphin: Use of a Recombinant Bactericidal Enzyme as a Mastitis Therapeutic. *Journal of Dairy Science*, *74*(12), 4175–4182. https://doi.org/10.3168/JDS.S0022-0302(91)78612-8

Oliveira, H., Melo, L. D. R., Santos, S. B., Nobrega, F. L., Ferreira, E. C., Cerca, N., … Kluskens, L. D. (2013). Molecular Aspects and Comparative Genomics of Bacteriophage Endolysins. *Journal of Virology*, *87*(8), 4558–4570. https://doi.org/10.1128/JVI.03277-12

Oren, Z., & Shai, Y. (1998). Mode of action of linear amphipathic α-helical antimicrobial peptides. *Biopolymers*, *47*(6), 451–463. https://doi.org/10.1002/(SICI)1097-0282(1998)47:6<451::AID-BIP4>3.0.CO;2-F

Park, I. Y., Park, C. B., Kim, M. S., & Kim, S. C. (1998). Parasin I, an antimicrobial peptide derived from histone H2A in the catfish, *Parasilurus asotus*. *FEBS Letters*, *437*(3), 258–262. https://doi.org/10.1016/S0014-5793(98)01238-1

Park, J., Yun, J., Lim, J.-A., Kang, D.-H., & Ryu, S. (2012). Characterization of an endolysin, LysBPS13, from a *Bacillus cereus* bacteriophage. *FEMS Microbiology Letters*, *332*(1), 76–83. https://doi.org/10.1111/j.1574-6968.2012.02578.x

Park, S., Jun, S. Y., Kim, C.-H., Jung, G. M., Son, J. S., Jeong, S. T., … Kang, S. H. (2018). Characterisation of the antibacterial properties of the recombinant phage endolysins AP50-31 and LysB4 as potent bactericidal agents against *Bacillus anthracis*. *Nature Scientific Reports*, *8*(18). https://doi.org/10.1038/s41598-017-18535-z

Park, Y.-B., Kim, J.-B., Shin, S.-W., Kim, J.-C., Cho, S.-H., Lee, B.-K., … Oh, D.-H. (2009). Prevalence, Genetic Diversity, and Antibiotic Susceptibility of Bacillus cereus Strains Isolated from Rice and Cereals Collected in Korea. *Journal of Food Protection*, *72*(3), 612–617. https://doi.org/10.4315/0362-028X-72.3.612

Paskaleva, E. E., Mundra, R. V., Mehta, K. K., Pangule, R. C., Wu, X., Glatfelter, W. S., … Kane, R. S. (2015). Binding domains of *Bacillus anthracis* phage endolysins recognize cell culture age-related features on the bacterial surface. *Biotechnology Progress*, *31*(6), 1487–1493. https://doi.org/10.1002/btpr.2172

Peng, Q., & Yuan, Y. (2018). Characterization of a novel phage infecting the pathogenic multidrug-resistant *Bacillus cereus* and functional analysis of its endolysin. *Applied Microbiology and Biotechnology*, *102*(18), 7901–7912. https://doi.org/10.1007/s00253-018-9219-7

Pires, D. P., Oliveira, H., Melo, L. D. R., Sillankorva, S., & Azeredo, J. (2016). Bacteriophage-encoded depolymerases: their diversity and biotechnological applications. *Applied Microbiology and Biotechnology*, *100*(5), 2141–2151. https://doi.org/10.1007/s00253-015-7247-0

Porter, C. J., Schuch, R., Pelzek, A. J., Buckle, A. M., McGowan, S., Wilce, M. C. J., … Whisstock, J. C. (2007). The 1.6 Å Crystal Structure of the Catalytic Domain of PlyB, a Bacteriophage Lysin Active Against *Bacillus anthracis*. *Journal of Molecular Biology*, *366*(2), 540–550. https://doi.org/10.1016/j.jmb.2006.11.056

Poullain, V. (2007). The evolution of specificity in evolving and coevolving antagonistic interactions between a bacteria and its phage. *Evolution*, *62*(1), 1–11. https://doi.org/10.1111/j.1558-5646.2007.00260.x

Proença, D., Velours, C., Leandro, C., Garcia, M., Pimentel, M., & São-José, C. (2015). A two-component, multimeric endolysin encoded by a single gene. *Molecular Microbiology*, *95*(5), 739–753. https://doi.org/10.1111/mmi.12857

Publications service, F. (2007). On an invisible microbe antagonistic toward dysenteric bacilli: brief note by Mr. F. D'Herelle, presented by Mr. Roux. *Research in Microbiology*, *158*(7), 553–554. https://doi.org/10.1016/j.resmic.2007.07.005

Rasko, D. A., Ravel, J., Økstad, O. A., Helgason, E., Cer, R. Z., Jiang, L., … Read, T. D. (2004). The genome sequence of *Bacillus cereus* ATCC 10987 reveals metabolic adaptations and a large plasmid related to *Bacillus anthracis* pXO1. *Nucleic Acids Research*, *32*(3), 977–988. https://doi.org/10.1093/nar/gkh258

Schuch, R. & Nelson, D. (1986). A bacteriolytic agent that detects and kills *bacillus anthracis*. *Exp. Biol. J. Gen. Physiol*, *124*(117), 5–13. https://doi.org/10.1038/nature01026

Regeimbal, J. M., Jacobs, A. C., Corey, B. W., Henry, M. S., Thompson, M. G., Pavlicek, R. L., … Hall, E. R. (2016). Personalized Therapeutic Cocktail of Wild Environmental Phages Rescues Mice from *Acinetobacter baumannii* Wound Infections. *Antimicrobial Agents and Chemotherapy*, *60*(10), 5806–16. https://doi.org/10.1128/AAC.02877-15

Roh, J. Y., Choi, J. Y., Li, M. S., Jin, B. R., & Je, Y. H. (2007). *Bacillus thuringiensis* as a specific, safe, and effective tool for insect pest control. *Journal of Microbiology and Biotechnology*, *17*(4), 547–59. Retrieved from http://www.ncbi.nlm.nih.gov/pubmed/18051264

Royet, J., & Dziarski, R. (2007). Peptidoglycan recognition proteins: pleiotropic sensors and effectors of antimicrobial defences. *Nature Reviews Microbiology*, *5*(4), 264–277. https://doi.org/10.1038/nrmicro1620

Saedi, M. S., Garvey, K. J., & Ito, J. (1987). Cloning and purification of a unique lysozyme produced by *Bacillus* phage phi 29. *Proceedings of the National Academy of Sciences of the United States of America*, *84*(4), 955–8. Retrieved from http://www.ncbi.nlm.nih.gov/pubmed/3469652

Sali, A., & Blundell, T. L. (1993). Comparative protein modelling by satisfaction of spatial restraints. *Journal of Molecular Biology*, *234*(3), 779–815. https://doi.org/10.1006/jmbi.1993.1626

Sambrook, J., Fritsch, E. F., & Maniatis, T. (1989). Molecular cloning: a laboratory manual. *Molecular Cloning: A Laboratory Manual.*, (Ed. 2). Retrieved from

https://www.cabdirect.org/cabdirect/abstract/19901616061

São-José, C. (2018). Engineering of Phage-Derived Lytic Enzymes: Improving Their Potential as Antimicrobials. *Antibiotics*, *7*(2), 29. https://doi.org/10.3390/antibiotics7020029

Scallan, E., Hoekstra, R. M., Angulo, F. J., Tauxe, R. V, Widdowson, M.-A., Roy, S. L., … Griffin, P. M. (2011). Foodborne illness acquired in the United States--major pathogens. *Emerging Infectious Diseases*, *17*(1), 7–15. https://doi.org/10.3201/eid1701.091101p1

Schaffer, C., & Messner, P. (2005). The structure of secondary cell wall polymers: how Gram-positive bacteria stick their cell walls together. *Microbiology*, *151*(3), 643–651. https://doi.org/10.1099/mic.0.27749-0

Schmelcher, M., Donovan, D. M., & Loessner, M. J. (2012). Bacteriophage endolysins as novel antimicrobials. *Future Microbiology*, *7*(10), 1147–71. https://doi.org/10.2217/fmb.12.97

Schmelcher, M., & Loessner, M. J. (2014). Application of bacteriophages for detection of foodborne pathogens. *Bacteriophage*, *4*(2), e28137. https://doi.org/10.4161/bact.28137

Schmelcher, M., Shabarova, T., Eugster, M. R., Eichenseher, F., Tchang, V. S., Banz, M., & Loessner, M. J. (2010). Rapid multiplex detection and differentiation of *Listeria* cells by use of fluorescent phage endolysin cell wall binding domains. *Applied and Environmental Microbiology*, *76*(17), 5745–56. https://doi.org/10.1128/AEM.00801-10

Schmelcher, M., Tchang, V. S., & Loessner, M. J. (2011). Domain shuffling and module engineering of *Listeria* phage endolysins for enhanced lytic activity and binding affinity. *Microbial Biotechnology*, *4*(5), 651–662. https://doi.org/10.1111/j.1751-7915.2011.00263.x

Scholte, C. M., Nelson, D. C., Garcia, M., Linden, S. B., Elsasser, T. H., Kahl, S., … Moyes, K. M. (2018). Short communication: Recombinant bacteriophage endolysin PlyC is nontoxic and does not alter blood neutrophil oxidative response in lactating dairy cows. *Journal of Dairy Science*, *101*(7), 6419–6423. https://doi.org/10.3168/jds.2017-13908

Schooley, R. T., Biswas, B., Gill, J. J., Hernandez-Morales, A., Lancaster, J., Lessor, L., … Hamilton, T. (2017). Development and Use of Personalized Bacteriophage-Based Therapeutic Cocktails To Treat a Patient with a Disseminated Resistant *Acinetobacter baumannii* Infection. *Antimicrobial Agents and Chemotherapy*, *61*(10), AAC.00954-17. https://doi.org/10.1128/AAC.00954-17

Schuch, R., Fischetti, V. A., & Nelson, D. (2009). A Genetic Screen to Identify Bacteriophage Lysins. *Methods in Molecular Biology (Clifton, N.J.)*, *502*(3), 365–370. https://doi.org/10.1007/978-1-60327-565-1

Schuch, R., Nelson, D., & Fischetti, V. A. (2002). A bacteriolytic agent that detects and kills *Bacillus anthracis*. *Nature*, *418*(6900), 884–889. https://doi.org/10.1038/nature01026

Schuch, R., Pelzek, A. J., Raz, A., Euler, C. W., Ryan, P. A., Winer, B. Y., … Fischetti, V. A. (2013). Use of a Bacteriophage Lysin to Identify a Novel Target for Antimicrobial Development.

PLoS ONE, *8*(4), e60754. https://doi.org/10.1371/journal.pone.0060754

Sheehan, M. M., García, J. L., Ló Pez, R., & García, P. (1997). The lytic enzyme of the pneumococcal phage Dp-1: a chimeric lysin of intergeneric origin. *Molecular Microbiology*, *25*(4), 717–725. Retrieved from https://onlinelibrary.wiley.com/doi/pdf/10.1046/j.1365-2958.1997.5101880.x

Sheehan, M. M., García, J. L., López, R., & García, P. (1996). Analysis of the catalytic domain of the lysin of the lactococcal bacteriophage Tuc2009 by chimeric gene assembling. *FEMS Microbiology Letters*, *140*(1), 23–8. Retrieved from http://www.ncbi.nlm.nih.gov/pubmed/8666197

Shen, M., & Sali, A. (2006). Statistical potential for assessment and prediction of protein structures. *Protein Science*, *15*(11), 2507–2524. https://doi.org/10.1110/ps.062416606

Shen, Y., Barros, M., Vennemann, T., Gallagher, D. T., Yin, Y., Linden, S. B., … Nelson, D. C. (2016). A bacteriophage endolysin that eliminates intracellular streptococci. *ELife*, *5*. https://doi.org/10.7554/eLife.13152

Soding, J., Biegert, A., & Lupas, A. N. (2005). The HHpred interactive server for protein homology detection and structure prediction. *Nucleic Acids Research*, *33*(Web Server), W244–W248. https://doi.org/10.1093/nar/gki408

Son, B., Yun, J., Lim, J.-A., Shin, H., Heu, S., Ryu, S., … Visser, H. de. (2012). Characterization of LysB4, an endolysin from the *Bacillus cereus*-infecting bacteriophage B4. *BMC Microbiology*, *12*(1), 33. https://doi.org/10.1186/1471-2180-12-33

Sozhamannan, S., McKinstry, M., Lentz, S. M., Jalasvuori, M., McAfee, F., Smith, A., … Read, T. D. (2008). Molecular Characterization of a Variant of *Bacillus anthracis*-Specific Phage AP50 with Improved Bacteriolytic Activity. *Applied and Environmental Microbiology*, *74*(21), 6792–6796. https://doi.org/10.1128/AEM.01124-08

Stenfors Arnesen, L. P., Fagerlund, A., & Granum, P. E. (2008). From soil to gut: *Bacillus cereus* and its food poisoning toxins. *FEMS Microbiology Reviews*, *32*(4), 579–606. https://doi.org/10.1111/j.1574-6976.2008.00112.x

Stone, R. (2002). Stalin's Forgotten Cure. *Science*. American Association for the Advancement of Science. https://doi.org/10.2307/3832619

Straub, M. E. and, & Applebaum, M. (1933). STUDIES ON COMMERCIAL BACTERIOPHAGE PRODUCTS. *JAMA: The Journal of the American Medical Association*, *100*(2), 110. https://doi.org/10.1001/jama.1933.02740020028009

Sulakvelidze, A., Alavidze, Z., & Morris, J. G. (2001). Bacteriophage Therapy, *45*(3), 649–659. https://doi.org/10.1128/AAC.45.3.649-659.2001

Summers, W. C. (2001). Bacteriophage Therapy. *Annual Review of Microbiology*, *55*(1), 437–451. https://doi.org/10.1146/annurev.micro.55.1.437

Thomas, D. J. I., Morgan, J. A. W., Whipps, J. M., & Saunders, J. R. (2000). Plasmid Transfer between the *Bacillus thuringiensis* Subspecies *kurstaki* and *tenebrionis* in Laboratory Culture and Soil and in Lepidopteran and Coleopteran Larvae. *Applied and Environmental Microbiology*, *66*(1), 118–124. https://doi.org/10.1128/AEM.66.1.118-124.2000

Tirado, C., & Schmidt, K. (2001). WHO Surveillance Programme for Control of Foodborne Infections and Intoxications: Preliminary Results and Trends Across Greater Europe. *Journal of Infection*, *43*(1), 80–84. https://doi.org/10.1053/jinf.2001.0861

Twort, F. W. (1915). AN INVESTIGATION ON THE NATURE OF ULTRA-MICROSCOPIC VIRUSES. *The Lancet*, *186*(4814), 1241–1243. https://doi.org/10.1016/S0140-6736(01)20383-3

U. S. Centers for Disease Control and Prevention. (2015). The U.S. Foodborne Diseases Active Surveillance Network (FoodNet). Retrieved from https://www.cdc.gov/foodnet/about.html

Vaaral, M., & Vaara2, T. (1981). *Outer Membrane Permeability Barrier Disruption by Polymyxin in Polymyxin-Susceptible and-Resistant Salmonella typhimurium Downloaded from*. *Antimicrobial agents and chemotherapy* (Vol. 19). Retrieved from http://aac.asm.org/

Van der Auwera, G. A., Timmery, S., Hoton, F., & Mahillon, J. (2007). Plasmid exchanges among members of the Bacillus cereus group in foodstuffs. *International Journal of Food Microbiology*, *113*(2), 164–172. https://doi.org/10.1016/J.IJFOODMICRO.2006.06.030

Ventola, C. L. (2015). The antibiotic resistance crisis: part 1: causes and threats. *P & T : A Peer-Reviewed Journal for Formulary Management*, *40*(4), 277–83. Retrieved from http://www.ncbi.nlm.nih.gov/pubmed/25859123

Vollmer, W. (2008). Structural variation in the glycan strands of bacterial peptidoglycan. *FEMS Microbiology Reviews*, *32*(2), 287–306. https://doi.org/10.1111/j.1574-6976.2007.00088.x

Vollmer, W., Blanot, D., & De Pedro, M. A. (2008). Peptidoglycan structure and architecture. *FEMS Microbiology Reviews*. https://doi.org/10.1111/j.1574-6976.2007.00094.x

Wadsworth, A. B. (1912). STUDIES ON PNEUMOCOCCUS INFECTION IN ANIMALS : FIRST PAPER. *The Journal of Experimental Medicine*, *16*(1), 54–77. https://doi.org/10.1084/JEM.16.1.54

Wu, H., Huang, J., Lu, H., Li, G., & Huang, Q. (2014). GMEnzy: A Genetically Modified Enzybiotic Database. *PLoS ONE*, *9*(8), e103687. https://doi.org/10.1371/journal.pone.0103687

Yan, L., & Adams, M. E. (1998). Lycotoxins, antimicrobial peptides from venom of the wolf spider Lycosa carolinensis. *The Journal of Biological Chemistry*, *273*(4), 2059–66. https://doi.org/10.1074/JBC.273.4.2059

Yim, J.-H., Kim, K.-Y., Chon, J.-W., Kim, D.-H., Kim, H.-S., Choi, D.-S., … Seo, K.-H. (2015). Incidence, Antibiotic Susceptibility, and Toxin Profiles of *Bacillus cereus sensu lato* Isolated from Korean Fermented Soybean Products. *Journal of Food Science*, *80*(6), M1266–M1270. https://doi.org/10.1111/1750-3841.12872

Yoong, P., Schuch, R., Nelson, D., & Fischetti, V. A. (2006a). PlyPH, a Bacteriolytic Enzyme with a Broad pH Range of Activity and Lytic Action against *Bacillus anthracis*. *Journal of Bacteriology*, *188*(7), 2711–2714. https://doi.org/10.1128/JB.188.7.2711-2714.2006

Yuan, Y., Peng, Q., & Gao, M. (2012). Characteristics of a broad lytic spectrum endolysin from phage BtCS33 of *Bacillus thuringiensis*. *BMC Microbiology*, *12*(1), 297. https://doi.org/10.1186/1471-2180-12-297

Zaman, S. Bin, Hussain, M. A., Nye, R., Mehta, V., Mamun, K. T., & Hossain, N. (2017). A Review on Antibiotic Resistance: Alarm Bells are Ringing. *Cureus*, *9*(6), e1403. https://doi.org/10.7759/cureus.1403

Zhou, G., Zheng, D., Dou, L., Cai, Q., & Yuan, Z. (2010). Occurrence of psychrotolerant *Bacillus cereus* group strains in ice creams. *International Journal of Food Microbiology*, *137*(2–3), 143–146. https://doi.org/10.1016/j.ijfoodmicro.2009.12.005

Zipperle Jr., G. F., Ezzell Jr., J. W., & Doyle, R. J. (1984). Glucosamine substitution and muramidase susceptibility in *Bacillus anthracis*. *Canadian Journal of Microbiology*, *30*(5), 553–559. https://doi.org/10.1139/m84-083